The Dissertation Committee for Nikolaos Vergos
certifies that this is the approved version of the following dissertation:

Tearing Mode Dynamics in Tokamak Plasmas

Committee:

Richard Fitzpatrick, Supervisor

Boris Breizman

Richard Hazeltine

François Waelbroeck

Gary Hallock

Tearing Mode Dynamics in Tokamak Plasmas

by

Nikolaos Vergos, Dipl.

DISSERTATION

Presented to the Faculty of the Graduate School of

The University of Texas at Austin

in Partial Fulfillment

of the Requirements

for the Degree of

DOCTOR OF PHILOSOPHY

THE UNIVERSITY OF TEXAS AT AUSTIN

May 2016

Dedicated to my parents.

Acknowledgments

This dissertation is the culmination of several years of work, and, if it could talk, it would have many stories of stressful, sleepless nights, but also tales of accomplishment, pride, and exhilaration. Even though the acknowledgments section is placed in the beginning of this document, it is the last one I am writing chronologically, as I am savoring the reflection over my years at the University of Texas at Austin and the Institute for Fusion Studies.

There is a clear dichotomy transcending academic studies; working towards a PhD is rightfully considered to be a long, lonesome journey with many obstacles along the way, planned or, more often, not. However, there is an inherent truth in the proverb "*it takes a village*". No man is an island, and I would like to dedicate this section to the people that helped me reach this milestone. They have tirelessly provided me with invaluable mentorship and support all these years, helping me steer through sometimes tumultuous waters.

First and foremost, I would like to humbly extend my thanks to my undergraduate advisor, Dr. Kyriakos Hizanidis of the National Technical University of Athens, in Greece. I would have never decided to take the leap of faith and move halfway across the world to pursue graduate studies in Plasma Physics had it not been for his passionate, unwavering support. My

life changed forever, and I have him to thank for it.

The main reason I applied to The University of Texas, in the first place, was the opportunity to work under the guidance of Professor Richard Fitzpatrick. It has been a privilege to have him as my graduate advisor, and I benefited immensely from our interactions. My enormous gratitude goes to him for a variety of reasons: our meetings provided me with invaluable intuition, and his world-class expertise in Plasma Physics, his patience in training, and his phenomenal approach to teaching helped sculpt me into a scholar. Especially during the last few months, while I was writing this dissertation, his hands-on assistance and constant feedback have helped me feel confident of the quality of this work.

I am honored to have highly esteemed scientists support me by agreeing to participate in my dissertation committee. Professors Richard Hazeltine and Boris Breizman have been role models over the years: their teachings and many insightful discussions have inspired me with dedication to obtaining a strong theoretical background as a prerequisite for successful research work. My most sincere thanks are extended to Dr. François Waelbroeck for his dual role as a dissertation committee member and as the Director of the Institute for Fusion Studies during my years in graduate school. None of this would have been possible without the generous support of the IFS, and I'm especially thankful to Dr. Waelbroeck for agreeing to send me to Oxford, UK in 2012, so that I could participate in the annual CCFE Plasma Physics Summer School. This has been a unique learning experience. Last, but not least, I wish to thank

Dr. Gary Hallock for being a part of my committee.

A special place in my heart is reserved for Drs. Greg Sitz and Roger Bengtson. Having the opportunity to teach undergraduate physics (and serve as an Assistant Instructor) throughout my graduate studies was way more than just a way to pay the bills; it shaped me as a teacher, provided me with enormous experience, and personal/professional growth. Teaching physics to non-majors taught me how to decompose complicated ideas, and it served as a constant reminder that one can't really claim they have learned something, until they are able to explain it successfully.

These years at the Department of Physics and the Institute for Fusion Studies have been rather agreeable. I am grateful to Cathy Rapinett, James Halligan, Matt Ervin, and Lisa Gentry for helping me with administrative hurdles, but also for providing a friendly, welcoming environment.

Everyday life in RLM wouldn't have been the same without my friends, especially Ioannis Keramidas, Andy O'Hara, Roberto Hernández, Spyros Katsaros, and Brent Covele. Sometimes too long coffee breaks, and exploration of other brewed libations have definitely offered balance, and contributed to a well-rounded experience. I wish all of them luck in their further academic or professional endeavors. I am very thankful to my former roommate, Ioannis Mitliagkas; his unparalleled work ethic and true friendship have been a constant source of inspiration, and an emotional crutch in times of duress. Major kudos to him, along with Professors Constantine Caramanis and Alex Dimakis of the Department of Electrical and Computer Engineering: our Greek

Rebetiko music band, *Patzaria Skordalia*, has been an excellent creative outlet, a much needed catharsis, as well as a strong connection to our shared Hellenic culture, despite the distance from home.

Wrapping up this dedication, it goes without saying that the highest and most humble thanks go out to my family. Everything I have accomplished in life so far can be directly attributed to their unfaltering love and support. My only wish is to keep making them proud for many years to come.

Finally, I would like to thank my partner Boston, who has wholeheartedly believed in me, and has borne with me patiently throughout this strenuous period. He is making my life better.

This dissertation is a work of love, and I owe it to everyone I acknowledged, and to many more I did not. Thank you for believing in me.

Tearing Mode Dynamics in Tokamak Plasmas

Publication No. _____

Nikolaos Vergos, Ph.D.
The University of Texas at Austin, 2016

Supervisor: Richard Fitzpatrick

One of the most problematic instabilities in tokamak plasmas is tearing modes; they are driven by current and pressure gradients, and involve a reconfiguration of the magnetic and velocity fields localized into a narrow region located at a resonant magnetic surface. While the equilibrium magnetic field lines are located on concentric nested toroidal flux surfaces, the instability creates magnetic islands in which field lines connect flux tubes together, allowing for a high radial heat transport, and, thus, resulting in a loss of confinement, and, potentially, disruptions. In order for the magnetic field lines to break and reconnect, we need to take into account the resistivity of the plasma and solve the resistive magnetohydrodynamics (MHD) equations. The analytical solution consists of a boundary layer analysis (asymptotic matching) and takes advantage of the small radial width of the region where the perturbations vary significantly. Indeed, ideal magnetohydrodynamics can be used everywhere except in that narrow region where the full resistive problem must be solved.

This dissertation addresses two related problems in the study of resistive tearing modes, and their interactions with externally induced resonant magnetic perturbations (error-fields). First, an in-depth investigation of the bifurcated states of a rotating, quasi-cylindrical, tokamak plasma in the presence of a resonant error-field is performed, within the context of constant-ψ resistive MHD theory. The response of the rotating plasma is studied in both the linear, and the nonlinear regime. In general, there is a "forbidden band" of tearing mode rotation frequencies that separates a branch of high-frequency solutions from a branch of low-frequency solutions. When a high-frequency solution crosses the upper boundary of the forbidden band there is a bifurcation to a low-frequency solution, and vice versa. Second, the analysis is extended to include the study of braking and locking of tearing mode rotation by the interaction of the mode with an error-field. It is found that this interaction can brake the plasma rotation, suppress magnetic island evolution and drive locked modes.

Table of Contents

Acknowledgments **v**

Abstract **ix**

List of Figures **xiv**

Chapter 1. Introduction **1**

1.1 The Growing Demand for Energy in a Warming World 1

1.1.1 The Case for Fusion 4

1.1.2 Magnetic Confinement: The Tokamak 7

1.1.3 Outline of this Dissertation 11

1.2 Introduction to Magnetohydrodynamics 13

1.2.1 The MHD Equations 15

1.3 MHD Equilibria 22

1.3.1 Force Balance and β 23

1.3.2 Magnetic Flux Surfaces 24

1.3.3 Cylindrical Equilibria: The Z-pinch 26

1.3.4 Toroidal Equilibria 28

1.3.5 The Grad-Shafranov Equation 31

1.3.6 Shafranov Geometry 33

1.4 Magnetohydrodynamic Instabilities 34

1.4.1 Linearization of Magnetohydrodynamic Equations . . . 35

1.4.2 The MHD Eigenvalue Equation 39

1.4.3 The Energy Principle 41

1.5 Normal Modes of Cylindrical Equilibria 43

1.5.1 Kruskal-Shafranov and Suydam Stability Conditions . . 45

Chapter 2. Theory of Tearing Modes **48**
2.1 Magnetic Reconnection 48
2.2 Linear Tearing Mode Theory 51
2.3 Tearing Mode Dispersion Relation 56
2.4 Formation of Magnetic Islands 70
2.5 Nonlinear Tearing Mode Theory 73

Chapter 3. Resonant Magnetic Perturbation Response Theory 79
3.1 Introduction 79
3.1.1 Cylindrical Tokamak Equilibrium 80
3.1.2 Plasma Response to a Resonant Magnetic Perturbation 81
3.2 Linear Regime 83
3.2.1 Normalization Scheme 86
3.2.2 Linear Plasma Response Theory 87
3.2.3 Toroidal Torque Balance 91
3.2.4 Bifurcation Theory in Linear Response Regime 93
3.3 Nonlinear Regime 97
3.3.1 Analytic Approximations 104
3.3.2 Bifurcation Theory in Nonlinear Response Regime . . . 110

Chapter 4. Braking and Locking of Tearing Mode Rotation 114
4.1 Interaction of Tearing Mode with Resonant Magnetic Perturbation117
4.2 Plasma Equation of Toroidal Angular Motion Equation 119
4.3 No-slip constraint 119
4.4 Normalized Plasma Equation of Toroidal Angular Motion . . . 120
4.4.1 Solution of Normalized Plasma Equation of Toroidal Angular Motion 121
4.5 Torques 123
4.5.1 Electromagnetic Braking Torque 123
4.5.2 Viscous Restoring Torque 126
4.5.3 Toroidal torque balance 126
4.5.3.1 Time-Independent 128
4.5.3.2 Time-Dependent 129

4.6 Magnetic Island Phase Evolution 130
4.7 Magnetic Island Width Evolution 132
4.8 Time-averaged Normalized Toroidal Net Torque 134
4.9 Bifurcation theory 136

Chapter 5. Summary and Conclusion **141**

Appendices **147**

Appendix A. Derivation of the Grad-Shafranov Equation **148**
A.1 Derivation 148
A.2 Discussion 154

Appendix B. Poloidal Equations **155**
B.1 Plasma Equation of Poloidal Angular Motion 155
B.2 Normalized Plasma Equation of Poloidal Angular Motion . . . 156
B.2.1 Solution of Normalized Plasma Equation of Poloidal Angular Motion 157
B.3 Slip Frequency 158
B.4 Torques 159
B.4.1 Poloidal Electromagnetic Torque 159
B.4.2 Poloidal Viscous Torque 160
B.5 Magnetic Island Evolution Equations 160
B.6 Complete Equations 163

Bibliography **169**

Vita **176**

List of Figures

1.1 Change in average surface temperature (a) and change in average precipitation (b) based on multi-model mean projections for 2081-2100 relative to 1986-2005 3

1.2 Tokamak magnetic field and current 9

1.3 Schematic drawing of ITER 11

2.1 A reconnecting magnetic field configuration. Adopted from Fitzpatrick, *Plasma Physics: An Introduction* [17] 52

2.2 Generalized sheared magnetic field $\mathbf{B}_0 = B_{0y}(x)\hat{\mathbf{y}}+B_{0z}\hat{\mathbf{z}}$. Shown here are the magnetic field $\mathbf{B}$ and its components $B_{0y}\hat{\mathbf{y}}, B_{0z}\hat{\mathbf{z}}$. Note that we have oriented the y and z axes in such a way that $B_{0y}(x = 0) = 0$. Adopted from Ref. [50] 55

2.3 Magnetic field lines in the vicinity of a magnetic island. Adopted from Fitzpatrick, *Plasma Physics: An Introduction* [17] 72

3.1 Phase-space evolution of the reconnected flux induced in a rotating tokamak plasma by a resonant error-field in the linear response regime. 89

3.2 Evolution of magnetic island width in the linear response regime. 90

3.3 Evolution of electromagnetic torque in the linear response regime. 91

3.4 Solutions of the time-asymptotic torque-balance equation in the linear response regime. 95

3.5 Phase-space evolution of the reconnected flux induced in a rotating tokamak plasma by a resonant error-field in the nonlinear response regime. 102

3.6 Evolution of magnetic island width in the nonlinear response regime. 104

3.7 Evolution of electromagnetic torque in the nonlinear response regime. 105

3.8 Solutions of the time-asymptotic torque-balance equation in the nonlinear response regime. 111

[...] Ποιὸς ἀλήθεια ὁ κόσμος ποὺ
ὑπερέχει
ποιὸ τὸ ‘νῦν’ καὶ ποιὸ τὸ ‘αἰὲν’
τοῦ κόσμου:
...
Νῦν Νῦν τὸ μηδέν
καὶ ΑΙΕΝ Ο ΚΟΣΜΟΣ Ο
ΜΙΚΡΟΣ, Ο ΜΕΓΑΣ!

Odysseas Elytis, *The Axion Esti*

Chapter 1

Introduction

1.1 The Growing Demand for Energy in a Warming World

Global warming is a fact. Many of the observed changes in the century-scale rise in the average temperature of the earth's climate system since the 1950s are unprecedented over tens to thousands of years. On 20 January 2016, NASA scientists reported[1] that earth's 2015 surface temperatures were the warmest since modern record keeping began in 1880, according to independent analyses by NASA and the National Oceanic and Atmospheric Administration (NOAA). Human-made carbon dioxide (CO_2) continues to increase above levels not seen in hundreds of thousands of years; currently, about half of the carbon dioxide released from the burning of fossil fuels is not absorbed by vegetation and the oceans and remains in the atmosphere.

Scientific understanding of global warming is increasing. The Intergovernmental Panel on Climate Change (IPCC), a scientific body under the auspices of the United Nations, reported in 2014 that scientists were more

[1]GISTEMP Team, 2016: GISS Surface Temperature Analysis (GISTEMP). NASA Goddard Institute for Space Studies. Dataset accessed 2016-04-07 at http://data.giss.nasa.gov/gistemp/

than 95% certain that global warming is mostly being caused by increasing concentrations of greenhouse gases (GHG) and other human (anthropogenic) activities [12]. Climate model projections, summarized in the report, indicated that during the 21st century the global surface temperature is likely to rise a further 0.3 to 1.7 °C for their lowest emissions scenario using stringent mitigation, and 2.6 to 4.8 °C for their highest. These findings, illustrated in Fig. 1.1, have been recognized by the national science academies of the major industrialized nations and are not disputed by any scientific body of national or international standing.

Therefore, in the last few decades there has been a discernible change of focus of the global interest towards greater protection of the natural environment. It has become more than evident that the growing need for energy and resources from both the developed and the very populous developing countries has lead to a rapid diminution of global reserves, pollution of the environment, dangerous climate change, and subsequently lowering of the people's quality of life on earth. Discussion of terms like *sustainable development* is frequently in the spotlight, and an increasing number of both public and private investment is being directed to *renewable energy sources* (e.g., photovoltaics, wind farms) as more environmentally friendly. Unfortunately, according to all growth scenarios, mankind's energy needs will keep rising in growing rates since billions of people, particularly in China and India, are covering the distance to the western standards of living, and the planet does not have the "luxury" to undergo a new industrial revolution. Confronting the energy needs of humanity, con-

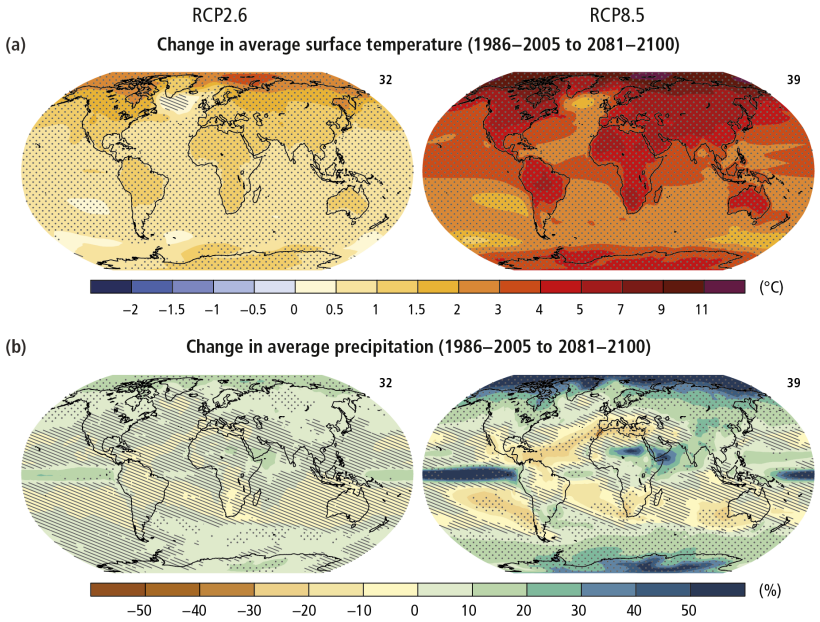

Figure 1.1: Change in average surface temperature (a) and change in average precipitation (b) based on multi-model mean projections for 2081-2100 relative to 1986-2005 under the RCP2.6 (left) and RCP8.5 (right) scenarios. The number of models used to calculate the multi-model mean is indicated in the upper right corner of each panel. Stippling (i.e., dots) shows regions where the projected change is large compared to natural internal variability and where at least 90% of models agree on the sign of change. Hatching (i.e., diagonal lines) shows regions where the projected change is less than one standard deviation of the natural internal variability. Adopted from the IPCC *Climate Change 2014 Synthesis Report* [12]

sidering the exhaustion of the conventional sources (i.e., fossil fuels) as a fact, is expected to be overtaken in the future by applying *controlled thermonuclear fusion* technology in power generation.

1.1.1 The Case for Fusion

Fusion is the fundamental energy source of the universe. It is the process that powers the sun and the stars. In a fusion reaction, energy is released when the nuclei of two light atoms (such as hydrogen) fuse together to form a heavier one. When they combine, a release of energy is expected in accordance with Einstein's formula:

$$E = m\,c^2 \tag{1.1}$$

Tapping into this energy source offers the prospect of a long-term, safe, environmentally friendly option to meet the energy needs of a growing world population. Fusion is a particularly attractive energy solution, as it uses a fuel that is abundant or can be manufactured easily, and it makes generation of large amounts of energy possible. The hydrogen isotopes used are deuterium, which can be readily extracted from sea water (there is around 30 grams of deuterium in every cubic meter of water), and tritium, which can be generated from lithium, an abundant light metal.

In hydrogen atoms the nucleus comprises only one proton. In deuterium the nucleus contains an additional neutron, and in tritium there are two neutrons and one proton. The fusion of one deuterium nucleus with a tritium nucleus results in a new helium nucleus (also known as an alpha particle), a neutron, and energy - lots of it! One gram of fusion fuel could generate 100,000 kWh of electricity - to supply the equivalent power one would need to burn eight metric tons of coal. The extra neutron can be used to generate

more tritium fuel from lithium.

$$D + T \rightarrow {}^{4}_{2}He + n + 17.6\,MeV \tag{1.2}$$

Fusion occurs naturally in the sun at temperatures of 10 - 15 million °C, producing the energy that sustains life on earth. However, in the sun, the fusion fuel is heated and compressed by massive gravitational forces. On earth, we cannot use gravity, so the challenge for fusion researchers is to compensate by heating a lower density plasma to a higher temperature (about 100 million °C, or 10 times hotter than the core of the sun) with excellent thermal insulation to initiate self-sustaining fusion reactions. Fusion reactions occur at high temperatures when the nuclei collide with sufficient energy to overcome the natural repulsive forces of their electrical charges. Such temperatures are well above the threshold at which a gas is completely ionized and becomes a *plasma*, the so-called fourth state of matter. In an ionized plasma, the positively-charged nuclei and negatively-charged electrons of atoms are separated and move about freely like molecules in a gas. More than 99% of our universe exists as plasma.

To reach fusion temperatures, powerful heating is necessary, and heat loss must be kept to a minimum by keeping the hot plasma thermally insulated from the reactor walls - a process known as *confinement*. This is an extremely difficult task, both in terms of understanding the complex physical processes that occur, and the need for sophisticated technologies. Fusion research has developed two different technologies: magnetic confinement and inertial confinement. Magnetic confinement uses strong magnetic fields to provide the

thermal insulation of the plasma, and allows the possibility of steady state operation, whilst inertial confinement uses high-power lasers or ion beams to heat and compress minuscule pellets of fuel to very high density, but only permits ignition for a very brief time period.

Nuclear energy is not broadly considered as environmentally friendly or sustainable. This can be attributed to the nuclear fission reactions currently used to generate electricity (associated with tragic accidents, like the *Fukushima Daiichi* nuclear disaster in 2011) but also to construct weapons of catastrophic power. Nuclear fusion, on the other hand, promises a safe and clean choice for energy generation, and offers the chance for a steady and virtually inexhaustible global energy supply. Several factors make it particularly attractive for large-scale, base-load electricity production:

1. Virtually inexhaustible fuel supply. The basic fuels are distributed widely around the globe. Deuterium is abundant and can be extracted easily from sea water. Lithium, from which tritium can be produced, is a readily available light metal in the earth's crust.

2. No greenhouse gas emissions: Fusion power will not generate gases such as carbon dioxide that are causing growing concern with regard to global warming and other damaging effects on the environment.

3. Suitable for the large-scale electricity production required for the increasing energy needs of modern cities. A fusion power station will generate a large amount of electricity around the clock.

4. Waste from fusion will not be a long-term burden on future generations. Only reactor structures close to the fusion plasma will become irradiated. Any radioactive waste generated will be small in volume and the radioactivity will decay over several decades with the possibility of reuse after about 100 years.

5. The transport of radioactive materials is not required in the day-to-day operation of a fusion power station. The radioactive tritium can be generated and consumed as needed within the reactor.

6. The system has inherent safety aspects. Only very small amounts of fuel are present in the reactor at any one time. Any malfunction results in a rapid shutdown: "runaway" or "meltdown" accidents are impossible as no chain reaction is involved.

7. Very low risk of radioactive emissions to the environment. Extensive safety studies have shown that a fusion power station can be operated without significant risk of radioactive emissions. Even in a worst case accident scenario there would be no need to evacuate the local population.

1.1.2 Magnetic Confinement: The Tokamak

As we have already discussed, nuclear fusion reactions take place at very high temperatures, and the ionized plasma needs to be contained for sufficiently long periods of time in order for outward energy and particle fluxes

to be kept to a minimum. A *tokamak* is a device, the purpose of which is to confine the high-temperature plasma on a set of nested toroidal (donut-shaped) magnetic flux surfaces. The term "tokamak" comes to us from a Russian acronym that stands for "toroidal chamber with magnetic coils" (toroidal'naya kamera s magnitnymi katushkami). Charged particles are forced to follow the magnetic field lines by rapidly circulating around the flux surfaces and "along" the closed magnetic field line loops within the device. Outward diffusion of heat and particles from the core of the plasma towards the outer edge is normally a very slow process, as a consequence of the very small gyroradii of the charged particles.

In a tokamak the main magnetic field is produced in the toroidal direction by a set of coils surrounding a toroidal vacuum vessel. A current flowing through the plasma, in the toroidal direction, provides a further magnetic field in the poloidal direction and heats the plasma; this current is driven by the toroidal electric field induced by means of a transformer. As the current in the primary transformer circuit is ramped up, a varying magnetic flux in the transformer's core is produced, inducing in turn a toroidal electric field in the secondary transformer circuit, i.e., the plasma. This is illustrated in Fig. 1.2.

Even though these concepts will be analyzed in detail in subsequent sections and chapters, let us provide a very brief overview of the mechanism behind instabilities: The combination of the toroidal and poloidal component of the magnetic field results in helical field lines, which form toroidal magnetic flux surfaces. For a plasma in equilibrium (i.e., magnetic pressure is balanced

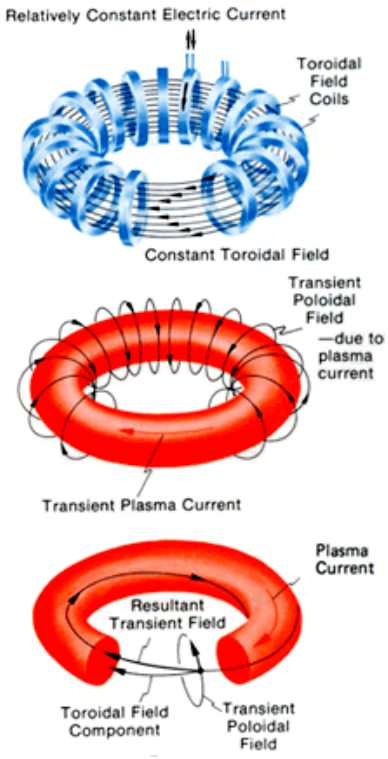

Figure 1.2: Tokamak magnetic field and current. Shown is the toroidal field and the coils (blue) that produce it, the plasma current (red) and the poloidal field produced by it, and the resulting twisted field when these are overlaid. Adopted from the Princeton Plasma Physics Laboratory website

by the plasma pressure), no pressure gradient along field lines is allowed, leading to isobaric magnetic surfaces. As the heat transport along the field lines is very fast, the surfaces are also isothermal. The number of toroidal windings necessary for a field line to complete a poloidal orbit is defined in terms of parameter q, also known as the safety factor. When q is an irrational number, the field line is ergodic, i.e., it covers the entire toroidal surface. For rational values of $q = m/n$, the field line closes upon itself after m toroidal and n

poloidal windings, respectively. These surfaces, in particular at low rational q, are critical with respect to magnetic field perturbations. As a consequence, the magnetic configuration, ideally structured as a set of nested surfaces, is prone to magnetic reconnection phenomena at the aforementioned rational surfaces, resulting generally in a loss of particle and energy confinement. In a tokamak, the toroidal field used to stabilize against MHD instabilities is strong enough to satisfy the Kruskal-Shafranov stability condition which we will refer to later in this chapter. There is a plethora of excellent reviews and textbooks on tokamak experiments, equilibrium, and diagnostics. The reader is strongly encouraged to refer to John Wesson's excellent, comprehensive reference [47].

At present, there are several tokamak reactors devoted to the study of the physics of plasmas located all around the world. However, the most important scientific endeavor of our times is arguably the design and construction of the *International Thermonuclear Experimental Reactor* (ITER) in Cadarache, Southern France: this is an international engineering and research project oriented towards demonstrating the technical and scientific viability of fusion as an energy source. After many delays, which is to be expected in a multinational collaboration, the facility is expected to finish its construction phase in 2019, will start commissioning the reactor that same year, and will initiate plasma experiments in 2020 with full deuterium-tritium experiments starting in 2027. When ITER becomes operational, it will become the largest magnetic confinement plasma physics experiment in use, surpassing the Joint European Torus (situated in Abingdon, Oxfordshire, UK). The first commercial demon-

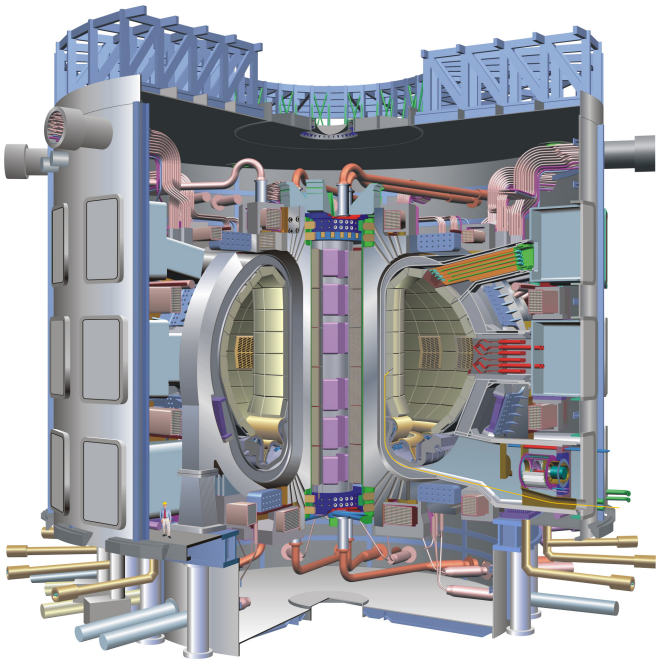

Figure 1.3: Schematic drawing of ITER

stration fusion power station, named DEMO, is proposed to follow on from the ITER project, so, despite the anecdotal nature of the well-known adage, commercial fusion electricity might actually be "50 years down the road".

1.1.3 Outline of this Dissertation

This dissertation is structured as follows:

1. The second half of Chapter 1 is a whirlwind overview of Magnetohydrodynamics (MHD), the theoretical framework of studying plasmas as electrically conducting fluids. The fundamental concept behind MHD is that magnetic fields can induce electrical currents in a moving conduc-

tive fluid, which in turn polarizes the fluid and reciprocally changes the magnetic field itself. The set of equations that describe MHD is a combination of the Navier-Stokes equations of fluid dynamics and Maxwell's equations of electromagnetism. These differential equations must be solved simultaneously, either analytically or numerically.

2. The theory of tearing modes, their topological properties and temporal evolution both in the linear and nonlinear regimes, are extensively discussed in Chapter 2.

3. Chapter 3 is where the groundwork of Resonant Magnetic Perturbation Response Theory is laid: a general analysis of the constant-ψ, resistive MHD theory of the response of a rotating, quasi-cylindrical tokamak plasma to an error-field, as well as the investigation of bifurcations between dynamically stable solution branches of the torque-balance equation.

4. In Chapter 4, the focus will be shifted to an exhaustive investigation of the braking and locking of tearing mode rotation by the interaction of the mode with resonant magnetic perturbations.

5. Finally, in Chapter 5, conclusions and perspectives considered in the thesis are summarized.

6. Supplementary information, such as the consideration of often negligible poloidal equations, is presented in the Appendices.

1.2 Introduction to Magnetohydrodynamics

Magnetohydrodynamics (MHD) is the macroscopic theory of electrically conducting fluids, providing a powerful and practical theoretical framework for describing both laboratory and astrophysical plasmas. It was developed by the Swedish electrical engineer and plasma physicist *Hannes Alfvén*, who won the 1970 Nobel Prize in Physics for this achievement. Our goal is to present a basic overview of this theory, in order to create the necessary framework for the study of resistive instabilities. For this Chapter, Professor Michael Coppins of *Imperial College London* has graciously allowed the use of his MHD Lecture notes from the 2012 *Culham Plasma Physics Summer School* [11].

For a plasma, the MHD approximation can be derived in a systematic manner by taking moments of the kinetic equations for ions and electrons, as done for instance by Braginskii [8]. MHD describes phenomena with length scales L, timescales τ and velocities V, where:

1. $L \gg \lambda_D$ (Debye length), which is an expression of the quasineutrality condition, i.e. charge density $\rho_q = 0$.

2. $L \gg r_L$ (average ion Larmor radius), which allows us to neglect some terms in Ohm's Law.

3. $\tau \gg$ ion-electron equilibration time, which allows us to use a *scalar* pressure $p = p_i + p_e$,

4. $V \ll c$, which allows us to neglect displacement current in Ampère's Law.

Phenomena described by magnetohydrodynamics are *macroscopic* (large-scale) and *slow* (low-frequency). However, in fact, MHD is routinely used in situations where some of the approximations are not valid, and the popularity of the theory can be attributed to:

1. The simplicity of the model. It is the simplest mathematical description of a conducting fluid interacting with a magnetic field. More sophisticated models are very hard to solve.

2. The ubiquity of MHD phenomena. The phenomena described by MHD are found experimentally to approximate closely to particularly important aspects of real plasma behavior, e.g., field line freezing, Alfvén waves, MHD equilibria, and MHD instabilities.

1.2.1 The MHD Equations

The equations governing MHD phenomena are:

$$\frac{\partial \rho}{\partial t} + \nabla \cdot (\rho\, \mathbf{v}) = 0, \qquad \text{(Continuity)}$$

$$\rho \left(\frac{d\mathbf{v}}{dt} \right) = -\nabla p + \mathbf{j} \times \mathbf{B}, \qquad \text{(Momentum)}$$

$$\frac{d}{dt} \left(\frac{p}{\rho^{\gamma}} \right) = 0, \qquad \text{(Internal Energy)}$$

$$\mathbf{E} + \mathbf{v} \times \mathbf{B} = \eta\, \mathbf{j}, \qquad \text{(Ohm's Law)}$$

$$\frac{\partial \mathbf{B}}{\partial t} = -\nabla \times \mathbf{E}, \qquad \text{(Faraday's Law)}$$

$$\mu_0\, \mathbf{j} = \nabla \times \mathbf{B}, \qquad \text{(Ampère's Law)}$$

$$\nabla \cdot \mathbf{B} = 0, \qquad \text{(Gauss' Law)}$$

where the variables appearing in the above system of equations are:

1. Mass density $\rho = n_e\, m_e + n_i\, m_i \simeq n\, m_i$. Here, we assume quasineutrality ($n_e = n_i = n$), and neglect electron mass ($m_e \to 0$).

2. Fluid velocity $\mathbf{v}$

3. Pressure $p = p_e + p_i = n_e\, k_B\, T_e + n_i\, k_B\, T_i$,. This reduces to $p = 2\, n\, k_B\, T$, since we assume equal temperatures for the electrons and ions. Recall that MHD describes slow phenomena, therefore the electron-ion energy equilibration time is long compared to the momentum exchange time. This implies $T_i \simeq T_e = T/2$ [20].

4. The ratio of specific heats γ, which assumes the value $5/3$ for an adiabatic equation of state. This equation of state is only applicable in the absence

of shocks, because it assumes that the entropy of a fluid element does not change.

5. Electric current density $\mathbf{j}$, electric field $\mathbf{E}$, and magnetic field $\mathbf{B}$.

6. Convective derivative $\dfrac{d}{dt} = \left(\dfrac{\partial}{\partial t} + \mathbf{v}\cdot\nabla\right)$, which is the rate of change following a fluid element.

The continuity equation, $\partial\rho/\partial t + \nabla\cdot(\rho\,\mathbf{v}) = 0$, is an exact moment of the kinetic equation. It assumes conservation of mass, i.e., no sources or sinks within the fluid. An alternative form of the continuity equation is $d\rho/dt = -\rho\nabla\cdot\mathbf{v}$. The fluid will be assumed to be *incompressible*, i.e., the density ρ of each fluid element is constant, or $\nabla\cdot\mathbf{v} = 0$.

The momentum equation is the equation of motion in our model. Very few approximations are needed to obtain this from the exact moment of the kinetic equation. Let us consider the force balance for a fluid element of volume δV and mass $\rho\,\delta V$. The inertial term is

$$\rho\,\delta V\,\frac{d\mathbf{v}}{dt} \equiv \rho\,\delta V\left[\frac{\partial\mathbf{v}}{\partial t} + (\mathbf{v}\cdot\nabla)\,\mathbf{v}\right] \tag{1.3}$$

The acceleration is caused by the total force on the fluid element consisting of the following parts:

1. The thermal pressure force. Assuming conditions close to local thermodynamic equilibrium, the pressure tensor is isotropic, exerting the force

$$-\oint p\,d\mathbf{F} = -\delta V\,\nabla p, \tag{1.4}$$

where the integral is over the surface of the volume element, and $d\mathbf{F} = \hat{\mathbf{n}}\, dF$ is the surface element.

2. The magnetic force. The force on a particle of charge q_i is the Lorentz force, $q_i\,(\mathbf{E} + \mathbf{v} \times \mathbf{B})$. Thus, the force on a macroscopic fluid element is the sum of the forces acting on its individual particles, $\delta q\,\mathbf{E} + \delta\mathbf{j} \times \mathbf{B}$, where δq is the net charge, and $\delta\mathbf{j}$ is the electric current carried by the fluid element. Due to the quasineutrality condition, $\delta q \simeq 0$, and the magnetic force is the macroscopic Lorentz force, $\delta V\,\mathbf{j} \times \mathbf{B}$.

3. The gravitational force: $\delta V\,\rho\,\mathbf{g} = -\,\delta V\,\rho\,\nabla\phi_g$, where ϕ_g is the gravitational potential. While this force is negligible in laboratory plasmas, it may play an important role in astrophysical systems.

Thus, the force balance equation becomes

$$\rho\left[\frac{\partial \mathbf{v}}{\partial t} + (\mathbf{v}\cdot\nabla)\,\mathbf{v}\right] = -\,\nabla p + \mathbf{j} \times \mathbf{B} - \rho\nabla\phi_g, \tag{1.5}$$

where the gravitational force term is usually omitted.

There is a need for many approximations in order to obtain the internal energy equation from the exact moment of the kinetic equation. The mass density, $\rho\,(\mathbf{x}, t)$, obeys the continuity equation which follows from mass conservation. No assumption about the relation between mass and charge is implied, concerning the kind and number of charge carriers, (i.e., the degree of ionization in the plasma), except for the *quasineutrality* condition - requirement that positive and negative charges balance within each macroscopic fluid

element. The pressure, $p(\mathbf{x}, t)$, contains the thermodynamic properties of the fluid. A plasma follows approximately the ideal gas law, $p = (n_i + n_e)\, k_B\, T = (R/\mu)\, \rho\, T$, where $n_{i,e}$ are the number densities of ions and electrons, k_B is Boltzmann's constant, $R = c_p - c_v$ is the difference of specific heats, and μ is the mean atomic weight ($\mu \simeq 1/2$ in a hydrogen plasma). In the MHD approximation, variations of the thermodynamic state are assumed to be sufficiently fast, and on sufficiently large spatial scales, that dissipation effects, particularly heat conduction, are negligible. Thus, changes of state are considered to be *adiabatic* (i.e., $p\, V^{\gamma} =$ constant for a fluid element), which can be written as

$$\frac{d}{dt}\left(\frac{p}{\rho^{-\gamma}}\right) = 0. \tag{1.6}$$

This implies that

$$\frac{\partial p}{\partial t} + \mathbf{v} \cdot \nabla p + \gamma\, p\, \nabla \cdot \mathbf{v} = 0,$$

where $\gamma = c_p/c_v$ is the ratio of the specific heats, which assumes the value $5/3$ for an adiabatic equation of state, as we have mentioned. This energy equation is only applicable in the absence of shocks, because it assumes that the entropy of a fluid element does not change.

As we have already seen, a very useful limiting case, valid for fluid velocities slow compared to the propagation speed of compressional waves, is that of incompressibility, i.e.,

$$\nabla \cdot \mathbf{v} = 0 \tag{1.7}$$

In this case, the density of a fluid element remains constant, and without much loss of generality, we can assume a *homogeneous density distribution*

that can be normalized such that $\rho = 1$. Condition (1.7) does not, however, imply that the pressure too is only advected, as Eq. (1.6) might suggest, since incompressibility corresponds to $\gamma \to \infty$. In fact, the pressure is no longer an independent dynamic variable, but it is determined by the nonlinear terms in the force balance equation (1.5), the divergence of which yields *Poisson's Equation* for ρ. The incompressibility limit is particularly suitable for high-density fluids such as liquid metals, where the equation of state differs from the ideal gas law, but since the sound velocity is usually much higher than the flow speeds, these properties do not enter the flow dynamics. In the following, we will consider either the case of fully compressible fluids with $\gamma = 5/3$, or the case of incompressibility, assuming homogeneous density in the latter.

Ohm's Law can be obtained from the exact moment equation after many approximations. The dynamics of the magnetic field follows from Faraday's Law. In order to express the electric field in terms of known quantities, a Galilean transformation (i.e., the non-relativistic limit of a Lorentz transformation) is performed:

$$\mathbf{x}' = \mathbf{x} - \mathbf{V}\,t, \quad t' = t.$$

Ampère's Law and Faraday's Law transform in the following way:

$$\nabla' \times \mathbf{B}' = \mu_0\,\mathbf{j}', \tag{1.8}$$

$$\frac{\partial \mathbf{B}'}{\partial t'} = -\nabla' \times \mathbf{E}', \tag{1.9}$$

where $\mathbf{B}' = \mathbf{B}$ and $\mathbf{E}' = \mathbf{E} + \mathbf{V} \times \mathbf{B}$. In a fluid element with a velocity $\mathbf{V}$ at time t, the velocity vanishes in the transformed system. For a fluid at

rest, however, Ohm's Law in the simplest case, $\mathbf{E}' = \eta\,\mathbf{j}$, η being the electrical resistivity, indicates that the electric field vanishes, $\mathbf{E}' = 0$ (i.e., stationary perfect conductor), neglecting dissipative effects for the moment. Hence, in the laboratory frame we have $\mathbf{E} = -\,\mathbf{V} \times \mathbf{B}$. Performing this transformation for each fluid element, we may replace the uniform transformation velocity $\mathbf{V}$ by the actual fluid velocity $\mathbf{v}\,(\mathbf{x}, t)$. This is how, for an infinitely conducting fluid we retrieve the *ideal MHD* Ohm's Law: $\mathbf{E} + \mathbf{v} \times \mathbf{B} = 0$.

In magnetized plasmas resistivity is actually anisotropic, but in the framework of MHD it is usually assumed that η is just a scalar constant. Fusion plasmas are very good conductors: $\eta \sim 10^{-9}\,\Omega\mathrm{m}$ (*cf.* copper: $\eta \sim 1.7 \times 10^{-8}\,\Omega\mathrm{m}$).

Other equations are *implicit* in MHD:

1. Charge conservation: $\partial\rho_q/\partial t + \nabla \cdot \mathbf{j} = 0$. In MHD $\rho_q = 0$, which yields $\nabla \cdot \mathbf{j} = 0$, but this is implicit in the MHD form of Ampère's Law:

$$\nabla \cdot \mathbf{j} = \frac{1}{\mu_0} \nabla \cdot (\nabla \times \mathbf{B}) = 0 \tag{1.10}$$

2. Gauss's Law: $\nabla \cdot \mathbf{B} = 0$ for the non-existence of magnetic monopoles. Faraday's Law implies:

$$\frac{\partial}{\partial t}\,(\nabla \cdot \mathbf{B}) = \nabla \cdot \frac{\partial \mathbf{B}}{\partial t} = -\,\nabla \cdot (\nabla \times \mathbf{E}) = 0, \tag{1.11}$$

   i.e., if $\nabla \cdot \mathbf{B} = 0$ initially then it stays zero.

Substituting Ohm's Law and Ampère's Law into Faraday's Law, we yield the following expression for the evolution of the magnetic field (MHD induction equation):

$$\frac{\partial \mathbf{B}}{\partial t} = \nabla \times (\mathbf{v} \times \mathbf{B}) + \frac{\eta}{\mu_0} \nabla^2 \mathbf{B} \tag{1.12}$$

The convection of the magnetic field by the plasma flow is described by the first term on the right hand side of Eq. (1.12), whereas the second term describes diffusion. When the first term is dominant, the magnetic flux is *frozen into* the the plasma, and the topology of the magnetic field does not change. On the other hand, when the diffusive term is not negligible, the topology of the magnetic field is free to change. The relative magnitude of the two terms on the right-hand side of the magnetic field evolution equation, Eq. (1.12), is conventionally measured in terms of the *Lundquist number*:

$$S \equiv \frac{\mu_0 \, v_A \, L}{\eta}, \tag{1.13}$$

which is the dimensionless ratio of an Alfvén wave crossing timescale to a resistive diffusion timescale. Here, v_A is the Alfvén velocity, and L is the characteristic length scale of the plasma. If $S \gg 1$, then convection dominates and the frozen flux condition prevails, whereas, in the opposite limit, diffusion dominates, and the coupling between the plasma flow and the magnetic field is weak.

In a tokamak the condition $S \gg 1$ is typically satisfied, which leads to the conclusion that, in *most* parts of the plasma, resistivity plays no role, and the plasma can be treated as a perfectly conducting fluid. In this limit, the resistive model described above reduces to ideal MHD, where $\eta \to 0$. However, in a *resistive layer*, where the tearing mode instability occurs, the effect of the magnetic diffusion is responsible for the *magnetic reconnection* of the field lines. In this case, the ideally stable magnetic topology is modified, leading to a new equilibrium with a lower magnetic energy.

1.3 MHD Equilibria

Slowly varying magnetically confined plasma configurations are of fundamental interest. They are usually well approximated by magnetostatic equilibria. The archetypical plasma configurations are one-dimensional: the sheet pinch and the cylindrical pinch. Even though these systems are highly idealized, they exhibit many features of real systems. The study of *cylindrical equilibria* is particularly useful; many plasma configurations are approximately cylindrical, and such configurations may be idealized as cylinders of perfectly circular cross-section which are long enough that end effects can be neglected. Such equilibria are one-dimensional: properties vary with r, but are independent of θ and z in the cylindrical coordinate system. Special cases of cylindrical equilibria are the Θ-*pinch* and the Z-*pinch*.

1.3.1 Force Balance and β

Let us recall the MHD equation of motion (force balance equation):

$$\rho \frac{\partial \mathbf{v}}{\partial t} + \rho (\mathbf{v} \cdot \nabla) \mathbf{v} = -\nabla p + \mathbf{j} \times \mathbf{B} \tag{1.14}$$

The rightmost term, $\mathbf{j} \times \mathbf{B}$, can be written as a sum of two constituent terms:

$$\mathbf{j} \times \mathbf{B} \equiv \nabla \left(\frac{B^2}{2\mu_0} \right) + \frac{(\mathbf{B} \cdot \nabla) \mathbf{B}}{\mu_0}, \tag{1.15}$$

where the first term corresponds to *magnetic pressure*, and the second term corresponds to *magnetic tension*. A naïve, simple requirement for magnetic confinement in fusion is that we want the plasma to "sit quietly" in the reactor. Hence, the plasma must be in *force balance*. We will focus on magnetostatic plasma configurations with *steady flows*: $\partial/\partial t \to 0$. In this case:

$$\rho (\mathbf{v} \cdot \nabla) \mathbf{v} + \nabla p = \mathbf{j} \times \mathbf{B} \tag{1.16}$$

The $\rho (\mathbf{v} \cdot \nabla) \mathbf{v}$ term varies as $\rho v^2/L$ and the $\mathbf{j} \times \mathbf{B}$ term varies as $j B \sim B^2/\mu_0 L$. The ratio of these two terms is v^2/v_A^2, where $v_A = \sqrt{B^2/\mu_0 \rho}$ is the Alfvén velocity. Usually $v \ll v_A$, thus, one can neglect flows in the force balance equation, and obtain the standard MHD force balance criterion:

$$\nabla p = \mathbf{j} \times \mathbf{B} \tag{1.17}$$

The formal simplicity of this equation is deceptive; the existence of strict solutions has only been shown for axisymmetric systems, while in the general non-axisymmetric case equilibria seem to exist only in an approximate sense.

There is a further simplification of the force balance equation, known as the *force-free configuration*; $\mathbf{v} \to 0$, $p \to 0$ which leads to $\mathbf{j} \times \mathbf{B} = \mathbf{0}$, i.e., a current-carrying plasma in which $p \ll B^2/2\,\mu_0$. Such configurations are important in space, e.g. the sun's corona.

A convenient measure of the plasma pressure is given by the *plasma beta (β)*, which is defined as the ratio of thermal pressure to magnetic pressure:

$$\beta \equiv \frac{2\,\mu_0\,p}{B^2} \tag{1.18}$$

Beta is also a measure of the efficiency of magnetic confinement in a fusion device. It is normally measured in terms of the total magnetic field. However, in any real-world design, the strength of the field varies over the volume of the plasma, so to be specific, the average beta is sometimes referred to as the "beta toroidal". In tokamak design, the total field is a combination of the external toroidal field and the current-induced poloidal field, so the "beta poloidal" is sometimes used to compare the relative strengths of these fields. Finally, because the external magnetic field is the driver of reactor cost, "beta external" is used to consider just this contribution.

1.3.2 Magnetic Flux Surfaces

An important concept in the context of MHD Equilibrium is the *flux surface*, which is a surface such that $\mathbf{B}$ is everywhere perpendicular to its normal. More formally, a given smooth surface S with normal $\hat{\mathbf{n}}$ is a *flux*

surface of a smooth vector field $\mathbf{B}$ when:

$$\mathbf{B} \cdot \hat{\mathbf{n}} = 0 \tag{1.19}$$

everywhere on S. In other words, the magnetic field does not cross the surface S anywhere, i.e., the magnetic flux traversing S is zero and the "number" of magnetic field lines inside is the same everywhere. It is then possible to define a scalar flux function f, such that its value is constant on the surface S, and

$$\mathbf{B} \cdot \nabla f = 0 \tag{1.20}$$

The force balance equation implies that p is constant along any magnetic field line (since $\mathbf{B} \cdot \nabla p = 0$), which is an expression of the underlying assumption that transport along the magnetic field lines is much faster than transport perpendicular to it. The force balance equation also implies that the surface $p =$ constant is a flux surface (assuming flux surfaces exist). Also: $\mathbf{j} \cdot \nabla p = 0$, which means that p is constant along lines of $\mathbf{j}$ as well.

Magnetically confined plasmas can be pictured as a set of nested flux surfaces. Pressure is uniform over each surface but it varies from one surface to another, and the innermost surface is just a line: the *magnetic axis*. $\mathbf{j}$ and $\mathbf{B}$ lines lie on flux surfaces, but j and B are not necessarily uniform over the surface; the field lines might be closer together in some places. We will revisit flux surfaces when we discuss toroidal equilibria.

1.3.3 Cylindrical Equilibria: The Z-pinch

As we have already mentioned, an important one-dimensional equilibrium is the *cylindrical pinch*. Let $\mu_0 = 1$ for simplicity in this discussion. The equilibrium quantities are

$$p(r) \quad \text{and} \quad \mathbf{B} = [0,\, B_\theta(r),\, B_z(r)]\,. \tag{1.21}$$

Following the force balance equation:

$$\frac{dp}{dr} = j_\theta\, B_z - j_z\, B_\theta \tag{1.22}$$

The plasma confinement is, in general, due to both poloidal and axial currents. Special cases, interesting primarily for historical reasons, are $B_\theta = j_z = 0$, called the Θ-*pinch*, since the current flows in the θ-direction, and $B_z = j_\theta = 0$, called the Z-*pinch*, since the current flows in the z - direction. We will briefly discuss the Z-pinch.

The Z-pinch is the simplest magnetic confinement configuration: it is effectively a long, straight wire made of plasma. There are no external coils, and the only magnetic field is due to the current in the plasma. The force balance equation can be written as:

$$\frac{d}{dr}\left(p + \frac{B_\theta}{2\,\mu_0}\right) = -\,\frac{B_\theta^2}{\mu_0\, r}, \tag{1.23}$$

where the right hand side of the equation corresponds to the radially inward force due to magnetic tension, i.e., the *pinch effect*, discovered by Pollock and Barraclough in 1905, and, independently, in 1907 by Edwin Northrup [35].

The simplest theoretical Z-pinch is one in which current flows in an infinitely narrow layer on the surface (skin current):

$$B_\theta = \begin{cases} 0, & r < a \\ \dfrac{\mu_0 I}{2\pi r}, & r > a \end{cases} \tag{1.24}$$

In the plasma $\mathbf{j} = \mathbf{0} = \nabla p$. This is an example of a plasma configuration, in which there is a discontinuity in the magnetic field due to a current layer. The plasma/vacuum boundary condition is

$$p = \frac{B^2_{(r=a)}}{2\,\mu_0} = \frac{\mu_0\, I^2}{8\pi^2\, a^2}, \tag{1.25}$$

since $B_{(r=a)} = \mu_0\, I/2\pi\, a$. From the ideal gas law, $p = 2\, n\, k_B\, T$, we obtain $\mu_0\, I^2 = 8\pi^2\, a^2\, p$ and the *Bennett relation* [4]:

$$\mu_0\, I^2 = 16\pi\, N\, k_B\, T, \tag{1.26}$$

where $N = n\,\pi\, a^2$ is the line density, or the number of ions or electrons per unit length. In a steady-state Z-pinch the current and magnetic field would have resistively diffused throughout the plasma. However, the Bennett relation still applies to any Z-pinch equilibrium surrounded by vacuum.

Unfortunately, despite its simplicity, the Z-pinch has two major drawbacks as a magnetic confinement device for fusion:

1. It has ends: the plasma current is produced by applying a large potential difference between electrodes, and there are large energy losses to the ends.

2. It is highly susceptible to MHD instabilities.

1.3.4 Toroidal Equilibria

An ideal magnetically confined plasma would be bounded by a *closed* flux surface, unlike the open flux surfaces of the Z-pinch (which ends on electrodes).

As we have seen, magnetic field-lines lie on flux surfaces, i.e., $\mathbf{B}$ is everywhere tangential to the surface. According to the *Poincaré-Hopf theorem* (colloquially known as the *hairy ball theorem*): "*you can't comb a hairy ball flat without creating a cowlick*", or, more formally, there is no non-vanishing continuous vector field tangential to a sphere. Therefore, it is impossible to have a spherical flux surface. But, luckily, there is no "hairy donut" theorem! As a matter of fact, in three dimensions, the only closed flux surface corresponding to a non-vanishing vector field is a *topological toroid*. This fact lies at the basis of the design of magnetic confinement devices.

Assuming the flux surfaces have this toroidal topology, the flux function f defines a set of nested surfaces, so it makes sense to use this function to label the flux surfaces, i.e., f may be used as a "radial" coordinate. Each toroidal surface f encloses a volume $V(f)$. The surface corresponding to an infinitesimal volume V is essentially a line that corresponds to the toroidal axis (called magnetic axis when B is a magnetic field).

The flux F through an arbitrary surface S is given by

$$F = \int_S \mathbf{B} \cdot \hat{\mathbf{n}}\, dS. \tag{1.27}$$

When B is a magnetic field with toroidal nested flux surfaces, the magnetic field lines are helices on these surfaces, and two magnetic fluxes can be defined from two corresponding surfaces:

1. The *poloidal flux* is defined as $\psi = \int_{S_p} \mathbf{B} \cdot \hat{\mathbf{n}}\, dS$, where S_p is a ring-shaped ribbon, stretched between the magnetic axis and the flux surface f. (Complementarily, S_p can be taken to be a surface spanning the central hole of the torus [7]).

2. Likewise, the *toroidal flux* is defined by $\phi = \int_{S_t} \mathbf{B} \cdot \hat{\mathbf{n}}\, dS$, where S_t is a poloidal section of the flux surface.

It is common to use ψ or ϕ to label the flux surfaces instead of the unphysical label f.

A very useful quantity characterizing the magnetic field line twist is the *rotational transform,* ι, or its inverse, called the *safety factor,* q, commonly used in tokamak physics:

$$q(r) = \iota^{-1}(r) = \frac{r\, B_z(r)}{R\, B_\theta(r)}, \tag{1.28}$$

where ι is the angle by which a field line is rotated in poloidal direction when advancing by a distance R in the axial direction. The dependence of ι or q on r indicates how the field line twist varies between different surfaces of $r =$ const., a quantitative measure being the *shear parameter*,

$$s(r) = \frac{d \ln q}{d \ln r}. \tag{1.29}$$

All field lines on a given flux surface have the same q (otherwise, field lines would cross), but q varies from one surface to another.

In three dimensions (as opposed to the effectively two-dimensional axisymmetric situation), the existence of flux surfaces (nested or not) is not guaranteed [23]. Assuming an initial situation with nested magnetic surfaces, the rotational transform of the field line on the surface may either be *irrational* so that the field line covers the surface entirely (ergodically), or *rational*. In the latter case, the field line does not cover a surface but constitutes a one-dimensional structure ($q = m/n$, where m and n are integers: the field line meets up on itself after m toroidal and n poloidal rotations). Physically, a rational surface is sensitive to small perturbations, and flute-like instabilities may develop that lead to the formation of magnetic islands, and stochastic regions (assuming non-zero resistivity). Since the field line trajectories are described by Hamiltonian equations, the KAM theorem is relevant.

For a large aspect-ratio torus we can "open out" the flux surface to make a cylinder of length $2\pi R_0$ and radius (distance from magnetic axis) r. Opening that out we get a rectangle of sides $2\pi R_0$ and $2\pi r$. Thus, the ratio of toroidal to poloidal magnetic field is

$$\frac{B_\phi}{B_\theta} = \frac{q\, 2\pi R_0}{2\pi r}, \tag{1.30}$$

giving

$$q(r) = \frac{r B_\phi(r)}{R_0 B_\theta(r)}. \tag{1.31}$$

It should be noted that the force balance equation does not describe any detail on scales smaller than the gyroradius. In combination with the existence of stochastic field regions, this means that the concept of flux surface can only be approximate, and not exact. Furthermore, the force balance equation depends on a number of assumptions, such as that of static equilibrium, whereas fusion-grade plasmas are clearly strongly driven systems far from equilibrium. Nevertheless, ideal MHD equilibrium theory is extremely useful for the description and understanding of magnetically confined plasmas.

1.3.5 The Grad-Shafranov Equation

To obtain geometrically more general equilibria than a one-dimensional pinch, it appears that all we have to do is to deform this configuration into the desired shape. For instance, by bending a cylindrical pinch into a torus, squeezing it into a strongly noncircular cross-section, or applying certain axial corrugations, all of which seem to imply purely quantitative changes. This is, however, not true. Apart from the problem of practical evaluation, which requires rather sophisticated numerical techniques, the transition to higher-dimensional configurations, in general, introduces qualitatively new features, which in the three-dimensional case lead to a basic existence problem. Biskamp [5] presents a very elegant and rigorous consideration of the most general case of two-dimensional equilibrium. However, we are going to follow a different, perhaps more pedagogic, approach to study *axisymmetric toroidal configurations*: the complete, step-by-step derivation of the *Grad-Shafranov* (GS)

equation.

Let us start by mentioning that the historically correct, but impractical, name of this equation should be the *Grad-Lüst-Rubin-Schlüter-Shafranov equation*, since it has been independently derived by Lüst and Schlüter (1957), Shafranov (1958), and Grad and Rubin (1958).

For two-dimensional equilibria, the force-balance equation, $\nabla p = \mathbf{j} \times \mathbf{B}$, can be rewritten as a second order, nonlinear, elliptic, partial differential equation, obtained from the reduction of the ideal MHD equations to two dimensions - often for the case of toroidal axisymmetry (the case relevant in a tokamak):

$$\Delta^* \psi = -\mu_0 R^2 \frac{dp}{d\psi} - \frac{1}{2}\frac{dF^2}{d\psi}, \tag{1.32}$$

where $p(\psi)$ is the pressure, $F(\psi) = R B_\phi$, and the magnetic field and current are, respectively, given by:

$$\mathbf{B} = \frac{1}{R} \nabla\psi \times \hat{\mathbf{e}}_\phi + \frac{F}{R} \hat{\mathbf{e}}_\phi, \tag{1.33}$$

$$\mu_0 \mathbf{j} = \frac{1}{R}\frac{dF}{d\psi} \nabla\psi \times \hat{\mathbf{e}}_\phi - \frac{1}{R} \Delta^* \psi \, \hat{\mathbf{e}}_\phi. \tag{1.34}$$

The *elliptic operator* Δ^* is:

$$\Delta^* \psi \equiv R^2 \nabla \cdot \left(\frac{1}{R^2} \nabla\psi \right) = R \frac{\partial}{\partial R} \left(\frac{1}{R} \frac{\partial \psi}{\partial R} \right) + \frac{\partial^2 \psi}{\partial Z^2} \tag{1.35}$$

The nature of the equilibrium, whether it be a tokamak, reversed-field-pinch, etc., is largely determined by the choices of the two functions, $F(\psi)$ and $p(\psi)$, as well as the boundary conditions. The Grad-Shafranov equation

is rather peculiar because it involves two new functions, ψ and F, and the flux function ψ appears as both an independent and a dependent variable. The full derivation of the Grad-Shafranov equation, including both the outline of the main steps, and the mathematical details is presented in the Appendix.

1.3.6 Shafranov Geometry

It is useful to briefly discuss Shafranov Geometry [24], and the concept of *Shafranov shift*, i.e., the outward radial displacement, $\Delta(r)$, of the center of flux surfaces with minor radius r induced by plasma pressure. Typically, the shift is linear in beta, and it tends to be important for tokamaks, due to the fact that the magnetic configuration is largely, or partly, imposed externally.

As we know, a common axisymmetric toroidal geometry, typical of experimental tokamaks as well as some pinch devices, has a circular boundary in the poloidal plane. The outermost flux surface, effectively determined by interaction with the boundary, can be presumed nearly circular, i.e., circular in poloidal cross-section. In general, the interplay of plasma forces and toroidal curvature will distort interior surfaces away from circularity. This was first note by Shafranov in 1966; for the special case of small plasma pressure and large aspect ratio, the inner flux surfaces remain approximately circular. Shafranov geometry refers to an approximate toroidal equilibrium - a large aspect-ratio, small beta solution to the Grad-Shafranov equation - characterized by nested flux surfaces with circular cross-sections. This is not a cylindrical equilibrium; toroidal curvature is manifested in a relative shift of

the centers of the circles corresponding to different surfaces.

The origin of the Shafranov shift is easily understood: the center of flux surfaces is displaced from the magnetic axis due to the net outward force on the plasma. The flow of current along the toroidal direction in the plasma causes an outward hoop force, which causes expansion in R. In an Ohmic tokamak, the hoop force is substantial and dominates at low beta. As we have seen, pressure is constant along a flux surface, but the area on the outside of a flux surface is larger than the area on the inside, which causes an outward "tire tube" force: a pressurized torus will tend to expand in both minor and major radius, as in the inflation of an unconfined inner tube. Finally, since B_ϕ is larger on the inside of a flux surface, there is a net outward force on the poloidal current.

1.4 Magnetohydrodynamic Instabilities

The macroscopic stability of plasmas in magnetic fields is one of the primary research subjects in the area of controlled thermonuclear fusion, and both theoretical and experimental investigations are being actively pursued. A plasma consists of many moving charged particles, and has many magnetohydrodynamic degrees of freedom, as well as degrees of freedom in velocity space. When a certain mode of perturbation grows, it enhances diffusion. Heating a plasma increases the kinetic energy of the charged particles, but, at the same time, may induce fluctuations in the electric and magnetic fields, which, in turn, augment anomalous diffusion, and lead to loss of confinement [32].

Therefore, it is very important to determine whether any particular perturbed mode is stable (damped mode) or unstable (growing mode). In the stability analysis, it is assumed that the deviation from the equilibrium state is small, so that a *linearized approximation* can be used. We will consider instabilities that can be described by linearized MHD equations. These are called *magnetohydrodynamic instabilities*, or macroscopic instabilities. A general review of MHD instabilities can be found in Ref. [2].

A small perturbation $\mathbf{F}(\mathbf{r}, t)$ of the first order is expanded in terms of its Fourier components:

$$\mathbf{F}(\mathbf{r}, t) = \mathbf{F}(\mathbf{r}) \exp(-i\,\omega\,t), \quad \omega = \omega_r + i\,\omega_i, \tag{1.36}$$

and each term can be treated independently in the linearized approximation. A dispersion relation is solved for ω, and the stability of the perturbation depends on the sign of the imaginary part ω_i: unstable for $\omega_i > 0$, and stable for $\omega_i < 0$. When $\omega_r \neq 0$, the perturbation is oscillatory, and when $\omega_r = 0$, it grows or damps monotonically.

1.4.1 Linearization of Magnetohydrodynamic Equations

Plasma stability problems can be studied by analyzing infinitesimal perturbations from the equilibrium state. All variables are written in the form $x = x_0 + x_1$, where the subscript 0 corresponds to the equilibrium, unperturbed value, and the subscript 1 corresponds to the small perturbation (second order and higher terms will be neglected). Furthermore, the following properties of equilibrium state will be used:

1. Equilibrium is steady-state, i.e., $\partial/\partial t \to 0$ for equilibrium quantities.

2. $\mathbf{v}_0 = 0$.

3. The zeroth-order equations are: $\nabla p_0 = \mathbf{j}_0 \times \mathbf{B}_0$, $\nabla \times \mathbf{B}_0 = \mu_0 \mathbf{j}_0$, $\nabla \cdot \mathbf{B}_0 = 0$.

The process of linearization can be quite tedious due to the presence of many higher-order terms that will eventually get discarded as negligible. Let us demonstrate it for one equation - e.g., the MHD equation of motion - before presenting the full set of linearized MHD equations. Recall that the equation of motion is written as

$$\rho \frac{\partial \mathbf{v}}{\partial t} + \rho \left(\mathbf{v} \cdot \nabla \right) \mathbf{v} = -\nabla p + \mathbf{j} \times \mathbf{B}. \tag{1.37}$$

We will now write all variables (except time) in the form $x = x_0 + x_1$. The equation assumes the rather complicated form:

$$\begin{aligned} &\rho_0 \frac{\partial \mathbf{v}_0}{\partial t} + \rho_0 \frac{\partial \mathbf{v}_1}{\partial t} + \rho_1 \frac{\partial \mathbf{v}_0}{\partial t} + \rho_1 \frac{\partial \mathbf{v}_1}{\partial t} + \\ &\quad + \rho_0 \left(\mathbf{v}_0 \cdot \nabla \right) \mathbf{v}_0 + \rho_1 \left(\mathbf{v}_0 \cdot \nabla \right) \mathbf{v}_1 + \rho_0 \left(\mathbf{v}_1 \cdot \nabla \right) \mathbf{v}_0 + \rho_1 \left(\mathbf{v}_0 \cdot \nabla \right) \mathbf{v}_0 + \\ &\quad + \rho_0 \left(\mathbf{v}_1 \cdot \nabla \right) \mathbf{v}_1 + \rho_1 \left(\mathbf{v}_0 \cdot \nabla \right) \mathbf{v}_1 + \rho_1 \left(\mathbf{v}_1 \cdot \nabla \right) \mathbf{v}_0 + \rho_1 \left(\mathbf{v}_1 \cdot \nabla \right) \mathbf{v}_1 = \\ &\quad = -\nabla p_0 - \nabla p_1 + \mathbf{j}_0 \times \mathbf{B}_0 + \mathbf{j}_0 \times \mathbf{B}_1 + \mathbf{j}_1 \times \mathbf{B}_0 + \mathbf{j}_1 \times \mathbf{B}_1 \end{aligned} \tag{1.38}$$

Taking into account that $\mathbf{v}_0 = 0$, $\nabla p_0 = \mathbf{j}_0 \times \mathbf{B}_0$, and neglecting higher-order terms, Eq. (1.38) assumes the much simpler form:

$$\rho_0 \frac{\partial \mathbf{v}_1}{\partial t} = -\nabla p_1 + \mathbf{j}_0 \times \mathbf{B}_1 + \mathbf{j}_1 \times \mathbf{B}_0. \tag{1.39}$$

Similar procedures yield the set of the first-order, linearized ideal MHD equations:

$$\frac{\partial \rho_1}{\partial t} = -\mathbf{v}_1 \cdot \nabla \rho_0 - \rho_0 \nabla \cdot \mathbf{v}_1, \qquad \text{(Continuity)}$$

$$\rho_0 \frac{\partial \mathbf{v}_1}{\partial t} = -\nabla p_1 + \mathbf{j}_0 \times \mathbf{B}_1 + \mathbf{j}_1 \times \mathbf{B}_0, \qquad \text{(Momentum)}$$

$$\frac{\partial p_1}{\partial t} = -\mathbf{v}_1 \cdot \nabla p_0 - \gamma\, p_0 \nabla \cdot \mathbf{v}_1, \qquad \text{(Internal Energy)}$$

$$\mathbf{E}_1 = -\mathbf{v}_1 \times \mathbf{B}_0, \qquad \text{(Ohm's Law)}$$

$$\frac{\partial \mathbf{B}_1}{\partial t} = -\nabla \times \mathbf{E}_1, \qquad \text{(Faraday's Law)}$$

$$\mu_0 \mathbf{j}_1 = \nabla \times \mathbf{B}_1, \qquad \text{(Ampère's Law)}$$

$$\nabla \cdot \mathbf{B}_1 = 0. \qquad \text{(Gauss' Law)}$$

Eliminating $\mathbf{j}_0$, $\mathbf{j}_1$ and $\mathbf{E}_1$, allows us to write a more elegant and compact set of first-order, linearized MHD equations:

$$\frac{\partial \rho_1}{\partial t} + \nabla \cdot (\rho_0\, \mathbf{v}_1) = 0, \tag{1.40}$$

$$\rho_0 \frac{\partial \mathbf{v}_1}{\partial t} = -\nabla p_1 + \mathbf{j}_0 \times \mathbf{B}_1 + \mathbf{j}_1 \times \mathbf{B}_0, \tag{1.41}$$

$$\frac{\partial p_1}{\partial t} + \mathbf{v}_1 \cdot \nabla p_0 - \gamma\, p_0 \nabla \cdot \mathbf{v}_1 = 0, \tag{1.42}$$

$$\frac{\partial \mathbf{B}_1}{\partial t} = \nabla \times (\mathbf{v}_1 \times \mathbf{B}_0)\,. \tag{1.43}$$

Let us now define the displacement of the plasma from its equilibrium position as

$$\boldsymbol{\xi}\,(\mathbf{r}_0, t) = \mathbf{r} - \mathbf{r}_0 \tag{1.44}$$

The first derivative of that displacement will correspond to a perturbed velocity:

$$\mathbf{r} = \mathbf{r}_0 + \boldsymbol{\xi}, \tag{1.45}$$

giving

$$\mathbf{v} = \frac{d\mathbf{r}}{dt} = \frac{d\mathbf{r}_0}{dt} + \frac{d\boldsymbol{\xi}}{dt} = \frac{\partial \boldsymbol{\xi}}{\partial t} + \mathbf{v} \cdot \nabla \boldsymbol{\xi}, \tag{1.46}$$

since $d\mathbf{r}_0/dt = \mathbf{v}_0 = 0$. Linearizing yields:

$$\mathbf{v}_0 + \mathbf{v}_1 = \frac{\partial \boldsymbol{\xi}}{\partial t} + \mathbf{v}_0 \cdot \nabla \boldsymbol{\xi} + \mathbf{v}_1 \cdot \nabla \boldsymbol{\xi}, \tag{1.47}$$

giving

$$\mathbf{v}_1 = \frac{\partial \boldsymbol{\xi}}{\partial t}, \tag{1.48}$$

where $\mathbf{v}_1 \cdot \nabla \boldsymbol{\xi}$ has been neglected as a higher-order term. Equation (1.43) reduces to

$$\frac{\partial \mathbf{B}_1}{\partial t} = \nabla \times \left(\frac{\partial \boldsymbol{\xi}}{\partial t} \times \mathbf{B}_0 \right). \tag{1.49}$$

Equations (1.40) and (1.42) yield

$$\rho_1 = -\nabla \cdot (\rho_0 \, \boldsymbol{\xi}) \tag{1.50}$$

$$p_1 = \boldsymbol{\xi} \cdot \nabla p_0 - \gamma \, p_0 \nabla \cdot \boldsymbol{\xi} \tag{1.51}$$

Finally, substituting into the equation of motion, (1.41), yields the *linearized equation of motion* in terms of the displacement $\boldsymbol{\xi}$:

$$\rho_0 \frac{\partial^2 \boldsymbol{\xi}}{\partial t^2} = \mathbf{F}(\boldsymbol{\xi}), \tag{1.52}$$

where

$$\begin{aligned} \mathbf{F}(\boldsymbol{\xi}) = \nabla \left(\boldsymbol{\xi} \cdot \nabla p_0 + \gamma \, p_0 \nabla \cdot \boldsymbol{\xi} \right) + \frac{1}{\mu_0} \left(\nabla \times \mathbf{B}_0 \right) \times \nabla \times \left(\boldsymbol{\xi} \times \mathbf{B}_0 \right) + \\ + \frac{1}{\mu_0} \nabla \times \left[\nabla \times \left(\boldsymbol{\xi} \times \mathbf{B}_0 \right) \right] \times \mathbf{B}_0 = \\ = \nabla \left(p_1 + \frac{\mathbf{B}_0 \cdot \mathbf{B}_1}{\mu_0} \right) + \frac{1}{\mu_0} \left[\left(\mathbf{B}_0 \cdot \nabla \right) \mathbf{B}_1 + \left(\mathbf{B}_1 \cdot \nabla \right) \mathbf{B}_0 \right] \end{aligned} \tag{1.53}$$

Solving Eq. (1.52) for a given MHD equilibrium [i.e., given $p_0(\mathbf{r})$, $\mathbf{B}_0(\mathbf{r})$] yields the evolution of the small displacement $\boldsymbol{\xi}(\mathbf{r},t)$. One way to proceed is to consider the boundary conditions, and subsequently solve for $\boldsymbol{\xi}(\mathbf{r},t)$ as an initial value problem. We are going to follow a slightly different, hopefully more intuitive approach.

1.4.2 The MHD Eigenvalue Equation

Let us look for separable solutions of Eq. (1.52), in which all parts of the plasma have the same time evolution:

$$\boldsymbol{\xi}(\mathbf{r},t) = \hat{\boldsymbol{\xi}}(\mathbf{r})\,\Theta(t) \tag{1.54}$$

The operator $\mathbf{F}(\boldsymbol{\xi})$ involves second order spatial derivatives, thus:

$$\rho_0 \frac{\partial^2 \boldsymbol{\xi}}{\partial t^2} = \mathbf{F}(\boldsymbol{\xi}). \tag{1.55}$$

Taking into account the separation of variables we introduced, we obtain

$$\rho_0\,\hat{\boldsymbol{\xi}}\,\frac{\partial^2\Theta}{\partial t^2} = \Theta\mathbf{F}(\hat{\boldsymbol{\xi}}), \tag{1.56}$$

or

$$\frac{1}{\Theta}\frac{\partial^2\Theta}{\partial t^2} = \frac{\left[\mathbf{F}\left(\hat{\boldsymbol{\xi}}\right)\right]_x}{\rho_0\,\hat{\xi}_x} = \frac{\left[\mathbf{F}\left(\hat{\boldsymbol{\xi}}\right)\right]_y}{\rho_0\,\hat{\xi}_y} = \frac{\left[\mathbf{F}\left(\hat{\boldsymbol{\xi}}\right)\right]_z}{\rho_0\,\hat{\xi}_z} = -\,\omega^2 : \text{separation constant.} \tag{1.57}$$

The time part of Eq. (1.55) is:

$$\frac{\partial^2\Theta}{\partial t^2} = -\,\omega^2\,\Theta, \tag{1.58}$$

and the solution takes the form

$$\Theta = \exp\left(-i\,\omega\,t\right).$$

Separable solutions like this one are called *normal modes*; the whole plasma oscillates at a single angular frequency, ω.

The spatial part of Eq. (1.55) is:

$$-\,\rho_0\,\omega^2\,\hat{\boldsymbol{\xi}} = \mathbf{F}(\hat{\boldsymbol{\xi}}). \tag{1.59}$$

This is an *eigenvalue equation*, where ω^2 is the eigenvalue, and $\hat{\boldsymbol{\xi}}$ is the eigenfunction (or eigenmode). We can now write the *ideal MHD linear eigenvalue equation*:

$$\begin{aligned} -\,\rho_0\,\omega^2\,\hat{\boldsymbol{\xi}} = \nabla\left(\hat{\boldsymbol{\xi}}\cdot\nabla p_0 + \gamma\,p_0\nabla\cdot\hat{\boldsymbol{\xi}}\right) + \\ + \frac{1}{\mu_0}\left(\nabla\times\mathbf{B}_0\right)\times\nabla\times\left(\hat{\boldsymbol{\xi}}\times\mathbf{B}_0\right) + \\ + \frac{1}{\mu_0}\nabla\times\left[\nabla\times\left(\hat{\boldsymbol{\xi}}\times\mathbf{B}_0\right)\right]\times\mathbf{B}_0. \end{aligned} \tag{1.60}$$

Equation (1.60) is unfortunately rather complicated, since its spectrum contains continua, and its eigenfunctions do not form a complete basis set. However, the operator $\mathbf{F}$ is *self-adjoint* (Hermitian) [32]. Thus, the eigenvalue ω^2 is *real*, which means that ω is either purely real or purely imaginary. If ω is imaginary, then $\omega = i\,\omega_i$, which implies that $\exp\left(-i\,\omega\,t\right) = \exp\left(\omega_i\,t\right)$, i.e., exponential growth. We will look for solutions of the MHD eigenvalue equation for which ω is imaginary ($\omega^2 < 0$). Such solution represent *instabilities*.

For instance, the resistive tearing instability (tearing mode), which will be the main focus of this dissertation.

It is also important to note that the general discussion of the MHD eigenvalue equation has provided us with an extremely powerful tool; considering special cases for the equilibrium magnetic field $\mathbf{B}_0$, and the eigenfunction $\hat{\boldsymbol{\xi}}$, we can derive the entire gamut of MHD waves as solutions of the dispersion relation for each case.

1.4.3 The Energy Principle

We will now consider a different approach. As we have seen, the eigenvalue problem is complicated, and difficult to solve in general. When we introduce a potential energy associated with the displacement $\boldsymbol{\xi}$, the stability problem can be simplified. From Eq. (1.52), the equation of motion has the general form

$$\rho_0 \frac{\partial^2 \boldsymbol{\xi}}{\partial t^2} = \mathbf{F}(\boldsymbol{\xi}) = -\hat{\mathbf{K}}\,\boldsymbol{\xi}, \tag{1.61}$$

where $\hat{\mathbf{K}}$ is a linear operator. When this equation is integrated over the whole plasma, the equation of energy conservation becomes:

$$\frac{1}{2}\int \rho_0 \left(\frac{\partial \boldsymbol{\xi}}{\partial t}\right)^2 d\mathbf{r} + \frac{1}{2}\int \boldsymbol{\xi}\,\hat{\mathbf{K}}\,\boldsymbol{\xi}\, d\mathbf{r} = \text{const.} \tag{1.62}$$

The *kinetic energy*, T, and the *potential energy*, W, are:

$$T \equiv \frac{1}{2}\int \rho_0 \left(\frac{\partial \boldsymbol{\xi}}{\partial t}\right)^2 d\mathbf{r},$$
$$W \equiv \frac{1}{2}\int \boldsymbol{\xi}\,\hat{\mathbf{K}}\,\boldsymbol{\xi}\, d\mathbf{r},$$

respectively. Accordingly, if $W > 0$ for all possible displacements that satisfy boundary conditions, then the system is stable. This is the stability criterion of the *energy principle* [29]. W is called the *energy integral*. A proof of sufficiency for the Energy Principle as a condition for ideal-MHD stability is that, since energy is conserved, if $W > 0$ for all allowable displacements, then T can not grow exponentially without bound, i.e., the plasma is stable. The proof of necessity is more complicated.

In a normal mode, all parts of the plasma have the same time dependence $\propto \exp(-i\,\omega\,t)$. The frequency or growth rate of a perturbation can be obtained by the energy integral; when the perturbation varies as $\exp(-i\,\omega\,t)$, the equation of motion is

$$\omega^2\,\rho_0\,\boldsymbol{\xi} = \hat{\mathbf{K}}\,\boldsymbol{\xi}. \tag{1.63}$$

The solution of this eigenvalue problem is the same as the solution based on the calculus of variations, $\delta(\omega^2) = 0$, where

$$\omega^2 = \frac{\int \boldsymbol{\xi}\,\hat{\mathbf{K}}\,\boldsymbol{\xi}\,d\mathbf{r}}{\int \rho_0\,\boldsymbol{\xi}^2\,d\mathbf{r}}. \tag{1.64}$$

As $\hat{\mathbf{K}}$ is an Hermitian operator, ω^2 is real. As we have already discussed, in the MHD analysis of an ideal plasma with zero resistivity, the perturbation either increases or decreases monotonically, or else the perturbed plasma oscillates with constant amplitude.

1.5 Normal Modes of Cylindrical Equilibria

We have laid the ground for the basic formulation of magnetohydrodynamic instabilities. The next step is for us to consider a sharp-boundary, cylindrical configuration, since we have already discussed the merit of such MHD equilibria [32]. Our sharp-boundary plasma has radius a, with a longitudinal magnetic field B_{0z} inside the boundary, and a longitudinal magnetic field B_{ez}, and an azimuthal magnetic field $B_\theta = \mu_0 I/(2\pi r)$ outside. Both longitudinal magnetic fields are assumed to be constant. Since the equilibrium is independent of θ and z, eigenfunctions are harmonic functions of θ and z, and the displacement can be written as:

$$\hat{\boldsymbol{\xi}}(r,\theta,z) = \tilde{\xi}(r)\exp(i\,m\,\theta)\exp(i\,k\,z), \tag{1.65}$$

since $\partial/\partial\theta \to i\,m$ and $\partial/\partial z \to i\,k$.

The eigenvalue equation reduces to an one-dimensional, ordinary differential equation for $\tilde{\xi}(r)$. As a matter of fact, any displacement can be expressed as a superposition of such modes as in Eq. (1.65). For the remainder of this section, we will drop the tilde over ξ for simplicity. Since the term in $\nabla\cdot\boldsymbol{\xi}$ in the energy integral is positive, the incompressible perturbation is the most dangerous one. We will examine the most deleterious mode, $\nabla\cdot\boldsymbol{\xi} = 0$. The perturbation of the magnetic field, $\mathbf{B}_1 = \nabla\times(\boldsymbol{\xi}\times\mathbf{B}_0)$, inside the plasma is

$$\mathbf{B}_1 = i\,k\,B_{0z}\,\boldsymbol{\xi}. \tag{1.66}$$

The linearized equation of motion, (1.52) becomes

$$\left(-\omega^2\,\rho_0+\frac{k^2\,B_{0z}^2}{\mu_0}\right)\boldsymbol{\xi}=-\nabla\left(p_1+\frac{\mathbf{B}_0\cdot\mathbf{B}_1}{\mu_0}\right)\equiv\nabla p^* \tag{1.67}$$

As $\nabla\cdot\boldsymbol{\xi}=0$, it follows that $\nabla^2 p^*=0$, i.e., in cylindrical coordinates:

$$\left[\frac{d^2}{dr^2}+\frac{1}{r}\frac{d}{dr}\;-\left(k^2+\frac{m^2}{r^2}\right)\right]p^*(r)=0 \tag{1.68}$$

The solution of Eq. (1.68) without singularity at $r=0$ is given by the *modified Bessel function of the first kind* [1], $I_m(k\,r)$, so that $p^*(r)$ is:

$$p^*(r)=p^*(a)\,\frac{I_m(k\,r)}{I_m(k\,a)}. \tag{1.69}$$

Accordingly:

$$\xi_r(a)=\frac{k\,p^*(a)/I_m(k\,a)}{\omega^2\rho_0-k^2\,B_0^2}\,I'_m(k\,a) \tag{1.70}$$

As the perturbation of the vacuum magnetic field $\mathbf{B}_{1e}$ satisfies $\nabla\times\mathbf{B}=0$ and $\nabla\cdot\mathbf{B}=0$, $\mathbf{B}_{1e}$ is expressed as the gradient of a scalar magnetic potential, $\mathbf{B}_{1e}=\nabla\psi$. This function satisfies $\nabla^2\psi=0$ and $\psi\to 0$, as $r\to\infty$. Thus:

$$\psi=C\,\frac{K_m(k\,r)}{K_m(k\,a)}\exp(i\,m\,\theta+i\,k\,z), \tag{1.71}$$

where $K_m(k\,r)$ is the *modified Bessel function of the second kind* [1]. Taking boundary conditions into account, the *dispersion relation* is written as:

$$\frac{\omega^2}{k^2}=\frac{B_{0z}^2}{\mu_0\rho_0}-\frac{\left[k\,B_{ez}+(m/a)B_\theta\right]^2}{\mu_0\,\rho_0\,k^2}\frac{I'_m(k\,a)}{I_m(k\,a)}\frac{K_m(k\,a)}{K'_m(k\,a)}-\frac{B_\theta^2}{\mu_0\,\rho_0}\frac{1}{(k\,a)}\frac{I'_m(k\,a)}{I_m(k\,a)}. \tag{1.72}$$

The first and second terms represent the stabilizing effect of B_{0z} and B_{ez}, where $K_m/K'_m < 0$. If the propagation vector (axial wavenumber) $\mathbf{k}$ is normal to the magnetic field, i.e., if

$$(\mathbf{k} \cdot \mathbf{B}_e) = kB_{ez} + \frac{m}{a}B_\theta = 0, \tag{1.73}$$

the second stabilizing term of Eq. (1.72) becomes zero, so that a *flute-like* perturbation is dangerous. The third term is destabilizing.

The configuration described by the dispersion relation (1.72) is quite flexible, since it allows us to study different modes (instabilities) that appear for different values of m, the azimuthal mode number, and B_{ez}. For instance, the *sausage instability* for $m = 0$, the *kink instability* for $m = 1$, and other instabilities for $m \geq 2$, in which the plasma looks like a multi-stranded cable.

1.5.1 Kruskal-Shafranov and Suydam Stability Conditions

We will conclude our overview of the theory of Magnetohydrodynamics by introducing a special case of instability, where $|B_{ez}| > |B_\theta|$ in the dispersion relation (1.72). This is going to be a natural segue to tokamak configurations, where $B_\phi > B_\theta$, and also to the study of *resistive tearing modes* which will be the focus of the next chapter of this dissertation.

When $|B_{ez}| \gg |B_\theta|$, the term including $|k\,a| \ll 1$ predominates. Assuming $m > 0$, expanding the modified Bessel function yields:

$$\mu_0\,\rho_0\,\omega^2 = k^2\,B_{0z}^2 + \left(k\,B_{ez} + \frac{m}{a}\,B_\theta\right)^2 - \frac{m}{a^2}\,B_\theta^2. \tag{1.74}$$

Setting the first derivative of ω with respect to k equal to zero, we obtain

$$k\left(B_{0z}^2 + B_{ez}^2\right) + \frac{m}{a} B_\theta B_{ez} = 0 \tag{1.75}$$

In this case ω^2 assumes its minimum value:

$$\omega_{min}^2 = \frac{B_\theta^2}{\mu_0 \rho_0 a^2}\left(\frac{m^2 B_{0z}^2}{B_{ez}^2 + B_{0z}^2} - m\right) = \frac{B_\theta^2}{\mu_0 \rho_0 a^2} m\left(m\frac{1-\beta}{2-\beta} - 1\right), \tag{1.76}$$

where β is the beta parameter, which we introduced in Eq. (1.18). Thus, the plasma is unstable when $0 < m < (2-\beta)/(1-\beta)$. For a low-beta plasma, only the modes $m = 1$ and $m = 2$ become unstable. However, if

$$\left(\frac{B_\theta}{B_z}\right)^2 < (k\,a)^2 \tag{1.77}$$

is satisfied, then the plasma is stable even for $m = 1$, which is a mode that merits special consideration. Usually, the length of the plasma is finite, so that k cannot be smaller than $2\pi/L$, where $2\pi/k$ is the axial wavelength of the helically structured instability, (1.65). Therefore, when

$$\left|\frac{B_\theta}{B_z}\right| < \frac{2\pi\, a}{L}, \tag{1.78}$$

or $q > 1$, where q is the safety factor, the plasma is stable. This is the *Kruskal-Shafranov stability condition* [31, 42].

It is important to note that the discussion above is based on a "skin-current" (or sharp-boundary) model. Analysis of stability for a plasma cylinder with a *distributed* current is much more complicated. In most cases, the plasma current decreases gradually towards the boundary. Such diffuse configurations

are largely determined by the magnetic shear in the plasma volume. For instance, for perturbations with a large m, a sufficient stability criterion can be represented as [45]:

$$r\,B_z^2\left(\frac{\mu'}{\mu}\right)^2 + 8\,\frac{dp}{dr} > 0, \tag{1.79}$$

where $\mu \equiv B_\theta / r\,B_z$ is the pitch number of the magnetic field, and $\mu' = d\mu/dr$ characterizes the *shear*. This condition is called *Suydam's criterion*, and it is a necessary, but not always sufficient condition for stability, as it is derived from consideration of local-mode behavior only. Equation (1.79) indicates that the stability boundary involves two competing effects. The destabilizing term results from the combination of a negative pressure-gradient and the unfavorable curvature of the B_θ field. The stabilizing term, proportional to μ'^2, represents the work done in bending the field lines when interchanging two flux tubes in a system with shear. Newcomb derived the necessary and sufficient conditions for the stability of a cylindrical plasma [34].

Chapter 2

Theory of Tearing Modes

2.1 Magnetic Reconnection

Magnetic reconnection is a phenomenon which is of particular importance in solar system plasmas. In the solar corona, it results in the rapid release to the plasma of energy stored in the large-scale structure of the coronal magnetic field, an effect which is thought to give rise to *solar flares* [37]. Small-scale reconnection may play a role in heating the corona, and, thereby, driving the outflow of the solar wind. In the Earth's magnetosphere, magnetic reconnection in the magnetotail is thought to be the precursor for *auroral sub-storms* [39].

In order to start our discussion of magnetic reconnection, we need the MHD Ohm's Law, modified by resistivity:

$$\mathbf{E} + \mathbf{v} \times \mathbf{B} = \eta \, \mathbf{j} \tag{2.1}$$

Here, the resistivity η is assumed to be a constant for the sake of simplicity. Taking the curl of the previous equation, and making use of Faraday's Law and Ampère's Law, we obtain the following well known equation that governs the evolution of the magnetic field in a resistive MHD plasma:

$$\frac{\partial \mathbf{B}}{\partial t} = \nabla \times (\mathbf{v} \times \mathbf{B}) + \frac{\eta}{\mu_0} \nabla^2 \mathbf{B}. \tag{2.2}$$

The first term on the right hand side of this equation describes the *convection* of the magnetic field by the plasma flow. The second term describes the resistive *diffusion* of the field through the plasma. If the first term dominates, then magnetic flux is frozen into the plasma, and the topology of the magnetic field cannot change. On the other hand, if the second term dominates, then there is little coupling between the field and the plasma flow, and the topology of the magnetic field is free to change. Although resistivity often acts to damp out perturbations, in the framework of MHD it can also act as a destabilizing factor. Once the plasma is freed from the frozen flux constraint, magnetic field lines may tear and reconnect [6] to form a new configuration with lower potential energy. This constitutes the basic mechanism of the *tearing instability*.

The relative magnitude of the two terms on the right hand side of Eq. (2.2) is conventionally measured in terms of *magnetic Reynolds number*, or *Lundquist number*:

$$S = \frac{\mu_0 \, v \, L}{\eta} \simeq \frac{|\nabla \times (\mathbf{v} \times \mathbf{B})|}{|(\eta/\mu_0) \, \nabla^2 \mathbf{B}|}, \tag{2.3}$$

where v is the characteristic flow speed, and L the characteristic length scale of the plasma. If S is much larger than unity then convection dominates, and the *frozen flux* constraint prevails, whereas if S is much less than unity then diffusion dominates, and the coupling between the plasma flow and the magnetic field is relatively weak.

It turns out that in the solar system very large S values are virtually guaranteed by the the extremely large scale lengths of solar system plasmas.

For instance, $S \sim 10^8$ for solar flares, whilst $S \sim 10^{11}$ is appropriate for the solar wind and Earth's magnetosphere [37]. Of course, in calculating these values we have identified the scale length L with the overall size of the plasma under investigation. On the basis of this discussion, it seems reasonable to neglect diffusive processes altogether in solar system plasmas. Of course, this leads to very strong constraints on the behavior of such plasmas, since all cross field mixing of plasma elements is suppressed in this limit. Particles may freely mix along field lines (within limitations imposed by magnetic mirroring, etc.), but are completely ordered perpendicular to the field, since they always remain tied to the same field lines as they convect in the plasma flow.

Let us consider what happens when two initially separate plasma regions come into contact with one another, as occurs, for example, in the interaction between the solar wind and Earth's magnetic field. Assuming that each plasma is frozen to its own magnetic field, and that cross-field diffusion is absent, we conclude that the two plasmas will not mix, but, instead, that a thin *boundary layer* will form between them, separating the two plasmas and their respective magnetic fields. In equilibrium, the location of the boundary layer will be determined by pressure balance. Since, in general, the frozen fields on either side of the boundary will have differing strengths, and orientations tangential to the boundary, the layer must also constitute a *current sheet*. Thus, flux freezing leads inevitably to the prediction that in plasma systems space becomes divided into separate cells, wholly containing the plasma and magnetic field from individual sources, and separated from each other by thin

current sheets.

The "separate cell" picture constitutes an excellent zeroth order approximation to the interaction of solar system plasmas, as witnessed, for example, by the well defined planetary magnetospheres [40]. It must be noted, however, that the large S-values upon which the applicability of the frozen flux constraint was justified were derived using the *large* overall spatial scales of the systems involved. However, strict application of this constraint to the problem of the interaction of separate plasma systems leads to the inevitable conclusion that structures will form having *small* spatial scales, at least in one dimension: i.e., the thin current sheets constituting the cell boundaries. It is certainly not guaranteed that the effects of diffusion can be neglected in these boundary layers. In fact, we shall demonstrate that the localized breakdown of the flux freezing constraint in the boundary regions, due to diffusion, not only has an impact on the properties of the boundary regions themselves, but can also have a decisive impact on the large length scale plasma regions where the flux freezing constraint remains valid. This observation illustrates both the subtlety and the significance of the magnetic reconnection process.

2.2 Linear Tearing Mode Theory

Although the work in this dissertation focuses on periodic cylindrical geometry as a successful approximation for simulating the toroidal geometry of a tokamak reactor, the basic properties of tearing modes are clearly illustrated using a two-dimensional, slab geometry configuration. Let us consider the

interface between two infinitely extending plasmas containing magnetic fields of different orientations. The simplest imaginable field configuration is that illustrated in Fig. 2.1. Here, the field varies only in the x direction, and points only in the y direction. The field is directed in the $-y$ direction for $x < 0$, and in the $+y$ direction for $x > 0$. The interface is situated at $x = 0$. The sudden reversal of the field direction across the interface gives rise to a z-directed current sheet at $x = 0$.

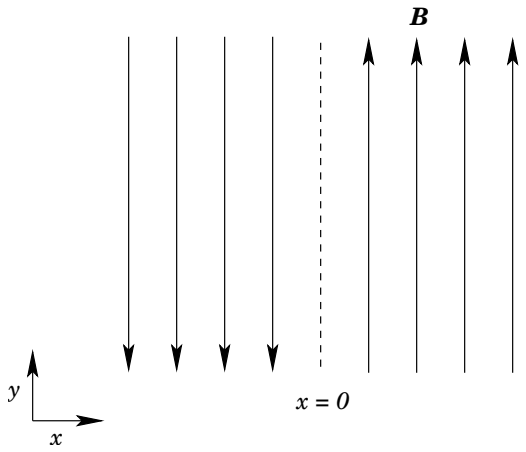

Figure 2.1: A reconnecting magnetic field configuration. Adopted from Fitzpatrick, *Plasma Physics: An Introduction* [17]

With the neglect of plasma resistivity, the field configuration shown in Fig. 2.1 represents a *stable* equilibrium state, assuming, of course, that we have normal pressure balance across the interface. However, as we shall see, when we take resistivity into account, this field configuration does not remain stable; we expect an instability to develop which relaxes the configuration to one possessing lower magnetic energy. This type of relaxation process inevitably entails the breaking and reconnection of magnetic field lines, and is,

therefore, termed *magnetic reconnection*. The magnetic energy released during the reconnection process eventually appears as plasma thermal energy. Thus, magnetic reconnection also involves plasma heating.

In the following, we shall outline the standard method for determining the *linear* stability of the type of magnetic field configuration shown in Fig. 2.1, taking into account the effect of plasma resistivity. We are particularly interested in plasma instabilities which are stable in the absence of resistivity, and only grow when the resistivity is nonzero. Such instabilities are conventionally termed *tearing modes*. Since magnetic reconnection is, in fact, a *nonlinear* process, we shall then proceed to investigate the nonlinear development of tearing modes.

The equilibrium magnetic field is

$$\mathbf{B}_0 = B_{0\,y}(x)\,\hat{\mathbf{y}}, \tag{2.4}$$

where $B_{0\,y}(-x) = -B_{0\,y}(x)$. The magnetic field reverses sign at the origin, giving rise to a z-directed current sheet at $x = 0$. It would be energetically favorable if the oppositely directed field lines on either side of the interface $x = 0$ could somehow meet up and annihilate (or cancel out) one another, since the magnetic energy, $U_B \sim \int B_{0y}^2\, dV$, would thereby be reduced. However, such motions are not allowed in ideal MHD because, by the frozen flux constraint, the magnetic flux through any plasma surface element in the $x - z$ plane must remain constant. Of course, when we allow a finite resistivity, the frozen flux constraint is relaxed, and field lines from one side of the interface can diffuse

across the plasma to annihilate its counterpart on the other side. We will see that, in cylindrical geometry, resistivity allows magnetic field lines to break and reconnect by means of a wave-like perturbation B_x, thus lowering magnetic energy via the formation of magnetic island chains.

Let us generalize the situation by allowing for the inclusion of an equilibrium magnetic field of the form

$$\mathbf{B}_0 = B_{0y}(x)\hat{\mathbf{y}} + B_{0z}\hat{\mathbf{z}}, \tag{2.5}$$

where the strong B_{0z} component is approximately uniform, but the B_{0y} component depends on x, so that overall $\mathbf{B}_0$ rotates as we move along in the x direction. We choose y and z axes so that $B_{0y} = 0$ when $x = 0$, but we could have oriented our axes so that $B_{0y} = 0$ for arbitrary x. Thus, the equilibrium described by Equation (2.4) is representative of a much more general set of equilibria. Such a configuration is illustrated in Fig. 2.2.

Since the equilibrium is stationary in time, and uniform in the y and z directions, it makes sense to assume that perturbations have the form

$$\psi\left(\mathbf{x}, t\right) = \psi\left(x\right)\, \mathrm{e}^{i\,\mathbf{k}\cdot\mathbf{x}+\gamma\, t}, \tag{2.6}$$

where γ is the instability growth rate and $\mathbf{k} = (0,\, k_y,\, k_z)$ is the wave vector. The resistive tearing instability satisfies

$$\mathbf{k} \cdot \mathbf{B}_0\left(x_s\right) = 0 \tag{2.7}$$

at the so called *resonant surface* $x = x_s$, where the tearing mode reconnects the magnetic field. For the simple equilibrium of Equation (2.4), the resonance

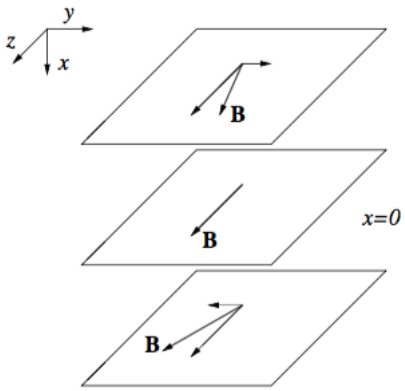

Figure 2.2: Generalized sheared magnetic field $\mathbf{B}_0 = B_{0y}(x)\hat{\mathbf{y}} + B_{0z}\hat{\mathbf{z}}$. Shown here are the magnetic field $\mathbf{B}$ and its components $B_{0y}\hat{\mathbf{y}}, B_{0z}\hat{\mathbf{z}}$. Note that we have oriented the y and z axes in such a way that $B_{0y}(x = 0) = 0$. Adopted from Ref. [50]

condition (2.7) is satisfied at $x_s = 0$, as one would expect. For the more general equilibrium we introduced with Equation (2.5), the resonance condition (2.7) can be satisfied at *any* value of x, since in the infinite plasma slab all values of $\mathbf{k}$ are allowed. Hence, any value of x is a potential candidate for the tearing instability. Let us focus on perturbations of the form

$$\psi\left(\mathbf{x}, t\right) = \psi(x)\, \mathrm{e}^{i\, k\, y + \gamma\, t}, \tag{2.8}$$

where, for ease of notation, we have written $k_y \to k$. In this case, for the equilibrium described by Equation (2.5), the resonance condition (2.7) is satisfied only at $x_s = 0$.

Let us note something about the physical significance of Eq. (2.7): the component of the wave vector parallel to the magnetic field, $k_{\|}$, is zero at the surface at which the tearing mode reconnects magnetic flux. Perturbations

with a significant $k_\parallel$ component expend energy bending the field lines. Consequently, if $k_\parallel \simeq 0$ then the perturbation expends very little energy bending field lines, and has plenty left for fluid motions which can enhance its growth [24].

2.3 Tearing Mode Dispersion Relation

Our goal is to obtain the tearing mode dispersion relation using linear analysis. This problem was first successfully treated in the classic paper by Furth, Killeen, and Rosenbluth [21]. Let us consider the infinite plasma slab with the equilibrium field of Equation (2.5) and resistive Ohm's Law (2.1). We will assume incompressible plasma flow with no zeroth order component.

We are starting our linear analysis with the linearized equations of *resistive* MHD [20] for assumed incompressible flow:

$$\frac{\partial \mathbf{B}}{\partial t} = \nabla \times (\mathbf{v} \times \mathbf{B}_0) + \frac{\eta}{\mu_0} \nabla^2 \mathbf{B}, \tag{2.9}$$

$$\rho_0 \frac{\partial \mathbf{v}}{\partial t} = -\nabla p + \frac{(\nabla \times \mathbf{B}) \times \mathbf{B}_0}{\mu_0} + \frac{(\nabla \times \mathbf{B}_0) \times \mathbf{B}}{\mu_0} \tag{2.10}$$

$$\nabla \cdot \mathbf{B} = 0, \tag{2.11}$$

$$\nabla \cdot \mathbf{v} = 0. \tag{2.12}$$

Here, ρ_0 is the equilibrium plasma mass density, $\mathbf{B}$ the perturbed magnetic field, $\mathbf{v}$ the perturbed plasma velocity, and p the perturbed plasma pressure. The x-component of Eq. (2.9) and the z-component of the curl of Eq. (2.10)

reduce to:

$$\gamma\, B_x = i\, k\, B_{0\,y}\, V_x + \frac{\eta}{\mu_0}\left(\frac{d^2}{dx^2} - k^2\right) B_x, \qquad (2.13)$$

$$\gamma\, \rho_0 \left(\frac{d^2}{dx^2} - k^2\right) V_x = \frac{i\, k\, B_{0\,y}}{\mu_0}\left(\frac{d^2}{dx^2} - k^2 - \frac{B''_{0\,y}}{B_{0\,y}}\right) B_x, \qquad (2.14)$$

respectively, where use has been made of Eqs. (2.11) and (2.12), and the fact that $\partial/\partial z \to 0$, which follows from our assumed form of perturbation, Eq. (2.8), and equilibrium, Eq. (2.5). Here, $'$ denotes d/dx. Note from Eq. (2.13) that, in the absence of resistivity, whenever $B_{0y} = 0$ we must have B_z vanish as well in order to prevent infinite plasma velocity. Finite resistivity η relaxes that constraint and allows the magnetic field lines to tear and reconnect across the $x = 0$ interface via finite B_x.

All the dynamics of the tearing mode is contained in the coupled set of Equations (2.13) and (2.14). Their solution is greatly facilitated by employing the method of *asymptotic matching* [3].

1. We divide the plasma into an "inner region", or layer of narrow width centered about $x = 0$, where resistivity and inertia are important, and an "outer region" comprising the bulk of the plasma, where ideal MHD holds, and, consequently, we may ignore resistivity and inertia.

2. The simplified versions of Eqs. (2.13) and (2.14) can be solved in each region, and then the resulting *inner* and *outer* solutions can be *matched* in an intermediate matching region.

3. We demand that the inner and outer solutions possess the same functional dependence on x in a region overlapping the inner and outer regions, where both solutions are valid.

4. By matching, we are able to obtain the dispersion relation for the tearing mode.

It is convenient to normalize Eqs. (2.13) and (2.14) using a typical magnetic field strength, B_0, and a typical scale length, a. Let us define the *Alfvén time-scale*

$$\tau_A = \frac{a}{v_A}, \tag{2.15}$$

where $v_A = B_0/\sqrt{\mu_0\,\rho_0}$ is the Alfvén velocity, and the *resistive diffusion* time-scale

$$\tau_R = \frac{\mu_0\,a^2}{\eta}. \tag{2.16}$$

As we have already seen, the ratio of these two time-scales is the Lundquist number:

$$S = \frac{\tau_R}{\tau_A}. \tag{2.17}$$

Let us introduce the *magnetic flux function* ψ, and the *plasma stream function* ϕ for convenience: $\psi = B_x/B_0$, $\phi = i\,k\,V_y/\gamma$. Also: $\bar{x} = x/a$, $F = B_{0\,y}/B_0$, $F' \equiv dF/d\bar{x}$, $\bar{\gamma} = \gamma\,\tau_A$, and $\bar{k} = k\,a$.

It follows that Eqs. (2.13) and (2.14) can be rewritten in normalized form as:

$$S\,\bar{\gamma}\,(\psi - F\,\phi) = \left(\frac{d^2}{d\bar{x}^2} - \bar{k}^2\right)\psi, \tag{2.18}$$

$$\bar{\gamma}^2\left(\frac{d^2}{d\bar{x}^2} - \bar{k}^2\right)\phi = -\bar{k}^2\,F\left(\frac{d^2}{d\bar{x}^2} - \bar{k}^2 - \frac{F''}{F}\right)\psi. \tag{2.19}$$

Comparison with Eqs. (2.13) and (2.14) shows that the term on the right hand side of Eq. (2.18) represents plasma *resistivity*, and the term on the left hand side of Eq. (2.19) represents plasma *inertia*. It is assumed that the tearing instability grows on a *hybrid* time scale, which is much less than τ_R but much greater than τ_A. It follows that

$$\bar{\gamma} \ll 1 \ll S\,\bar{\gamma}. \tag{2.20}$$

Therefore, throughout most of the plasma, we can neglect the right hand side of Eq. (2.18) and the left hand side of Eq. (2.19), which is equivalent to the neglect of plasma resistivity and inertia. In this case, Eqs. (2.18) and (2.19) simplify to

$$\phi = \frac{\psi}{F}, \tag{2.21}$$

$$\frac{d^2\psi}{d\bar{x}^2} - \bar{k}^2\,\psi - \frac{F''}{F}\,\psi = 0. \tag{2.22}$$

The first equation is simply the *flux freezing constraint*, which requires the plasma to move with the magnetic field, and the second is the linearized, static *force balance equation*: $\nabla \times (\mathbf{j} \times \mathbf{B}) = \mathbf{0}$.

Together, Eqs. (2.21) and (2.22) are known as the equations of *ideal MHD*, and are valid throughout the bulk of the plasma. However, it is clear that these equations *break down* in the immediate vicinity of the interface, where $\bar{x} \rightarrow 0$ and, consequently, $F \rightarrow 0$, and where the magnetic field reverses direction and the normalized "radial" plasma velocity ϕ approaches infinity. The ideal MHD equations break down close to the interface because the neglect

of plasma resistivity and inertia becomes untenable as $F \rightarrow 0$. Thus, there is a thin layer, in the immediate vicinity of the interface, $\bar{x} = 0$, where the behavior of the plasma is governed by the full MHD Equations, (2.18) and (2.19). Such singularities are resolved by including inertia and resistivity in the inner region.

We can simplify the full equations making use of the fact that $\bar{x} \ll 1$ and $d/d\bar{x} \gg 1$ in a thin layer, to obtain the following layer equations:

$$S\,\bar{\gamma}\,(\psi - \bar{x}\,\phi) = \frac{d^2\psi}{d\bar{x}^2}, \tag{2.23}$$

$$\bar{\gamma}^2\,\frac{d^2\phi}{d\bar{x}^2} = -\bar{x}\,\frac{d^2\psi}{d\bar{x}^2}, \tag{2.24}$$

where we have redefined the variables ϕ, $\bar{\gamma}$, and S, such that $\phi \rightarrow F'(0)\,\phi$, $\bar{\gamma} \rightarrow \gamma\,\tau_H$, and $S \rightarrow \tau_R/\tau_H$. These definitions hold throughout the rest of this section. Here,

$$\tau_H = \frac{\tau_A}{k\,a\,F'(0)} \tag{2.25}$$

is the *hydromagnetic time scale*, and it possesses a simple physical interpretation. Let us consider a shear Alfvén wave with wave number k traveling in the y direction. As we have already assumed, let the B_{0z} component in Equation (2.5) be very strong. In this case, we can write for the frequency of the wave:

$$\omega_A = k_\parallel\,v_A \simeq k\,v_A\,\frac{B_{0y}}{B_{0z}} \simeq k\,a\,v_A\frac{dB_{0y}/dx}{B_0}, \tag{2.26}$$

where we have approximated $B_{0y} \simeq \dfrac{dB_{0y}(0)}{dx}\,a$ and $B_{0z} \simeq B_0$. Recall that a and B_0 are a typical length scale and magnetic field strength, respectively.

From Equations (2.15), (2.25), (2.26), and the definition $F' \equiv \dfrac{d}{d\bar{x}}\left(B_{0y}/B_0\right)$, it is easily seen that $\tau_H = 1/\omega_A$. An estimate of the layer width can be obtained by combining Eqs. (2.23) and (2.24) to yield:

$$\gamma^2 \frac{d^2\phi}{dx^2} - \bar{x}^2\, S\, \bar{\gamma}\, \phi = -\,\bar{x}\, S\, \bar{\gamma}\, \psi. \tag{2.27}$$

In order to obtain the characteristic width of the layer, $\bar{\delta}$, we balance the two terms on the left hand side of the equation above:

$$x \sim \bar{\delta} = \left(\frac{\gamma}{S}\right)^{1/4} \tag{2.28}$$

Under most circumstances, $\gamma \sim S^{-3/5}$ for tearing mode growth [5], so our normalized layer width becomes

$$\bar{\delta} \sim S^{-2/5}. \tag{2.29}$$

Since $S \gg 1$, one can see that $\bar{\delta} \ll 1$ and it becomes even smaller with decreasing resistivity, and, conversely, increasing Lundquist number S. Let us summarize our plan of action:

1. We will integrate the "outer" equation, Eq. (2.22), from large $\bar{x}$ subject to appropriate boundary conditions (for instance $\psi\left(\bar{x} \to \infty\right) = 0$) to the layer edge $\bar{x} \sim \bar{\delta} \sim 0^+$, to obtain $\psi\left(\bar{x}\right)$ in the region $\bar{x} > 0$.

2. Similarly, we could obtain $\psi\left(\bar{x}\right)$ in the region $\bar{x} < 0^-$ by integrating Eq. (2.22) from large negative $\bar{x}$ (again subject to appropriate boundary conditions) up to the left boundary of the layer $\bar{x} \sim -\,\bar{\delta} \sim 0^-$. Maxwell's

equations demand that $\psi\,(\sim B_x)$ be continuous across the layer. Since we are working with a linear problem, we are free to multiply our two solutions by appropriate factors so as to satisfy this constraint. However, the current sheet at $x = 0$ demands that B_y is in general discontinuous across the layer, implying, by Eq. (2.11), a discontinuity in B_x'.

3. Our ideal MHD solution can be characterized by the real number:

$$\Delta' = \frac{1}{\psi}\left[\frac{d\psi}{d\bar{x}}\right]_{\bar{x}=0^-}^{\bar{x}=0^+}, \tag{2.30}$$

which is known as the *tearing stability index*, and is a measure of the perturbed current sheet flowing at $\bar{x} = 0$. In fact, Δ' turns out to be proportional to the "potential" magnetic energy that can be liberated by the tearing mode [48].

It is illustrative to consider the net electromagnetic energy flux into the non-ideal layer:

$$\mathcal{E} = -\left[S_x\left(\bar{x} = 0^+\right) - S_x\left(\bar{x} = 0^-\right)\right], \tag{2.31}$$

where

$$S_x = -\frac{1}{\mu_0} E_z\, B_y \tag{2.32}$$

is the "radial" component of the *Poynting vector*. A quick calculation shows that

$$\mathcal{E} \propto \gamma\,|\psi|^2\,\Delta', \tag{2.33}$$

with γ being the growth rate of the mode. Thus, for the mode to grow ($\gamma > 0$) and liberate magnetic energy from the equilibrium ($\mathcal{E} > 0$), we need $\Delta' > 0$.

Note that Δ' can be found solely from a consideration of the outer Equation (2.22), and is dependent only on the plasma equilibrium, the wave number k, and the boundary conditions at infinity. Without ever studying the inner region, we can obtain an expression for Δ', the source of free energy driving the instability, but we have no idea how it relates to the growth rate γ. As one might expect, to obtain the final piece of the puzzle, we must appeal to the *layer equations* (2.23) and (2.24) which depend on inertia, and, hence, on $\bar{\gamma}$.

The layer equations possess a trivial solution ($\phi = \phi_0$, $\psi = \bar{x}\,\phi_0$, where ϕ_0 is independent of $\bar{x}$), and a nontrivial solution for which $\psi(-\bar{x}) = \psi(\bar{x})$ and $\phi(-\bar{x}) = -\phi(\bar{x})$. The tearing mode corresponds to the latter, nontrivial solution. Due to the inclusion of resistivity, the layer equations represent a fourth order system with four undetermined coefficients. Recall, however, that our layer solutions must possess the same functional dependence on x as the outer solutions in the matching region.

The asymptotic behavior of the outer solutions ($\bar{x} \ll 1$) may be found by plugging a Frobenius power series solution into Equations (2.21) and (2.22) to find

$$\psi(x) \;\rightarrow\; a_0 + a_1\,|\bar{x}|, \tag{2.34}$$

$$\phi(x) \;\rightarrow\; \frac{\psi}{\bar{x}}, \tag{2.35}$$

to lowest order, where a_0 and a_1 represent the two arbitrary constants of the second order system of Eqs. (2.21) and (2.22). The inner solutions must exhibit

the same dependence on $\bar{x}$ far from the origin ($\bar{x} \gg \bar{\delta}$), so we can write down the asymptotic behavior of the inner solutions:

$$\psi(x) \rightarrow \left(\frac{\Delta(\bar{\gamma}, S)}{2} |\bar{x}| + 1 \right) \Psi, \tag{2.36}$$

$$\phi(x) \rightarrow \frac{\psi}{\bar{x}}, \tag{2.37}$$

where the parameters Ψ and $\Delta(\bar{\gamma}, S)$ represent two of the four undetermined constants associated with the fourth order system of Equations (2.23) and (2.24), and determined by solving the layer equations, subject to the above boundary conditions. The remaining constants correspond to the trivial solution and an exponentially growing solution, and may therefore be discarded.

Thus, we can now obtain the dispersion relation by solving the linear equations so as to determine the exact form of the coefficient $\Delta(\bar{\gamma}, S)$, and then using the matching criterion:

$$\Delta(\bar{\gamma}, S) = \Delta', \tag{2.38}$$

to determine the growth rate, γ, of the tearing instability.

Our next goal is to find the explicit form for $\Delta(\bar{\gamma}, S)$. Following Coppi et. al. [10], we Fourier transform the fourth order layer equations (2.23) and (2.24) into a second order equation, using the transform pair:

$$\hat{\phi}(t) = \frac{S^{1/3}}{2\pi} \int_{-\infty}^{\infty} \phi(\bar{x})\, e^{\,i\, S^{1/3}\, \bar{x}\, t}\, d\bar{x} \tag{2.39}$$

$$\phi(\bar{x}) = \int_{-\infty}^{\infty} \hat{\phi}(t)\, e^{\,i\, S^{1/3}\, \bar{x}\, t}\, dt, \tag{2.40}$$

with a similarly defined transform pair for ψ:

$$\hat{\psi}(t) = \frac{S^{1/3}}{2\pi}\int_{-\infty}^{\infty}\psi(\bar{x})\,e^{\,i\,S^{1/3}\,\bar{x}\,t}\,d\bar{x} \tag{2.41}$$

$$\psi(\bar{x}) = \int_{-\infty}^{\infty}\hat{\psi}(t)\,e^{\,i\,S^{1/3}\,\bar{x}\,t}\,dt, \tag{2.42}$$

where $\hat{\phi}(-t) = -\,\hat{\phi}(t)$.

The layer equations (2.23) and (2.24) can be Fourier transformed, and the results combined, to give

$$\frac{d}{dt}\left(\frac{t^2}{Q+t^2}\frac{d\hat{\phi}}{dt}\right) - Q\,t^2\,\hat{\phi} = 0, \tag{2.43}$$

where

$$Q = \gamma\,\tau_H^{2/3}\,\tau_R^{1/3}. \tag{2.44}$$

As one can see, the Fourier transformation pairs we have defined above differ from the "usual" Fourier transform,

$$\hat{\phi}(t) \sim \int_{-\infty}^{\infty}\phi\,(\bar{x})\,e^{-i\,\bar{x}\,t}\,d\bar{x}, \tag{2.45}$$

in that we include a *stretching* factor, $S^{1/3}$, inside the argument of the exponential function, so that Eq. (2.39) effectively yields the usual transform of $\phi\left(\bar{x}/S^{1/3}\right)$ rather than the one of $\phi(\bar{x})$ [50]. We do this because, even though $\phi(\bar{x})$ is localized in a region $x \sim \bar{\delta} \ll 1$, $\phi\left(\bar{x}/S^{1/3}\right)$ is localized in a much larger region $\bar{x}/S^{1/3} \sim \bar{\delta}$, which implies that $\bar{x} \sim \bar{\delta}\,S^{1/3} \sim S^{2/5}\,S^{1/3} \sim \mathcal{O}(1)$. We have used the earlier results that, under most circumstances, $\bar{\gamma} \sim S^{3/5}$ for tearing mode growth, and that the normalized layer width takes the form

$\bar{\delta} \sim S^{-2/5}$. Thus, we have effectively "stretched" the edge of the resistive layer out to $x \sim 1$. We need to investigate the behavior of ϕ in the matching region, which lies far from the non ideal layer edge. As we have argued, this matching region corresponds to $x \gg 1$ in the stretched coordinates of Eq. (2.39).

Recall that the Fourier transform takes large-$\bar{x}$ behavior to small-t. The most general small-t asymptotic solution of Equation (2.43) is

$$\hat{\phi}(t) \to \frac{b_{-1}}{t} + b_0 + \mathcal{O}(t), \tag{2.46}$$

where b_{-1} and b_0 are independent of t, and it is assumed that $t > 0$. Since $\phi(\bar{x})$ is odd, and so is $\hat{\phi}(t)$, it follows that $b_0 \to -\, b_0$ for $t < 0$.

When inverse Fourier transformed [36], the above expression leads to the following expression for the asymptotic behavior of ϕ at the edge of the non-ideal-MHD layer:

$$\phi(\bar{x}) \to b_{-1}\, \frac{\pi}{2}\, S^{1/3}\, \mathrm{sgn}(x) + \frac{b_0}{\bar{x}} + \mathcal{O}(|\bar{x}|^{-2}). \tag{2.47}$$

Since we are working at the edge of the non-ideal layer, the reflection of the constant term (i.e., $b_{-1} \to -\, b_{-1}$ for $x < 0$) does not necessarily demand that there is a discontinuity in ϕ.

From a comparison with Equations (2.36) and (2.37) (asymptotic behavior of inner solutions), it follows that

$$\Delta = \pi\, \frac{b_{-1}}{b_0}\, S^{1/3}. \tag{2.48}$$

Thus, the matching parameter Δ is determined from the two lowest order coefficients of the Fourier transformed layer solution. The next step is to determine this ratio from Eq. (2.48).

Let us search for an *unstable* tearing mode, characterized by $Q > 0$. It is convenient to assume that

$$Q \ll 1. \tag{2.49}$$

This ordering, which is known as the *constant-ψ approximation*, since it implies that $\psi(\bar{x})$ is approximately constant across the layer, will be justified later on.

In the limit $t \gg Q^{1/2}$, Equation (2.43) reduces to

$$\frac{d^2\hat{\phi}}{dt^2} - Q\,t^2\,\hat{\phi} = 0. \tag{2.50}$$

The solution to this equation which is well behaved in the limit $t \rightarrow \infty$ is written as $U(0, \sqrt{2}\,Q^{1/4}\,t)$, where $U(a, x)$ is a standard parabolic cylinder function [1].

In the limit

$$Q^{1/2} \ll t \ll Q^{-1/4} \tag{2.51}$$

we can make use of the standard small argument asymptotic expansion of $U(a, x)$ to write the most general solution to Equation (2.50) in the form

$$\hat{\phi}(t) = A\left[1 - 2\,\frac{\Gamma(3/4)}{\Gamma(1/4)}\,Q^{1/4}\,t + \mathcal{O}(t^2)\right], \tag{2.52}$$

where A is an arbitrary constant and Γ is the *Gamma function*.

In the limit

$$t \ll Q^{-1/4}, \tag{2.53}$$

Equation (2.43) reduces to

$$\frac{d}{dt}\left(\frac{t^2}{Q+t^2}\,\frac{d\hat{\phi}}{dt}\right) = 0. \tag{2.54}$$

The most general solution to this equation is written as:

$$\hat{\phi}(t) = B\left(-\frac{Q}{t} + t\right) + C + \mathcal{O}(t^2), \tag{2.55}$$

where B and C are arbitrary constants.

Matching coefficients between Equations (2.52) and (2.55) in the range of t satisfying the inequality (2.51) yields the following expression for the most general solution to Equation (2.43) in the limit $t \ll Q^{1/2}$:

$$\hat{\phi} = A\,\left[2\,\frac{\Gamma(3/4)}{\Gamma(1/4)}\,\frac{Q^{5/4}}{t} + 1 + \mathcal{O}(t)\right]. \tag{2.56}$$

Finally, a comparison of Eqs. (2.37), (2.39) and (2.56) allows us to express the matching parameter Δ in terms of the ratio b_1/b_0 and the growth rate γ, using Equation (2.48):

$$\Delta' = 2\pi\,\frac{\Gamma(3/4)}{\Gamma(1/4)}\,S^{1/3}\,Q^{5/4}. \tag{2.57}$$

The asymptotic matching condition (2.38) can be combined with the above expression for Δ' to give the *tearing mode dispersion relation*:

$$\gamma = \left[\frac{\Gamma(1/4)}{2\pi\,\Gamma(3/4)}\right]^{4/5}\,\frac{(\Delta')^{4/5}}{\tau_H^{2/5}\,\tau_R^{3/5}}. \tag{2.58}$$

Here, use has been made of the definitions of S and Q. According to this dispersion relation, the tearing mode is unstable whenever $\Delta' > 0$, and it

grows on the hybrid time-scale $\tau_H^{2/5}\,\tau_R^{3/5}$. It is easily demonstrated that the tearing mode is stable (purely decaying) whenever $\Delta' < 0$.

Recall that, in order to obtain Eq. (2.58), we used the *constant - ψ approximation*, (2.49). From Eqs. (2.36) and (2.38) we can see that ψ would indeed be approximately constant across the linear layer, provided that:

$$\Delta'\,\bar{\delta} \ll 1, \tag{2.59}$$

or, from Eq. (2.29), $\Delta' \ll S^{2/5}$, i.e., as long as the tearing mode does not become too unstable.

According to Eqs. (2.38), (2.49), and (2.57), a slightly stricter condition for the constant-ψ approximation to hold yields

$$\Delta' \ll S^{1/3} \tag{2.60}$$

Let us briefly discuss where the constant-ψ approximation comes from; it holds when the time scale on which the tearing mode grows is much larger than the time scale on which magnetic flux diffuses across the non-ideal layer.

From Eq. (2.50), the thickness of the non-ideal-MHD layer in t-space is

$$\delta_t \sim \frac{1}{Q^{1/4}}. \tag{2.61}$$

It follows from Eqs. (2.40) and (2.42) that the thickness of the layer in $\bar{x}$-space is

$$\bar{\delta} \sim \frac{1}{S^{1/3}\,\delta_t} \sim \left(\frac{\bar{\gamma}}{S}\right)^{1/4}. \tag{2.62}$$

When $\Delta' \sim \mathcal{O}(1)$ then $\bar{\gamma} \sim S^{-3/5}$, according to Eq. (2.52), giving $\bar{\delta} \sim S^{-2/5}$. It is clear, therefore, that if the Lundquist number, S, is very large, then the non-ideal-MHD layer centered on the interface, $\bar{x} = 0$, is *extremely narrow*. The time-scale for magnetic flux to diffuse across a layer of thickness $\bar{\delta}$ (in $\bar{x}$-space) is [cf., Equation (2.16)]

$$\tau \sim \tau_R \, \bar{\delta}^{\,2}. \tag{2.63}$$

If $\gamma \, \tau \ll 1$ then the tearing mode grows on a time scale which is far longer than the time scale on which magnetic flux diffuses across the non ideal layer. In this case, we would expect the normalized "radial" magnetic field, ψ, to be approximately *constant* across the layer, since any non-uniformities in ψ would be smoothed out via resistive diffusion. It follows from Equations (2.62) and (2.63) that the constant-ψ approximation holds provided that

$$\bar{\gamma} \ll S^{-1/3}, \tag{2.64}$$

i.e., $Q \ll 1$, which is in agreement with our old condition, Eq. (2.49).

2.4 Formation of Magnetic Islands

We have seen that, if $\Delta' > 0$, then a magnetic field configuration of the type shown in Fig. 2.1 is unstable to a tearing mode. We will investigate how a tearing instability affects the field topology as it develops. Since our magnetic field is divergence-free, and it does not depend on the z coordinate, it is convenient to express it in terms of a flux function:

$$\mathbf{B} = B_0 \, a \, \nabla\psi \times \hat{\mathbf{z}}, \tag{2.65}$$

where B_0 and a are a typical magnetic field strength and typical length scale, respectively.

Note that $\mathbf{B}\cdot\nabla\psi = 0$, since ψ is a flux function. By definition [24], it follows that $\mathbf{B}$ is tangent to surfaces of constant ψ, or that magnetic field lines run along contours of $\psi(x, y)$, as we have discussed in Chapter 1. In the vicinity of the interface $\bar{x} = 0$, we can write

$$\psi(\bar{x}, \bar{y}) \simeq \psi_0(\bar{x}) + \psi_1(\bar{x}, \bar{y}), \tag{2.66}$$

where ψ_0 generates the equilibrium magnetic field B_{0y}, and ψ_1 generates the perturbed magnetic field associated with the tearing mode. Here $\bar{x} = x/a$ and $\bar{y} = y/a$. In writing Equation (2.66) we have used the constant-ψ approximation which implies that, near $x = 0$:

$$B_x\left(\bar{x}, \bar{y}\right) \simeq B_x\left(\bar{y}\right), \tag{2.67}$$

$$\psi_1\left(\bar{x}, \bar{y}\right) \simeq \psi_1\left(\bar{y}\right). \tag{2.68}$$

The equilibrium magnetic field is assumed to be odd in $\bar{x}$, and, assuming that the phase of B_x varies in $\bar{\psi}$ like $\sin\left(\bar{k}\,\bar{y}\right)$, Equations (2.65) and (2.66) imply that, in the vicinity of the interface, we have:

$$\psi \simeq -\frac{F'(0)}{2}\,\bar{x}^{\,2} + \Psi\,\cos\bar{k}\,\bar{y}, \tag{2.69}$$

where Ψ is a constant, proportional to the amplitude of the perturbation B_x, and, as before:

$$F'(0) = \frac{1}{B_0}\frac{dB_{0y}(0)}{d\bar{x}}. \tag{2.70}$$

For convenience in our calculations, we introduce [2, 5]:

1. A normalized perturbed magnetic flux function $\chi = -\psi/\Psi$,

2. An "angular" coordinate $\theta = \bar{k}\,\bar{y}$, and

3. A "radial" coordinate $X = \bar{x}/\bar{W}$, where

4. $\overline{W} = 4\sqrt{\Psi/F'(0)}$.

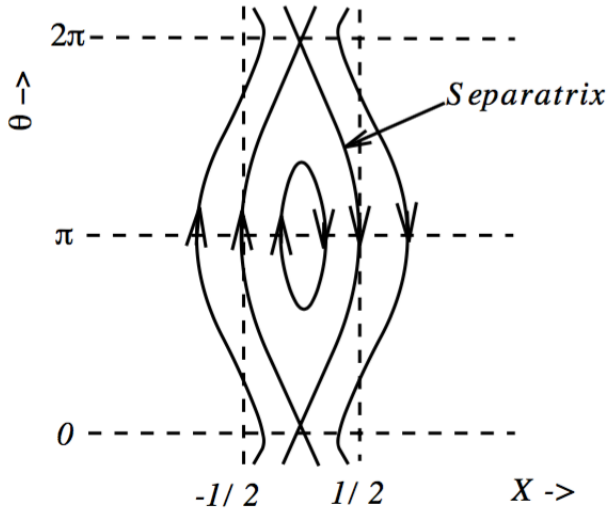

Figure 2.3: Magnetic field lines in the vicinity of a magnetic island. Adopted from Fitzpatrick, *Plasma Physics: An Introduction* [17]

In the vicinity of the interface, χ takes the form

$$\chi = 8\,X^2 - \cos\theta \tag{2.71}$$

Figure 2.3 shows the contours of χ plotted in X-θ space. These contours map out the magnetic flux surfaces. Inside a *magnetic separatrix* located at $\chi = 1$, the magnetic field tears and reconnects to form *magnetic islands* centered on the interface, $X = 0$.

Magnetic field lines situated outside the separatrix are displaced by the tearing mode, but still retain their original topology. By contrast, field lines inside the separatrix have been broken and reconnected, and now possess quite different topology. The reconnection obviously takes place at the "X-points," which are located at $X = 0$ and $\theta = 2\pi\, m$, where m is an integer. The maximum width of the reconnected region (in $\bar{x}$-space) is given by the *island width*, $\overline{W}$. Note that the island width is proportional to the square root of the perturbed "radial" magnetic field at the interface (i.e., $\overline{W} \propto \sqrt{\Psi}$).

2.5 Nonlinear Tearing Mode Theory

Linear Theory predicts that the tearing mode grows exponentially on the hybrid timescale $\tau_H^{2/5}\tau_R^{3/5}$, as we have deduced from the tearing mode dispersion relation, Equation (2.58). When the island exceeds the width of the linear layer (i.e., $\overline{W} > \bar{\delta}$), Rutherford [41] postulated that forces due to nonlinear eddy currents replace inertia as the dominant mechanism opposing mode growth. Consequently, the growth slows down considerably, with the island width growing on the extremely slow resistive diffusion time scale. The nonlinear evolution of the magnetic island width is governed by

$$0.8227\,\tau_R\,\frac{d\overline{W}}{dt} = \Delta'\left(\overline{W}\right), \tag{2.72}$$

where

$$\Delta'\left(\overline{W}\right) = \left[\frac{1}{\psi}\frac{d\psi}{d\bar{x}}\right]_{-\overline{W}/2}^{+\overline{W}/2} \tag{2.73}$$

is the tearing stability index [14]. It is the jump in the logarithmic derivative of ψ taken across the island [49]. It is clear that, once the tearing mode enters the nonlinear regime, i.e., once the normalized island width, $\overline{W}$, exceeds the normalized linear layer width, $S^{-2/5}$, the growth rate of the instability slows down considerably, until the mode eventually ends up growing on the extremely slow resistive timescale, τ_R. The tearing mode stops growing once it has attained a saturated island width $\overline{W}_0$, satisfying

$$\Delta'\left(\overline{W}_0\right) = 0. \tag{2.74}$$

The saturated width is a function of the original plasma equilibrium, but it does not depend on resistivity. In general, $\overline{W}_0$ is comparable with the characteristic length scale of the magnetic field configuration.

As before, in order to derive result (2.72), we shall work in slab geometry using our familiar equilibrium magnetic field, $\mathbf{B}_0 = B_{0y}(x)\hat{\mathbf{y}} + B_{0z}\hat{\mathbf{z}}$, which can be rewritten in terms of a flux function ψ:

$$\mathbf{B} = \nabla\psi \times \hat{\mathbf{z}} + B_{0z}\hat{\mathbf{z}} \tag{2.75}$$

As a consequence of the strong uniform B_{0z} component, we can assume incompressibility for the velocity $\mathbf{v}$, which therefore can be written in terms of a *stream function* ϕ:

$$\mathbf{v} = -\nabla\phi \times \hat{\mathbf{z}}. \tag{2.76}$$

As we did in the linear case, we are going to use a combination of Faraday's Law and Ohm's Law, which can be written in terms of the flux function ψ:

$$\frac{\partial\psi}{\partial t} + \mathbf{v}\cdot\nabla\psi = \eta\, j_z \tag{2.77}$$

Ampère's Law can also be written in terms of the flux function:

$$\nabla^2 \psi = \mu_0 \, j_z \tag{2.78}$$

Finally, the plasma equation of motion

$$\rho \left(\frac{\partial \mathbf{v}}{\partial t} + \mathbf{v} \cdot \nabla \mathbf{v} \right) = \nabla p + \mathbf{j} \times \mathbf{B}, \tag{2.79}$$

can be rewritten in terms of the *vorticity* $\omega_z = (\nabla \times \mathbf{v})_z$:

$$\rho \left(\frac{\partial \omega_z}{\partial t} + \mathbf{v} \cdot \nabla \omega_z \right) = \mathbf{B} \cdot \nabla j_z. \tag{2.80}$$

Recall that we had assumed that the tearing mode grows very slowly, and this was the basis for our constant-ψ approximation across the linear layer. This fundamental assumption allows us to neglect inertia, and leads to the implication that the left hand side of Equation (2.80) is equal to zero, hence, j_z is a flux function:

$$j_z = j_z(\psi) \tag{2.81}$$

Let us now expand the flux function:

$$\psi \left(x, y, t \right) = \psi_0 \left(x \right) + \tilde{\psi} \left(y, t \right), \tag{2.82}$$

where [5]:

$$\tilde{\psi} \left(y, t \right) = \sum_{n=1}^{\infty} \psi_n \left(y, t \right) = \sum_{n=1}^{\infty} \tilde{\psi}_n(t) \cos(nky). \tag{2.83}$$

We have assumed that $B_{0y} \simeq B'_{0y} \, x$ near $x = 0$, thus, $\psi_0(x) = B'_{0y} \, x^2/2$. In spite of the notation of Equations (2.82) and (2.83), $\tilde{\psi}$ still possesses some dependence on x. However, as in the previous section, we assume that the

constant-ψ approximation also applies to $\tilde{\psi}$. Namely, in our region of focus, described by a "radial" layer of extent much greater than the linear layer width δ and the island width W, we assume that $\tilde{\psi}$ is approximately constant. As we have already seen, this assumption is valid provided that

$$\Delta'_n W \ll 1, \quad \Delta'_n \bar{\delta} \ll 1, \tag{2.84}$$

where

$$\Delta'_n = \left[\frac{1}{\psi_n} \frac{d\psi_n}{dx} \right]_{0-}^{0+} \tag{2.85}$$

are the usual tearing stability indices. Let us now substitute the expanded flux function (2.82) into the combined Faraday's Law and Ohm's Law expression (2.77) to obtain:

$$\frac{\partial \tilde{\psi}}{\partial t} - \left(\frac{\partial \psi}{\partial y} \right)_{\psi} B'_{0y} x = \eta \left(j_z - j_{z0} \right). \tag{2.86}$$

The second term represents the nonlinear contribution $\mathbf{v} \cdot \nabla \psi$, expressed in terms of the velocity stream function ϕ introduced in Equation (2.76). It might seem that, in order to proceed, we would need to explicitly calculate ϕ, but Rutherford noticed that we could eliminate that term altogether by *flux surface averaging* [41]. The flux surface average operator on f is defined as:

$$\langle f \rangle_y \equiv \frac{1}{2\pi} \int_0^{2\pi/k} f \, k \, dy \tag{2.87}$$

After dividing Equation (2.86) by x, we average over y at constant ψ to yield:

$$j_z(\psi) = j_{z0} + \eta^{-1} \left\langle \frac{\partial \tilde{\psi}\left(y,t\right)/\partial t}{\left[\psi - \tilde{\psi}\left(y,t\right) \right]^{1/2}} \right\rangle_y \Bigg/ \left\langle \left[\psi - \tilde{\psi}\left(y,t\right) \right]^{1/2} \right\rangle_y . \tag{2.88}$$

For values of ψ lying within the separatrix, where the field lines are closed, the definition of the flux surface average operator needs to be modified, so that the limits of integration in Equation (2.87) will depend on ψ. Additionally, although we have eliminated the nonlinear term in Equation (2.86), the price we have to pay is that the flux surface average itself is highly nonlinear, i.e., the surfaces of constant ψ over which we integrate are those surfaces determined using *all* the harmonics in Equation (2.82).

We are integrating Equation (2.78) over our region of interest, projecting out the n^{th} harmonic by multiplying both sides by $\cos(n\,k\,y)$, flux-surface-averaging, and taking into account that the gradient discontinuity in ψ_n is captured by Δ'_n. We write:

$$\Delta'_n\tilde{\psi}_n = 2\,\mu_0 \left\langle \cos(nky) \int_{-\infty}^{+\infty} j_z\,dx \right\rangle_y = \\ = \frac{4\mu_0}{\eta\left(2\,B'_{0y}\right)^{1/2}} \int_{\psi_{min}}^{+\infty} d\psi \left\langle \frac{\partial\tilde{\psi}/\partial t}{(\psi-\tilde{\psi})^{1/2}} \right\rangle_y \left\langle \frac{\cos(n\,k\,y)}{(\psi-\tilde{\psi})^{1/2}} \right\rangle_y \Bigg/ \left\langle (\psi-\tilde{\psi})^{-1/2} \right\rangle_y . \tag{2.89}$$

We have "closed" our equation in the second equality by substituting Equation (2.88) for j_z, having switched the integration variable to ψ. Rutherford argued that in the case here the fundamental harmonic is linearly unstable, i.e., $\Delta'_1 > 0$, but all other harmonics are relatively strongly stable, i.e., $\Delta'_n/\Delta'_1 \ll 1$ for $n \geq 2$, then a solution exists in which the fundamental harmonic dominates: $|\tilde{\psi}_1| \gg |\tilde{\psi}_n|$, for $n \geq 2$. In this case, we can return to Equation (2.89), and explicitly evaluate the integrals to obtain the *island evolution equation*:

$$\Delta'_1\,\tilde{\psi}_1^{1/2} = \frac{2\mu_0 A}{\eta\left(B'_{0y}\right)^{1/2}} \frac{\partial\tilde{\psi}_1}{\partial t}, \tag{2.90}$$

where $A = 0.8227$.

The island does not grow indefinitely, but it eventually saturates. This saturation was studied heuristically by White et. al. [49], and rigorously by Thyagaraja [46], who, by matching the inner and outer solutions to higher order (i.e., continuing the expansion in Equation (2.86) past the lowest order terms), and using the flux surface averaging operator, was able to obtain the result:

$$\frac{\Lambda_1}{2}\,\tau_R\,\frac{d\overline{W}}{dt} = \Delta' - \Lambda_1\,\lambda_0^2\left(\frac{W}{4}\right)\ln\left(\frac{4}{W}\right), \tag{2.91}$$

where λ_0 is a constant related to the equilibrium current gradient, and $\Lambda_1 = 2A \simeq 1.645$. Equation (2.91) predicts that, at some width $\overline{W}_0$, the island will saturate when the right hand side becomes zero, or:

$$\Delta' = \Lambda_1\,\lambda_0^2\left(\frac{\overline{W}_0}{4}\right)\ln\left(\frac{4}{\overline{W}_0}\right). \tag{2.92}$$

There is no particular reason why $\overline{W}_0$ should be small. However, it should be noted that Equation (2.92) is only accurate in the limit $\overline{W}_0 \ll 1$. Even though ideal MHD breaks down in a small region $\bar{\delta} \sim S^{-2/5}$, the equilibrium magnetic field is changed over a region comparable with the size of the plasma.

Chapter 3

Resonant Magnetic Perturbation Response Theory

This Chapter presents the theory of the linear and nonlinear response of a rotating tokamak plasma to a resonant error-field[1]. It is an essential segue for the next Chapter, in which the braking of rotating tearing mode rotation due to interaction with error-fields is studied extensively.

3.1 Introduction

The aim of this Chapter of the dissertation is twofold:

1. First, we will present a general analysis of the constant-ψ, resistive magnetohydrodynamical theory of the response of a rotating, quasi-cylindrical tokamak plasma to a resonant magnetic perturbation (error-field). It has been demonstrated that constant-ψ regimes are the most appropriate regimes in ohmically heated tokamak plasmas. Hence, this constraint is not really restrictive. This analysis will cover both *linear plasma response*, where the width of the magnetic island chain induced

[1]The theory and results in this Chapter have been published in Ref. [16].

at the rational surface is much less than the linear layer width, as well as *nonlinear plasma response*, where the width of the driven magnetic island chain is permitted to greatly exceed the linear layer width. The analysis predicts that, in the presence of a resonant error-field, there is a forbidden band of plasma rotation frequencies which effectively separates relatively high-rotation from relatively low-rotation states.

2. Second, we will investigate bifurcations between the dynamically stable low-rotation and high-rotation solution branches of the torque balance equation, triggered as the amplitude of the error-field is varied. A high- to low-rotation bifurcation is invariably associated with a significant increase in the driven magnetic island width, and vice versa.

3.1.1 Cylindrical Tokamak Equilibrium

Let us consider a large aspect-ratio, low-β tokamak plasma whose magnetic flux surfaces map out almost concentric circles in the poloidal plane. Such a plasma can be satisfactorily approximated as a periodic cylinder. Let a be the *minor radius* of the plasma. We will adopt the standard right-handed cylindrical coordinates (r, θ, z). The system will be assumed to be periodic in the z-direction with period $2\pi\, R_0$, where $R_0 \gg a$ is the simulated plasma major radius. For consistency with the parameters of toroidal geometry, it is convenient to define the simulated toroidal angle $\phi = z/R_0$. Following this choice of coordinates, the equilibrium magnetic field $\mathbf{B}$ can be written as $\mathbf{B} = [0,\, B_\theta(r),\, B_\phi]$ and the associated equilibrium plasma current den-

sity $\mathbf{j}$ takes the form $\mathbf{j} = [0,\, 0,\, j_\phi(r)]$, where, according to *Ampère's Law*, $\nabla \times \mathbf{B} = \mu_0\, \mathbf{j}$:

$$\mu_0\, j_\phi(r) = \frac{1}{r} \frac{d\,(r\, B_\theta)}{dr}, \tag{3.1}$$

where μ_0 is the *vacuum permeability*: $\mu_0 = 4\pi \times 10^{-7}\,\mathrm{N/A^2}$ in SI units.

Recall that, in order to parameterize the helical pitch of the equilibrium magnetic field lines, we can introduce the local *safety factor* $q(r)$:

$$q\,(r) = \frac{r\, B_\theta}{R_0\, B_\phi} \tag{3.2}$$

In a conventional tokamak plasma, $q(r) \sim \mathcal{O}(1)$ and is a monotonically increasing function of r. In the following we shall adopt standard large aspect-ratio tokamak orderings [47], according to which $B_\phi \gg B_\theta$ and $R_0 \gg a$.

3.1.2 Plasma Response to a Resonant Magnetic Perturbation

We will consider the response of the plasma to a static, helical (m, n) magnetic perturbation, which will be henceforth referred to as an *error-field* for simplicity, even though it actually only represents one particular resonant harmonic of the total error-field. Recall that m stands for the *poloidal mode number* (m periods of the error-field in the poloidal, θ direction) and n is the *toroidal mode number* (n periods of the error-field in the simulated toroidal, ϕ direction). We shall describe the field as a superposition of the desired axisymmetric field, $\mathbf{B}$ and the accidentally produced non-axisymmentric error-field, $\delta\mathbf{B}$.

It is convenient to express both the perturbed magnetic field and the

perturbed plasma current density in terms of a *magnetic flux function*, $\psi(r,\theta,\phi,t)$ [14]:

$$\delta\mathbf{B} = \nabla\psi \times \hat{\mathbf{z}} \tag{3.3}$$

$$\mu_0\,\delta\mathbf{j} = -\nabla^2\psi\,\hat{\mathbf{z}}, \tag{3.4}$$

where $\hat{\mathbf{z}}$ is the unit vector in the z-direction of our coordinate system. The magnetic flux function can be represented as:

$$\psi(r,\theta,\phi,t) = \psi(r,t)\,\exp\left[i\,(m\,\theta - n\,\phi)\right]. \tag{3.5}$$

We shall also define the *inverse aspect-ratio* of the plasma:

$$\epsilon_a = \frac{a}{R_0} \ll 1. \tag{3.6}$$

The representation (3.5) holds provided that:

$$\frac{m}{n} \gg \frac{a}{R_0}. \tag{3.7}$$

As we have discussed in the previous Chapter, the response of the plasma to the applied error-field is governed by the equations of perturbed, marginally stable (i.e., $\partial/\partial t \rightarrow 0$), ideal MHD everywhere in the plasma, apart from a relatively narrow (in r) region in the vicinity of the rational surface, minor radius r_s, where $q(r_s) = m/n$. Let us also define two new quantities that will assist us with parameterizing the error field, and the response of the plasma in the vicinity of the rational surface:

1. Vacuum flux: $\Psi_v(t) = |\Psi_v|\,\mathrm{e}^{-i\,\phi_v}$ is defined to be the value of $\psi(r,t)$ at radius r_s in the presence of the error-field, but in the absence of the plasma. Here, ϕ_v is the helical phase of the error-field.

2. Reconnected flux: $\Psi_s(t) = |\Psi_s|\, e^{-i\,\phi_s}$ is defined to be the actual value of $\psi(r,t)$ at radius r_s. Here, ϕ_s is the helical phase of the reconnected flux.

The intrinsic stability of the (m,n) tearing mode is governed by the *tearing stability index* which we have introduced in the previous Chapter:

$$\Delta' = \left[\frac{d\ln\hat{\psi}}{d\ln r}\right]_{r_s-}^{r_s+}, \tag{3.8}$$

where $\hat{\psi}(r)$ is a solution of the marginally stable, ideal MHD equations for the case of an (m,n) helical perturbation that satisfies physical boundary conditions at $r=0$ and $r=a$ in the absence of the error-field.

According to resistive MHD theory [44], and the seminal 1973 paper by *P.H. Rutherford* [41], if $\Delta' > 0$ then the m,n tearing mode spontaneously reconnects magnetic flux at the rational surface to form a helical magnetic island chain. In the following, we will be assuming that $\Delta' < 0$, so that the m,n tearing mode is intrinsically stable; any magnetic reconnection and island formation that takes place at the rational surface is due solely to the error-field. Our further analysis will comprise two different constant-ψ, resistive MHD regimes at the rational surface: a *linear* and a *nonlinear* regime.

3.2 Linear Regime

The first constant-ψ, resistive MHD response regime at the rational surface is the so-called "visco-resistive" regime [14]. These terms will be used interchangeably in the remainder of this Chapter. Standard asymptotic matching between the marginally stable, ideal MHD solution in the outer region (i.e.,

everywhere apart from the immediate vicinity of the rational surface) and the linear layer solution in the vicinity of the rational surface yield [15]:

$$\Delta\,\Psi_s = \Delta'\,\Psi_s + 2\,m\,\Psi_v \tag{3.9}$$

For the case of the visco-resistive layer response regime:

$$\Delta = \frac{\delta_{VR}}{r_s}\,\tau_R\left(\frac{d}{dt} + i\,\omega\right), \tag{3.10}$$

where δ_{VR} is the linear layer width and d/dt is the growth rate in the frame of the plasma. Here:

$$\tau_H = \frac{R_0}{B_\phi}\frac{\sqrt{\mu_0\,\rho(r_s)}}{n\,s}, \tag{3.11}$$

$$\tau_R = \mu_0\,r_s\,\sigma(r_s) = \frac{\mu_0\,r_s^2}{\eta_\parallel}, \tag{3.12}$$

$$\tau_V = \frac{r_s^2\,\rho(r_s)}{\mu(r_s)}, \tag{3.13}$$

are the hydromagnetic, resistive diffusion, and viscous diffusion timescales respectively, at the rational surface. Moreover, $s = (d\ln q/d\ln r)_{r_s}$ is the local magnetic shear and $\rho(r), \sigma(r)$ and $\mu(r)$ are the equilibrium plasma mass density, electrical conductivity and perpendicular viscosity profiles, respectively.

Let us introduce expressions for the full (radial) width of the magnetic island chain that forms at the rational surface, and the vacuum island width:

$$W = 4\left(\frac{|\Psi_s|}{s\,r_{s\theta}(r_s)}\right)^{1/2}, \tag{3.14}$$

$$W_v = 4\left(\frac{|\Psi_v|}{s\,r_{s\theta}(r_s)}\right)^{1/2}. \tag{3.15}$$

Combining those equations and taking into account our definitions for the vacuum and the reconnected flux, we obtain:

$$\left(\frac{d}{d\hat{t}} + i\,\omega\right)\left(\hat{W}^2\,\mathrm{e}^{-i\,\phi_s}\right) = -\,\hat{W}^2\,\mathrm{e}^{-i\,\phi_s} + \hat{W}_v^2\,\mathrm{e}^{-i\,\phi_v}, \tag{3.16}$$

which can be rewritten as:

$$2\,\hat{W}\,\frac{d\hat{W}}{d\hat{t}} - i\,\hat{W}^2\,\frac{d\phi}{d\hat{t}} + i\,\hat{\omega}\,\hat{W}^2 = -\hat{W}^2 + \hat{W}_v^2\,\mathrm{e}^{i\,\phi}, \tag{3.17}$$

where $\phi = \phi_s - \phi_v$ is the relative helical phase of the magnetic island with respect to the error-field, and we have assumed that $d\phi_v/dt = 0$. Equations (3.9) and (3.10) give the governing equation for the visco-resistive regime:

$$\frac{\delta_{VR}}{r_s}\left(\frac{d}{dt} + i\,\omega\right)\Psi_s = \Delta'\Psi_s + 2\,m\,\Psi_v, \tag{3.18}$$

which leads to:

$$2\,\frac{\delta_{VR}}{W}\,\tau_R\,\frac{d}{dt}\left(\frac{W}{r_s}\right) = \Delta' + 2\,m\left(\frac{W_v}{W}\right)^2\cos\phi \tag{3.19}$$

and

$$\frac{\delta_{VR}}{r_s}\,\tau_R\left(\frac{d\phi_s}{dt} - \omega\right) = -2\,m\left(\frac{W_v}{W}\right)^2\sin\phi. \tag{3.20}$$

It can be demonstrated that zero net electromagnetic torque can be exerted on magnetic flux surfaces located in the bulk of the plasma that is governed by the equations of marginally stable, ideal MHD [14]. Thus, any electromagnetic torque exerted on the plasma by the error-field develops in the immediate vicinity of the rational surface, where ideal MHD breaks down.

In the visco-resistive, linear regime, the net toroidal electromagnetic torque acting on the layer takes the form [14],[15]:

$$T_{\phi_{EM}} = \frac{4\pi^2\, n\, m\, R_0}{\mu_0} \left|\Psi_v\right|^2 \left(\frac{2\, m}{-\Delta'}\right) \hat{T}_\phi, \tag{3.21}$$

where:

$$\hat{T}_\phi = \left(\frac{-\Delta'}{2\, m}\right) \left(\frac{W}{W_v}\right)^2 \sin\phi. \tag{3.22}$$

3.2.1 Normalization Scheme

Let us introduce some normalized quantities in order to facilitate calculations:

$$\hat{W} = \frac{0.8227}{2} \frac{W}{\delta_{VR}}, \tag{3.23}$$

$$\hat{W}_v = \frac{0.8227}{2} \frac{W_v}{\delta_{VR}} \left(\frac{2\, m}{-\Delta'}\right)^{1/2}, \tag{3.24}$$

$$\hat{t} = t \Big/ \left[\frac{\delta_{VR}}{r_s} \frac{\tau_R}{(-\Delta')}\right], \tag{3.25}$$

$$\hat{\omega} = \omega \left[\frac{\delta_{VR}}{r_s} \frac{\tau_R}{(-\Delta')}\right] \tag{3.26}$$

And, without loss of generality, we can set:

$$\phi_v = 0 \tag{3.27}$$

Equations (3.19) and (3.20), governing the response of the plasma to the error-field in the linear regime, become:

$$\frac{d\hat{W}}{d\hat{t}} = \frac{\hat{W}}{2}\left(-1 + \frac{\hat{W}_v^2}{\hat{W}^2}\cos\phi\right), \tag{3.28}$$

$$\frac{d\phi}{d\hat{t}} = \hat{\omega} - \frac{\hat{W}_v^2}{\hat{W}^2}\sin\phi. \tag{3.29}$$

The normalized toroidal electromagnetic torque exerted in the vicinity of the rational surface takes the form

$$\hat{T}_\phi = \frac{\hat{W}^2}{\hat{W}_v^2}\sin\phi. \tag{3.30}$$

Equations (3.28) and (3.29) hold when:

$$\hat{W} \ll 1. \tag{3.31}$$

3.2.2 Linear Plasma Response Theory

Let us define:

$$X = \hat{W}^2\cos\phi, \tag{3.32}$$

$$Y = \hat{W}^2\sin\phi, \tag{3.33}$$

where X is the component of the normalized reconnected magnetic flux, driven by the error-field, that is *in phase* with the error-field, and Y is the corresponding component that is in *phase-quadrature*.

The equations that govern the plasma response to the resonant magnetic perturbation in the linear regime now take the form:

$$\frac{dX}{d\hat{t}} = -X - \hat{\omega}\, Y + \hat{W}_v^2, \tag{3.34}$$

$$\frac{dY}{d\hat{t}} = -Y + \hat{\omega}\, X. \tag{3.35}$$

For convenience, let us combine X and Y into $Z \equiv X + i\, Y$:

$$\frac{dZ}{d\hat{t}} = (-1 + i\,\omega)\, Z + \hat{W}_v^2 \tag{3.36}$$

The solution of Eq. (3.36) is

$$Z = \left(\frac{1 + i\,\hat{\omega}}{1 + \hat{\omega}^2}\right) \hat{W}_v^2 \left\{1 - \exp\left[(i\,\omega - 1)\,\hat{t}\right]\right\} + Z_0 \exp\left(i\,\omega - 1\right)\hat{t}, \tag{3.37}$$

where $Z_0 = X_0 + i\, Y_0$ at $t = t_0$. This solution can be analyzed into its X and Y components as follows:

$$X = \left(\frac{1}{1 + \hat{\omega}^2}\right) \hat{W}_v^2 \left\{1 - \left[\cos\left(\hat{\omega}\,\hat{t}\,\right) - \hat{\omega} \sin\left(\hat{\omega}\,\hat{t}\,\right)\right] \mathrm{e}^{-\hat{t}}\right\} +$$

$$+ \left[X_0 \cos\left(\hat{\omega}\,\hat{t}\,\right) - Y_0 \sin\left(\hat{\omega}\,\hat{t}\,\right)\right] \mathrm{e}^{-\hat{t}}, \tag{3.38}$$

$$Y = \left(\frac{1}{1 + \hat{\omega}^2}\right) \hat{W}_v^2 \left\{\hat{\omega} - \left[\hat{\omega} \cos\left(\hat{\omega}\,\hat{t}\,\right) - \hat{\omega} \sin\left(\hat{\omega}\,\hat{t}\,\right)\right] \mathrm{e}^{-\hat{t}}\right\} +$$

$$+ \left[Y_0 \cos\left(\hat{\omega}\,\hat{t}\,\right) + X_0 \sin\left(\hat{\omega}\,\hat{t}\,\right)\right] \mathrm{e}^{-\hat{t}}. \tag{3.39}$$

The linear response of the plasma to the error-field can be visualized (see Fig. 3.1) as a trajectory in the $X - Y$ *phase-space*. The evolution is an exponential decay to the fixed point X_∞, Y_∞ where:

$$X_\infty = \left(\frac{1}{1 + \hat{\omega}^2} \right) \hat{W}_v^2 \tag{3.40}$$

$$Y_\infty = \left(\frac{\hat{\omega}}{1 + \hat{\omega}^2} \right) \hat{W}_v^2 \tag{3.41}$$

At the fixed point [26, 27, 38]:

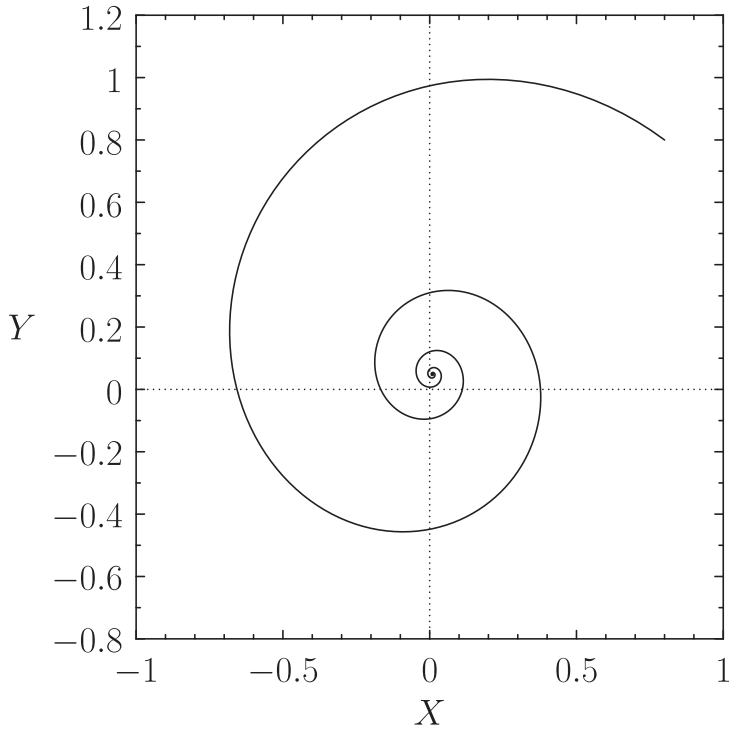

Figure 3.1: Phase-space evolution of the reconnected flux induced in a rotating tokamak plasma by a resonant error-field in the linear response regime.

$$\phi = \tan^{-1} \hat{\omega} \,, \tag{3.42}$$

$$\left(\frac{\hat{W}}{\hat{W}_v} \right)^4 = \frac{1}{1 + \hat{\omega}^2} \,, \tag{3.43}$$

$$\hat{T}_\phi = \frac{\hat{\omega}}{1 + \hat{\omega}^2} \,. \tag{3.44}$$

We can also visualize the time-asymptotic behavior of the magnetic island width (Fig. 3.2) and the electromagnetic torque (Fig. 3.3), which clearly assume a constant value, as a result of the exponential decay to the fixed point.

It is important to note that, in the limit of strong plasma rotation, the time-

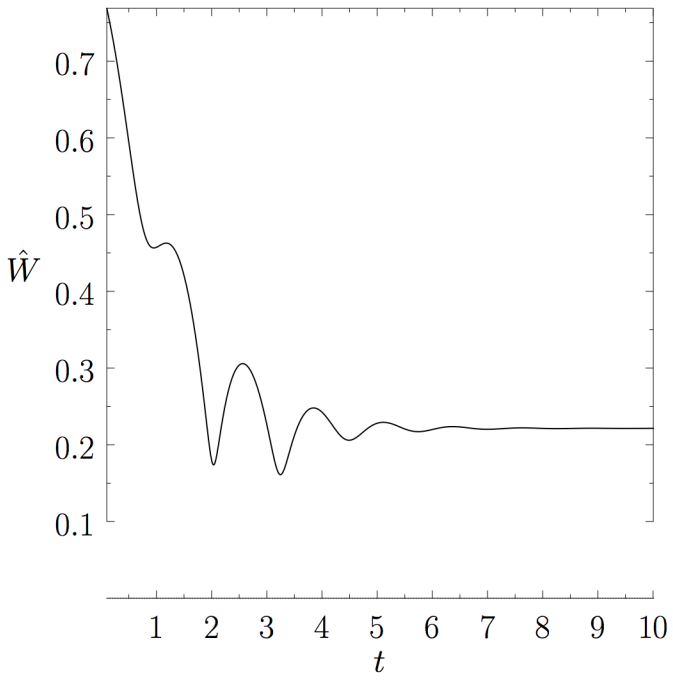

Figure 3.2: Evolution of magnetic island width in the linear response regime.

asymptotic linear response shares many features with the *small locked island*

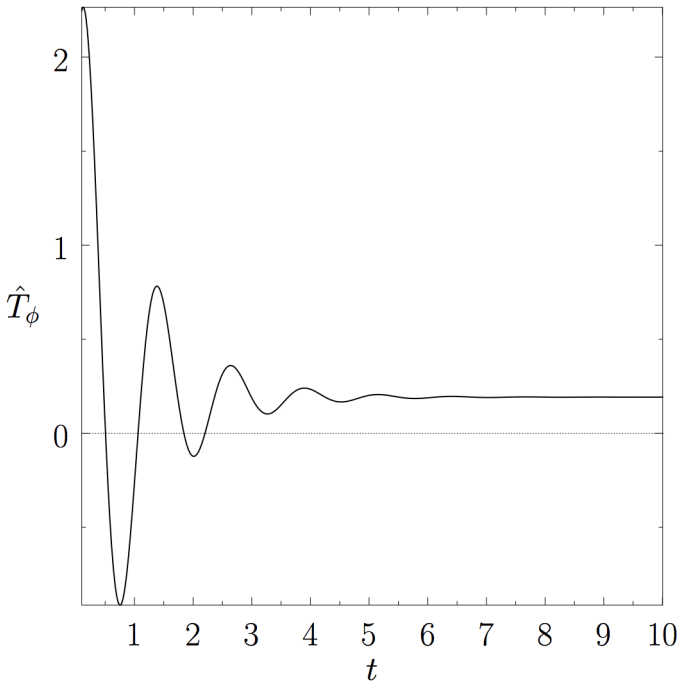

Figure 3.3: Evolution of electromagnetic torque in the linear response regime.

regime which we are going to discuss in Chapter 4. The visco-resistive regime is valid provided $\hat{W} \ll 1$, or $\hat{W}_v^2 \ll (1+\hat{\omega}^2)^{1/2}$.

3.2.3 Toroidal Torque Balance

In general, the time-asymptotic toroidal electromagnetic torque, $T_{\phi_{EM}}$, exerted by an error-field to the plasma varies in time. However, the typical variation timescale is of order the rotation period, which is typically much shorter than the global viscous diffusion timescale. Therefore, we can reasonably assume that the plasma averages over any oscillations in the torque, and it responds primarily to a time-averaged torque, $\langle T_{\phi_{EM}} \rangle$. Let us also

suppose that the modification to the plasma angular velocity profile due to the time-averaged electromagnetic toroidal torque is $\Delta\Omega_\phi(r)$. At the edge of the plasma, we can impose the appropriate spatial boundary condition, $\Delta\Omega_\phi(a) = 0$, which implies that the plasma rotation is effectively *clamped* at the edge and not substantially modified by the error-field [14].

In the vicinity of the rational surface, perpendicular viscosity gives rise to a localized viscous torque that aims to oppose the modification to the plasma rotation profile due to the error-field-induced toroidal electromagnetic torque. This localized viscous torque is:

$$\delta T_{\phi_{VS}} = -\frac{4\pi^2 R_0^3}{\displaystyle\int_{r_s}^{a} \frac{dr}{r\mu}} \frac{(\omega_0 - \omega)}{n}, \tag{3.45}$$

where ω_0 is the *natural frequency*: $\omega_0 = m\,\Omega_{\theta_0}(r_s) - n\,\Omega_{\phi_0}(r_s)$ with Ω_{θ_0}, Ω_{ϕ_0} being the poloidal and toroidal angular velocity profiles of the plasma, respectively, in the *absence* of the error-field. The change in the plasma toroidal angular velocity at the rational surface due to the error-field can be expressed as:

$$\omega = \omega_0 - n\,\Delta\Omega_\phi(r_s) \tag{3.46}$$

Incidentally, ω is the modified angular frequency of a magnetic island chain that is forced to co-rotate with the plasma.

In a steady-state, the localized viscous torque acting on the plasma in the vicinity of the rational surface must balance the time-averaged electromag-

netic torque, $T_{\phi_{VS}} + \langle T_{\phi EM} \rangle = 0$, which implies:

$$\hat{W}_v^4 \, \hat{T}_\phi = R^4 \, (\hat{\omega}_0 - \hat{\omega}) \, . \tag{3.47}$$

The quantity R in Eq. (3.47) is defined as

$$R = \left[\frac{2^5 \, (0.8227)^4}{(2.104)^6} \frac{\delta_{VR}}{r_s} \left(\frac{B_\phi}{B_\theta(r_s)} \right)^2 \Bigg/ \int_{r_s}^{a} \frac{dr}{r} \frac{\mu(\hat{r}_s)}{\mu(r)} \right]^{1/4} . \tag{3.48}$$

Here, we have made use of the expression for the normalized angular frequency $\hat{\omega}$, as defined in Eq. (3.26).

3.2.4 Bifurcation Theory in Linear Response Regime

From Eqs. (3.44) and (3.47), we can obtain a combined expression for the linear response regime:

$$\hat{W}_v^4 \, \frac{\hat{\omega}}{1 + \hat{\omega}^2} = R^4 \, (\hat{\omega}_0 - \hat{\omega}) \tag{3.49}$$

Equation (3.49) can assume the rather convenient algebraic form:

$$f \, (x) \equiv \gamma \, x^3 - \gamma \, x^2 + \frac{\beta}{3} \, x - \frac{1}{27} = 0, \tag{3.50}$$

where:

$$x = \frac{\hat{\omega}}{\hat{\omega}_0}, \tag{3.51}$$

$$\beta = \frac{1}{9} \left[1 + \left(\frac{\hat{W}_v}{R} \right)^4 \right], \tag{3.52}$$

$$\gamma = \frac{\hat{\omega}_0}{27}. \tag{3.53}$$

In Equation (3.50), x parameterizes the actual plasma rotation in the presence of the error-field, β parameterizes the error-field amplitude, and γ parameterizes the intrinsic plasma rotation in the absence of the error-field. The time-asymptotic torque balance equation (3.50) is solved numerically, and it can be seen that, at fixed $\gamma < 1$, x increases monotonically with increasing β. On the other hand, for $\gamma > 1$, there is a range of x values in which x increases with increasing β.

Solutions for which the the plasma rotation decreases with increasing error-field amplitude are dynamically stable, whereas solutions for which the plasma rotation increases with increasing error-field amplitude are dynamically unstable.

The general solution of the torque balance equation exhibits a *forbidden band* [14, 15] of plasma rotation frequencies when the intrinsic plasma rotation is sufficiently high. This band separates a branch of dynamically stable low-rotation solutions from a branch of dynamically stable high-rotation solutions. Thus, when a low-rotation solution crosses the lower boundary of the forbidden band, it becomes dynamically unstable and there is a *bifurcation* to a high-rotation solution. Conversely, when a high rotation solution crosses the upper boundary of the forbidden band, it becomes dynamically unstable and there is a bifurcation to the low rotation solution.

The numerical solution of the time-asymptotic torque balance equation, (3.50), is shown in Fig. 3.4. It can be seen that, at fixed intrinsic plasma rotation (i.e., fixed γ), x decreases monotonically with increasing β when $\gamma <$

1. On the other hand, there is a range of x values in which x increases with increasing β when $\gamma > 1$.

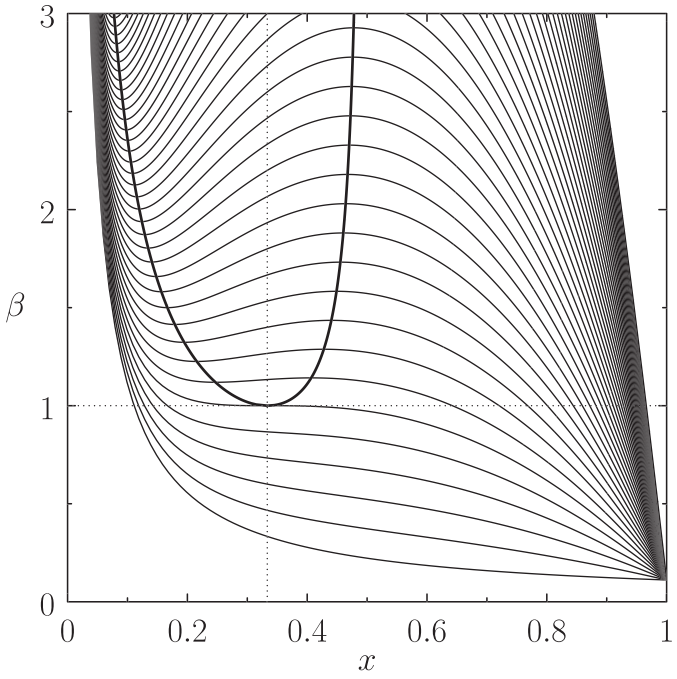

Figure 3.4: Solutions of the time-asymptotic torque-balance equation in the linear response regime. The thin curves show constant-γ solutions plotted in $x - \beta$ space. The curve that passes through the point $x = 1/3, \beta = 1$ corresponds to $\gamma = 1$. Curves that pass below (in β) this point correspond to $\gamma < 1$, and vice versa. The solutions lying inside the thick curve are dynamically unstable. [16].

Taking the limits, suppose that $\hat{\omega}_0 \gg 1$ (high rotation). Then, for $\hat{\omega} \sim \hat{\omega}_0$, Equation (3.49) can be written as:

$$\left(\frac{\hat{W}_v}{R}\right)^{1/4} \simeq \hat{\omega}\left(\hat{\omega}_0 - \hat{\omega}\right) \tag{3.54}$$

Bifurcation from the high rotation to the low rotation solution branch will occur when β exceeds the critical value:

$$\beta_+ \simeq 1 + \frac{3}{4}\left(\gamma - 1\right) \tag{3.55}$$

Bifurcation from the low rotation to the high rotation solution branch will occur when β falls below the critical value:

$$\beta_- \simeq 1 + \left(\frac{4}{3}\right)^{1/2}\left(\gamma^{1/2} - 1\right) \tag{3.56}$$

These expressions are valid only for $\gamma > 1$ ($\hat{\omega}_0 > \sqrt{27}$). For $\gamma \leq 1$, there is no forbidden band of plasma rotation frequencies, and, consequently, no bifurcations. From the expressions for β and γ, we can conclude that the bifurcation from the high-rotation to the low-rotation solution branch occurs when the normalized vacuum island width exceeds the critical value:

$$\hat{W}_{v_+} \simeq \left(8 + \frac{\hat{\omega}_0^2 - 27}{4}\right)^{1/4} R \tag{3.57}$$

Bifurcation from the low rotation to the high rotation solution branch will occur when when the normalized vacuum island width falls below the critical value:

$$\hat{W}_{v_-} \simeq \left[8 + 2\left(\hat{\omega}_0 - \sqrt{27}\right)\right]^{1/4} R \tag{3.58}$$

In general, $\hat{W}_{v_+} > \hat{W}_{v_-}$, thus the system exhibits hysteresis. Once $\hat{W}_v$ has exceeded the critical value required to trigger the bifurcation from a high-rotation to a low-rotation solution, its value must be significantly reduced before the reverse transition is triggered. Likewise, once $\hat{W}_v$ has fallen below the critical value required to trigger the bifurcation from a low-rotation to a high-rotation solution, its value must be significantly increased before the reverse transition is triggered.

3.3 Nonlinear Regime

We shall now investigate the so-called *Rutherford regime*. This is a nonlinear regime in which the reconnected magnetic flux induced by the error-field is governed by two equations:

1. *Rutherford Island Width Evolution Equation*:

$$0.8227 \frac{d}{dt}\left(\frac{W}{r_s}\right) = \Delta' + 2\, m \left(\frac{W_v}{W}\right)^2 \cos\phi \tag{3.59}$$

2. *No-slip Constraint*:

$$\frac{d\phi_s}{dt} = 0 \tag{3.60}$$

The no-slip constraint, (3.60), implies that the magnetic island chain is forced to co-rotate with the plasma at the rational surface.

As we have seen in Chapter 2,

$$W = 4 \left(\frac{|\Psi_s|}{s\, r_s\, B_\theta}\right)^{1/2} r_s \tag{3.61}$$

is the full radial width of the magnetic island chain that forms at the rational surface, and $B_\theta(r_s) = r_s\, B_\phi / R_0\, q(r_s)$ is the local equilibrium poloidal magnetic field. Also:

$$W_v = 4 \left(\frac{|\Psi_v|}{s\, r_s\, B_\theta} \right)^{1/2} r_s \tag{3.62}$$

is the vacuum island width.

The net toroidal electromagnetic torque exerted by the error-field in the vicinity of the rational surface is:

$$\hat{T}_\phi = \left(-\frac{\Delta'}{2\, m} \right) \left(\frac{W}{W_v} \right)^2 \sin\phi, \tag{3.63}$$

which is the same expression as for the linear regime case. The nonlinear regime holds when

$$W \gg \delta_{VR}\,; \tag{3.64}$$

that is, when the magnetic island width greatly exceeds the linear layer width. Conversely, we can express the validity regime for the linear regime as the one where the island width falls below the linear layer width.

Finally, both the linear (visco-resistive) and the nonlinear (Rutherford) regimes are only valid when the *constant-ψ* approximation holds, i.e.,

$$\omega \ll \left(\frac{\tau_R}{\tau_V^2 \tau_H^2} \right)^{1/3}, \quad \left(\frac{\tau_V}{\tau_R^2 \tau_H^2} \right)^{1/3}, \tag{3.65}$$

for the linear regime, and:

$$2\, m \left(\frac{W}{r_s} \right) \left(\frac{W_v}{W} \right)^2 \ll 1 \tag{3.66}$$

for the nonlinear regime.

Equations (3.59), (3.60) and (3.63) can be combined to give:

$$\frac{d\hat{W}}{d\hat{t}} = \frac{1}{2}\left(-1 + \frac{\hat{W}_v^2}{\hat{W}^2}\cos\phi\right), \tag{3.67}$$

$$\frac{d\phi}{d\hat{t}} = \hat{\omega}_0, \tag{3.68}$$

$$\hat{T}_\phi = \frac{\hat{W}_2}{\hat{W}_v^2}\sin\phi, \tag{3.69}$$

with the same normalization scheme as before.

Let us introduce $v \equiv \hat{W}^3$. The nonlinear response equation, (3.67), becomes:

$$\frac{dv}{d\hat{t}} = \frac{3}{2}\left(-v^{2/3} + \hat{W}_v^2\cos\phi\right) \tag{3.70}$$

Along with the normalized no-slip condition (3.68), we can consider a time-asymptotic solution of the form:

$$v\left(\hat{t}\right) = v_{transient}\left(\hat{t}\right) + v_{periodic}\left(\hat{t}\right), \tag{3.71}$$

where:

$$v_{transient}\left(\hat{t}\right) = \begin{cases} \left(\frac{\hat{t}_0 - \hat{t}}{2}\right)^3 & \text{if } \hat{t} < \hat{t}_0 \\ 0 & \text{if } \hat{t} \geq \hat{t}_0 \end{cases} \tag{3.72}$$

And $v_{periodic}\left(\hat{t}\right)$ is a periodic solution of

$$\frac{dv}{d\phi} = \frac{3}{2\,\hat{\omega}_0}\left(-v^{2/3} + \hat{W}_v^2\cos\phi\right) \tag{3.73}$$

In principle, Eq. (3.70) permits the variable v to pass through zero and become negative, which implies that the normalized magnetic island width, $\hat{W}$, also becomes negative. However, a magnetic island chain of negative width

is equivalent to a chain of equal and opposite, positive width in which the O-points are converted into X-points and vice versa. Such conversion implies a π radian helical phase shift. In order to maintain this definition, each time v passes zero and becomes negative we apply the transformation:

$$v \to -v, \tag{3.74}$$

$$\phi \to \phi - \pi. \tag{3.75}$$

The time-asymptotic solution of Eq. (3.70) is periodic in $\hat{t}$, with period $\hat{\tau} = \pi/\hat{\omega}$. Without loss of generality, we can set $\phi(0) = \phi_0$, which allows us to write:

$$\phi\left(\hat{t}\right) = \phi_0 + \hat{\omega}\,\hat{t}. \tag{3.76}$$

A suitable choice of ϕ_0 is one for which $v_{periodic}\,(0) = 0$. Then:

$$v(0) = \left(\frac{\hat{t}_0}{3}\right) \tag{3.77}$$

As we did with the visco-resistive regime case, we will express the nonlinear response equation (3.70) in terms of X and Y phase space coordinates:

$$X = v^{2/3}\cos\phi \tag{3.78}$$

$$Y = v^{2/3}\sin\phi \tag{3.79}$$

Unlike a typical trajectory in the linear regime, which decays to a fixed point, as we have seen, a typical phase-space trajectory in the nonlinear (Rutherford) regime asymptotes to a *closed loop (limit cycle)* that passes

through the origin, as we can see in Fig. 3.5. Assuming that $\hat{\omega} > 0$, the time-asymptotic trajectory orbits the loop in a counterclockwise fashion. Each time the loop passes through the origin the associated island width, $\hat{W}\left(\hat{t}\right)$, falls to zero. As we have already discussed, each time this occurs the island phase decreases discontinuously by π radians, in accordance with the transformation (3.75).

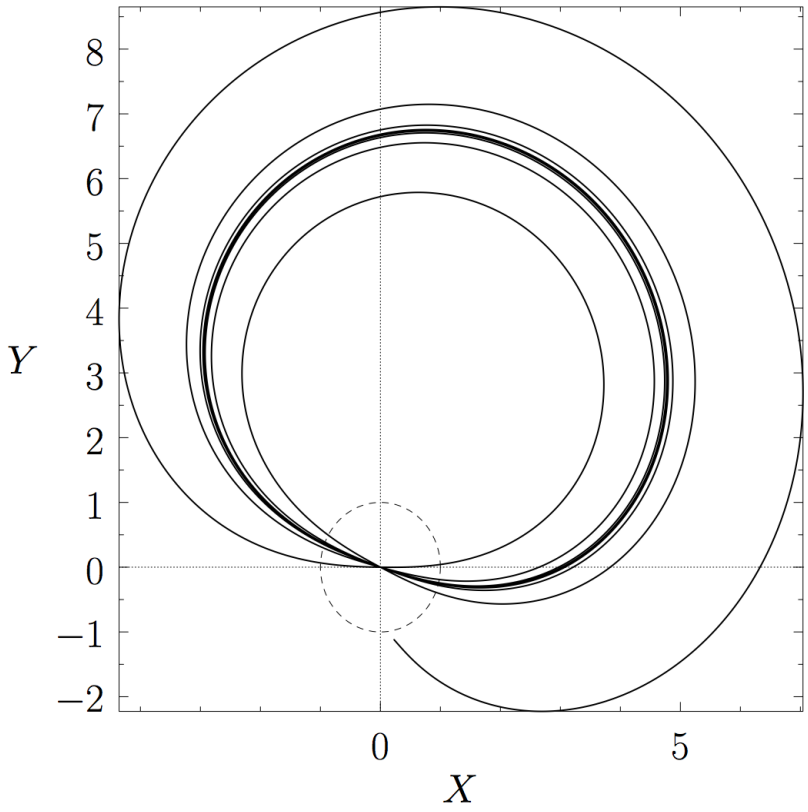

Figure 3.5: Phase-space evolution of the reconnected flux induced in a rotating tokamak plasma by a resonant error-field in the nonlinear response regime.

For a periodic solution of Eq. (3.70), let us introduce two auxiliary variables:

$$u \equiv \left(\frac{\hat{W}}{\hat{W}_v}\right)^3 = \frac{v(\phi)}{\hat{W}_v^3}, \tag{3.80}$$

and

$$\alpha \equiv \frac{2\,\hat{\omega}\,\hat{W}_v}{3}. \tag{3.81}$$

We can now rewrite Eq. (3.70) as:

$$\alpha\,\frac{du}{d\phi} = \cos\phi - u^{2/3} \tag{3.82}$$

Equation (3.82) must be solved subject to the following constraints, with a suitable choice of a mean helical phase ϕ_0:

$$u\left(\phi_0\right) = 0, \tag{3.83}$$

$$u\left(\phi_0 + \pi\right) = 0, \tag{3.84}$$

Hence: $\phi_0 \leq \phi\left(\hat{t}\right) \leq \phi_0 + \pi$. These constraints ensure that the island chain's width instantaneously passes through zero each time its helical phase decreases discontinuously from $\phi_0 + \pi$ to ϕ_0. Comparing to the linear regime case, we can visualize the clearly *oscillatory* time-asymptotic behavior of the magnetic island width (Fig. 3.6) and the electromagnetic torque (Fig. 3.7).

For given α, there is a single value of ϕ_0 that allows the previous constraints to be satisfied simultaneously. Once ϕ_0 and $u\left(\phi\right)$ have been determined numerically, we can calculate:

$$\left[\frac{\hat{W}\left(\phi\right)}{\hat{W}_v}\right]^4 = u^{4/3}, \tag{3.85}$$

$$\hat{T}_\phi = u^{2/3}\sin\phi. \tag{3.86}$$

In accordance with the no-slip constraint for the Rutherford regime, the helical phase of the magnetic island chain, ϕ, increases linearly in time. The chain's width grows from zero when $\phi = \phi_0$ to its maximum value when $\phi \simeq \phi_0 + \pi/2$, and then decays to zero again when $\phi = \phi_0 + \pi$. At this point, as we have discussed, the chain's phase decreases abruptly by π radians, and the cycle repeats ad infinitum.

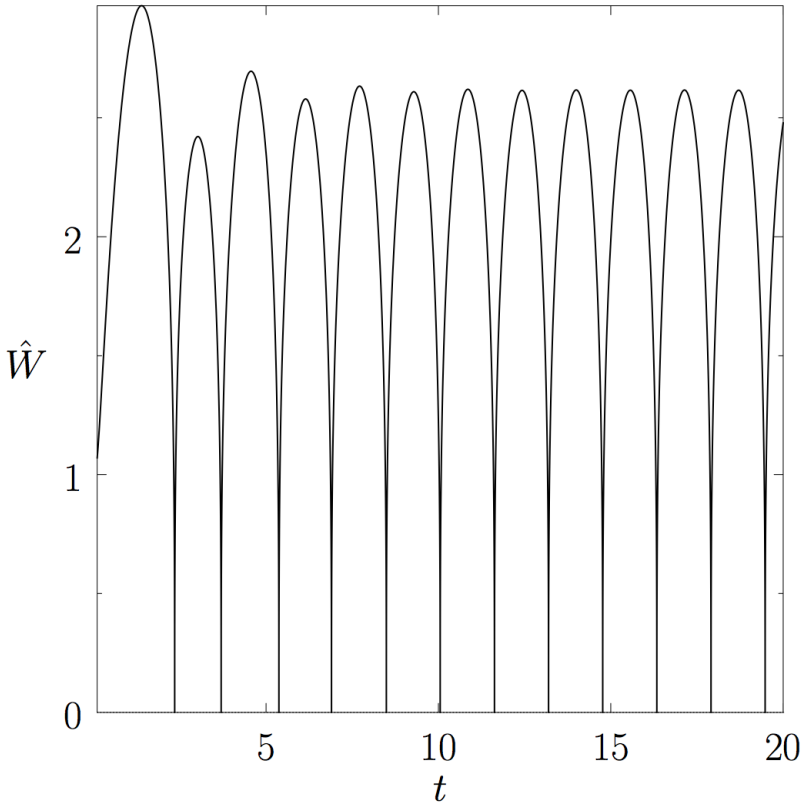

Figure 3.6: Evolution of magnetic island width in the nonlinear response regime.

3.3.1 Analytic Approximations

Due to the periodic character of the time-asymptotic nonlinear response of a rotating tokamak plasma to a resonant error-field, it is useful to define a *cycle average operator*:

$$\langle ... \rangle \equiv \frac{1}{\pi} \int_{\phi_0}^{\phi_0 + \pi} (...)\, d\phi \tag{3.87}$$

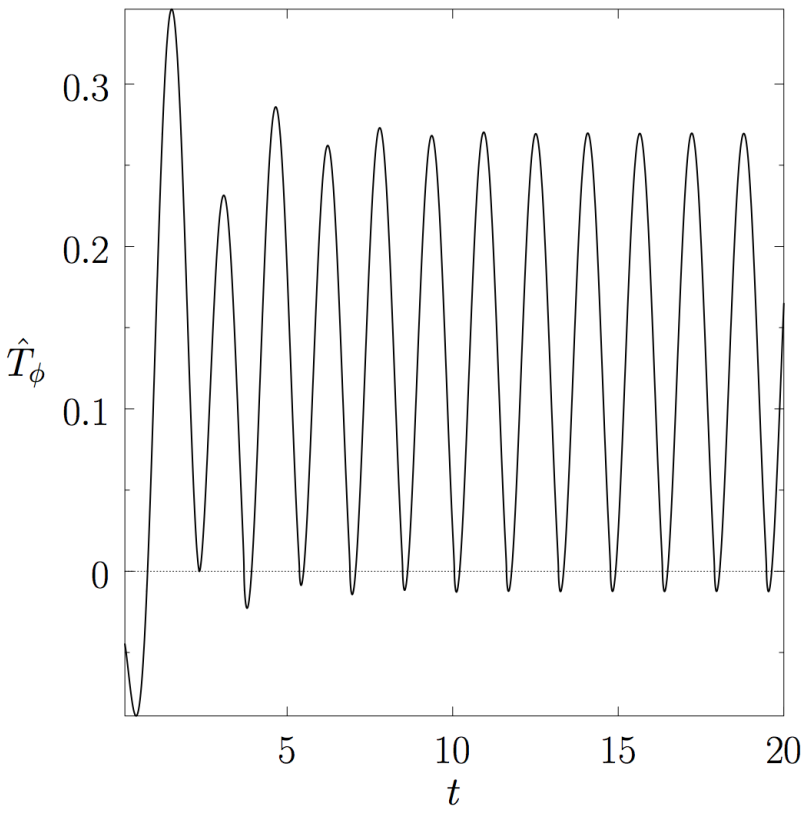

Figure 3.7: Evolution of electromagnetic torque in the nonlinear response regime.

So:

$$\langle \phi \rangle = \phi_0 + \frac{\pi}{2}, \tag{3.88}$$

which means that the mean helical phase of the magnetic island chain during its growth/decay cycle is $\phi_0 + \pi/2$. Averaging Eqs. (3.85) and (3.86) over one cycle yields:

$$\left\langle \left(\frac{\hat{W}}{\hat{W}_v} \right)^4 \right\rangle = \frac{1}{\pi} \int_{\phi_0}^{\phi_0+\pi} u^{4/3}\, d\phi, \tag{3.89}$$

and

$$\left\langle \hat{T}_\phi \right\rangle = \frac{1}{\pi} \int_{\phi_0}^{\phi_0+\pi} u^{2/3} \sin\phi \, d\phi \,. \tag{3.90}$$

In order for us to obtain the nonlinear equivalents for the equations (3.42), (3.43) and (3.44) describing the time-asymptotic linear response of the plasma to the resonant magnetic perturbation, we are going to study the extreme cases of high plasma rotation ($\alpha \gg 1$), and low plasma rotation ($\alpha \ll 1$), and interpolate between them.

1. Low Plasma Rotation:

   Let us consider the low plasma rotation limit, $\alpha \ll 1$. This limit is characterized by $\phi_0 \simeq \pi/2$. This implies that, during the island's growth/decay phase we have described, its helical phase always lies in the destabilizing range, $-\pi/2 < \phi < \pi/2$. On the other hand, the phase lies in the accelerating range, $-\pi < \phi < 0$, during half of the cycle, and in the decelerating range, $0 < \phi < \pi$, during the other half. Thus, in the low plasma rotation limit, the magnetic island achieves a relatively large peak width, and is subject to both accelerating and decelerating electromagnetic torques.

   Expanding in the small parameter α, the lowest order solution to Eq. (3.70) is:

   $$u \simeq \cos^{3/2}\phi \tag{3.91}$$

   By definition, ϕ_0 is the negative root of

   $$u\,(\phi_0) = 0, \tag{3.92}$$

thus: $\phi_0 = -\pi/2$. To next order, the solution to Equation (3.70) is:

$$u \simeq \cos^{3/2}\phi + \frac{9}{4}\,\alpha \cos\phi \sin\phi \tag{3.93}$$

Further examination of the numerical solution to Equation (3.70), as well as Eqs. (3.85), (3.86) and (3.93) result in:

$$\frac{\phi_0}{\pi} \simeq -\frac{1}{2} + 0.8235\,\alpha^2, \tag{3.94}$$

$$u \simeq \left(\cos\phi + \frac{3}{2}\,\alpha \cos^{1/2}\phi \sin\phi\right)^{3/2}, \tag{3.95}$$

$$\left(\frac{\hat{W}}{\hat{W}_v}\right)^4 \simeq \cos^2\phi + 3\,\alpha\cos^{3/2}, \tag{3.96}$$

$$T \simeq \cos\phi\sin\phi + \frac{3}{2}\,\alpha\cos^{1/2}\phi\sin^2\phi. \tag{3.97}$$

Hence, the averaged quantities to the same order will be:

$$\frac{\langle\phi\rangle}{\pi} \simeq 0.8235\,\alpha^2, \tag{3.98}$$

$$\left\langle \left(\frac{\hat{W}}{\hat{W}_v}\right)^4 \right\rangle \simeq 0.5, \tag{3.99}$$

$$\langle T\rangle \simeq \left(\frac{3}{2\pi}\int_{-\pi/2}^{\pi/2} \cos^{1/2}\phi\sin^2\phi\, d\phi\right)\alpha = 0.4577\,\alpha. \tag{3.100}$$

2. High Plasma Rotation:

Let us now consider the high plasma rotation limit, $\alpha \gg 1$. This is characterized by $\phi_0 \simeq 0$. The phase of the magnetic island chain lies in the destabilizing range, $-\pi/2 < \phi < \pi/2$ during half of its growth/decay cycle, and in the stabilizing range during the other half. The phase

always lies in the decelerating range, $0 < \phi < \pi$, and therefore, in the high plasma rotation limit, the magnetic island chain only achieves a relatively small peak width, and is subject to a continuously decelerating toroidal electromagnetic torque.

Expanding in the small parameter α^{-1}, the lowest (zeroth) order solution to Equation (3.70) is:

$$u \simeq \frac{\sin\phi}{\alpha} \tag{3.101}$$

And, to next (first) order, the solution to (3.70) is:

$$u \simeq \frac{\sin\phi}{\alpha} + \alpha^{-5/3} \int_{\phi}^{\pi/2} \sin^{2/3} x \, dx \tag{3.102}$$

According to Eqs. (3.85), (3.86), and (3.101), for the lowest order in α^{-1} we have:

$$\frac{\phi_0}{\pi} \simeq -\left(\frac{1}{\pi}\int_0^{\pi/2} \sin^{2/3}\phi \, d\phi\right) \alpha^{-2/3} = -0.3566\,\alpha^{-2/3}, \tag{3.103}$$

$$\left(\frac{\hat{W}}{\hat{W}_v}\right)^4 \simeq \frac{\sin^{4/3}\phi}{\alpha^{4/3}}, \tag{3.104}$$

$$T \simeq \frac{\sin^{5/3}\phi}{\alpha^{2/3}}. \tag{3.105}$$

The averaged quantities to the same order will be:

$$\frac{\langle\phi\rangle}{\pi} \simeq 0.5 - 0.3566\,\alpha^{-2/3}, \tag{3.106}$$

$$\left\langle\left(\frac{\hat{W}}{\hat{W}_v}\right)^4\right\rangle \simeq \left(\frac{1}{\pi}\int_0^{\pi} \sin^{4/3}\phi \, d\phi\right) \alpha^{-4/3} = 0.5798\,\alpha^{-4/3}, \tag{3.107}$$

$$\langle T\rangle \simeq \left(\frac{1}{\pi}\int_0^{\pi} \sin^{5/3}\phi \, d\phi\right) \alpha^{-2/3} = 0.5356\,\alpha^{-2/3}. \tag{3.108}$$

3. Intermediate Plasma Rotation:

   In order for us to yield analytic approximations for the cycled-average expressions in the intermediate plasma rotation regime where $\alpha \simeq 1$, we interpolate between the small-α results, Equations (3.99), (3.100), and the large-α results, Equations (3.107) and (3.108):

$$\frac{\langle \phi \rangle}{\pi} \simeq \frac{\alpha^2}{1+2\,\alpha^2} - \frac{0.1756\,\alpha^2}{1+0.4950\,\alpha^{8/3}}, \tag{3.109}$$

$$\left\langle \left(\frac{\hat{W}}{\hat{W}_v} \right)^4 \right\rangle \simeq \frac{0.5}{1+0.8624\,\alpha^{4/3}}, \tag{3.110}$$

$$\langle T \rangle \simeq \frac{0.4577\,\alpha}{1+0.8546\,\alpha^{5/3}}. \tag{3.111}$$

   Expressions (3.109), (3.110), and (3.111) are the nonlinear equivalents to the linear results from Equations (3.42), (3.43), and (3.44).

The plasma response to the error-field in the nonlinear regime is broadly similar in nature to that in the linear regime. As the plasma rotation (parameterized by α in the nonlinear regime) increases, the mean helical phase of the magnetic island chain shifts from 0 to $\pi/2$, the mean island width decreases, and the mean decelerating toroidal electromagnetic torque first increases, attains a maximum, and then decreases. The main difference is that in the linear regime the island chain is *locked* in a constant phase relation with respect to the error-field, whereas in the nonlinear case the phase relation is constantly changing due to the no-slip condition.

Finally, because the nonlinear regime is only valid for $\hat{W} \gg 1$, i.e., when the island width greatly exceeds the linear layer width, it follows that the

asymptotic response of the plasma to the error-field only lies in the nonlinear regime when

$$\hat{W}_v \gg \left(\frac{1 + 0.8624\,\alpha^{4/3}}{0.5} \right)^{1/4} \tag{3.112}$$

3.3.2 Bifurcation Theory in Nonlinear Response Regime

From the torque-balance criterion, (3.47), and the equation for time-asymptotic nonlinear response, (3.111), we can obtain a combined expression for the nonlinear response regime:

$$\hat{\omega}_0 - \hat{\omega} = \left(\frac{\hat{W}_v}{R} \right)^4 \frac{0.4577\,\alpha}{1 + 0.8546\,\alpha^{5/3}} \tag{3.113}$$

Equation (3.113) can similarly be expressed in the rather convenient algebraic form:

$$g(x) \equiv \gamma'\,x^{5/3} + \frac{1}{2}\frac{\beta'}{2^{1/3}}\,x - \frac{1}{32}\frac{1}{2^{1/3}} = 0, \tag{3.114}$$

where:

$$\beta' = \frac{1}{16}\left(1 + 0.3051\,\frac{\hat{W}_v^5}{R^4} \right), \tag{3.115}$$

$$\gamma' = \frac{0.3451}{32}\,\hat{W}_v^{5/3}\,\hat{\omega}_0^{5/3} \tag{3.116}$$

As we have discussed for the linear regime, x parameterizes the actual plasma rotation in the presence of the error-field, β' parameterizes the amplitude of the error-field and γ' parameterizes the intrinsic plasma rotation, i.e., in the absence of the error-field. The time-asymptotic torque-balance equation (3.114) is solved numerically (see Fig. 3.8), and it can be seen that, as before, the solution exhibits a forbidden band of plasma rotation frequencies when

$\gamma' > 1$, i.e., when the intrinsic plasma rotation is sufficiently high. This band separates a branch of dynamically stable low-rotation solutions from a branch of dynamically stable high-rotation solutions. When a low-rotation solution crosses the lower boundary of the forbidden band, it becomes dynamically unstable, and there is a bifurcation to a high-rotation solution. Conversely, when a high rotation solution crosses the upper boundary of the forbidden band, it becomes dynamically unstable, and there is a bifurcation to the low rotation solution.

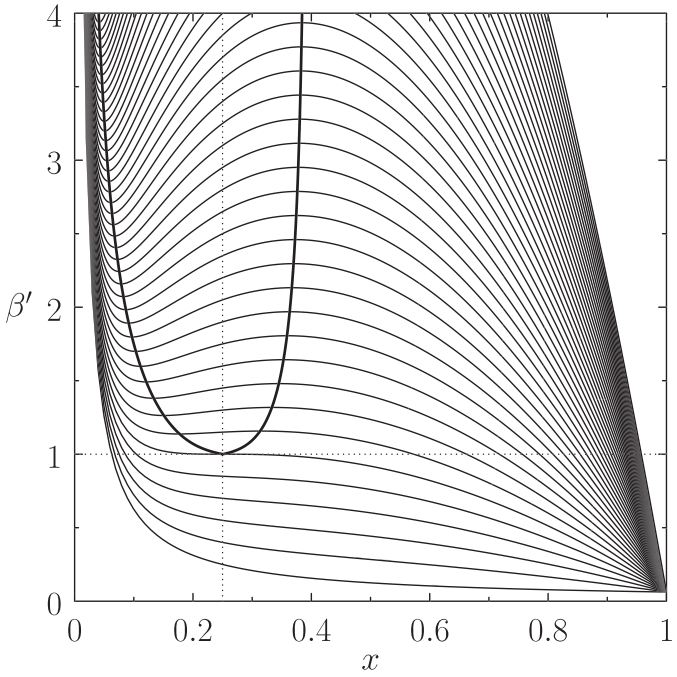

Figure 3.8: Solutions of the time-asymptotic torque-balance equation in the nonlinear response regime. The thin curves show constant-γ' solutions plotted in $x - \beta'$ space. The curve that passes through the point $x = 1/4, \beta' = 1$ corresponds to $\gamma' = 1$. Curves that pass below (in β') this point correspond to $\gamma' < 1$, and vice versa. The solutions lying inside the thick curve are dynamically unstable [16].

The critical values of β' for which the said bifurcations take place are determined numerically, and it can be seen that, to a good approximation, the bifurcation from the high rotation to the low rotation solution branch will occur when β' exceeds the critical value:

$$\beta'_{+} \simeq 1 + \frac{12}{5^{5/3}} \left(\gamma' - 1\right) \tag{3.117}$$

Bifurcation from the low rotation to the high rotation solution branch will occur when β' falls below the critical value:

$$\beta'_{-} \simeq 1 + \frac{1}{2} \frac{5}{54^{1/5}} \left({\gamma'}^{3/5} - 1\right) \tag{3.118}$$

These expressions are only valid for $\gamma' > 1$ (i.e., for $\hat{\omega}_0 > 15.15\, \hat{W}_v$). For $\gamma' \leq 1$, there is no forbidden band of plasma rotation frequencies and, consequently, no bifurcations.

From the expressions for β' and γ', we can conclude that the bifurcation from the high-rotation to the low-rotation solution branch occurs when the normalized island width exceeds the critical value $\hat{W}_{v_+}$, which is the positive root of:

$$\hat{W}^5_{v_+} - 0.4642\, \hat{\omega}_0^{5/3}\, R^4\, \hat{W}^{5/3}_{v_+} - 6.121\, R^4 \simeq 0 \tag{3.119}$$

Bifurcation from the low rotation to the high rotation solution branch occurs when the normalied island width falls below the critical value $\hat{W}_{v_-}$, which is the largest positive root of:

$$\hat{W}^5_{v_-} - 3.898\, \hat{\omega}_0\, R^4\, \hat{W}_{v_-} + 9.875\, R^4 \simeq 0 \tag{3.120}$$

In general, $\hat{W}_{v_+} > \hat{W}_{v_-}$; thus, the system exhibits hysteresis. Once $\hat{W}_v$ has exceeded the critical value required to trigger the bifurcation from a high-rotation to a low-rotation solution, its value must be significantly reduced before the reverse transition is triggered. Likewise, once $\hat{W}_v$ has fallen below the critical value required to trigger the bifurcation from a low-rotation to a high-rotation solution, its value must be significantly increased before the reverse transition is triggered.

Chapter 4

Braking and Locking of Tearing Mode Rotation

We will now shift our focus to the braking of tearing mode rotation by interaction of the mode with resonant magnetic perturbations (error-fields) in tokamak plasmas. As we have seen in Chapter 3, there is a "forbidden band" of tearing mode rotation frequencies that separates a branch of high frequency solutions from a branch of low frequency solutions. When a high-frequency solution crosses the upper boundary of the forbidden band (from above to below), there is a bifurcation to a low-frequency solution, and vice versa. The bifurcation thresholds predicted by simple torque balance theory (which takes into account the electromagnetic braking torque acting on the plasma, as well as the plasma viscous restoring torque, but neglects plasma inertia) are found to be essentially the same as those predicted by more complicated time-dependent mode braking theory (which takes inertia into account).

It has been shown that, according to ideal MHD, magnetic field lines are frozen into the electron fluid, and, hence, that magnetic flux tubes move together with the plasma with the electron fluid velocity (*frozen flux condition*); the magnetic flux through any closed contour in the plasma, each element

of which moves with the local electro fluid velocity, is a conserved quantity. Since, in general, $\mathbf{v}_e \neq 0$ in the laboratory frame, MHD modes in tokamaks are often observed to rotate in this frame [52].

Toroidal plasma rotation plays an important, and in some cases a critical, role in tokamaks. One reason for this is that, with sufficiently fast rotation, magnetic islands co-rotate with the plasma at their associated rational surfaces [14]. However, if the plasma rotation becomes too small then such islands can *lock* (i.e., become stationary in the laboratory frame of reference) [14, 9]. In many tokamaks it is found that the position of a locked mode of given helicity is always the same with respect to the vacuum vessel, indicating that there is a breaking of the axisymmetry of the external field; for example, an error-field due to imperfections in shape and misalignment of the external field coils. Because the plasma can not flow through a large island at any significant rate, mode locking also leads to a stopping of the plasma rotation at the resonant surface, and an appreciable slowing down of the plasma as a whole due to viscous coupling [52].

Mode locking is usually observed if tearing modes grow to a large amplitude, and it has a variety of negative consequences. It often results in a disruption [43, 13] (i.e., a total loss of plasma containment), which is thought to be because magnetic stochastization [30] due to the interaction among tearing modes at different resonant surfaces can only take place if the modes are locked together in phase; which is true, by definition, for locked modes.

Mode locking usually takes place in two distinct stages: First, the is-

land rotation frequency is reduced to a small fraction of its unperturbed value via electromagnetic torques associated with eddy currents induced in the conducting structures that inevitably surround the plasma. Typical examples of such structures include the vacuum vessel, and passive plates used to stabilize kink modes. These structures are simply referred to as the "wall"[18]. Second, the island locks to a static resonant error-field. (Such fields are always present in tokamak plasmas because of magnetic field-coil misalignments, poorly compensated coil feeds, et cetera) Generally speaking, unless the error-field in question is unusually large, mode locking is not possible without the prior braking action of eddy currents [14].

A theory of tearing mode rotation braking due to eddy currents excited in the wall was developed by Nave & Wesson [33]. According to this theory, the electromagnetic braking torque acting on the island is balanced by plasma inertia (because a significant fraction of the plasma is forced to co-rotate with the island as a consequence of the inability of the plasma to easily cross the island's magnetic separatrix, as well as the action of plasma perpendicular viscosity). In Nave & Wesson's theory, the island rotation frequency decelerates smoothly and reversibly as the island width increases. As we have already discussed, an alternative theory was subsequently developed by Fitzpatrick [14], in which the electromagnetic braking torque is balanced by plasma viscosity, and plasma inertia plays a negligible role.

Nave & Wesson's theory is appropriate to islands that grow comparatively rapidly; i.e., on a timescale that is small compared to the plasma momen-

tum confinement time. Fitzpatrick's theory, on the other hand, is appropriate to islands that grow comparatively slowly; i.e., on a timescale that is long compared to the momentum confinement time. According to Fitzpatrick's theory, if the intrinsic plasma rotation at the rational surface is sufficiently large, then there is a forbidden band of island rotation frequencies. This band, which has been directly observed experimentally [22], separates a branch of high-frequency solutions from a branch of low-frequency solutions. If the island width becomes sufficiently large that a high-frequency solution crosses the upper boundary of the forbidden band (from above to below) then there is a bifurcation to a low-frequency solution. This bifurcation is associated with a sudden collapse in the island rotation frequency to a comparatively low level. Such a collapse is almost certain to lead to mode locking. Fitzpatrick's theory of tearing mode rotation braking is based on the hypothesis that solutions of the steady-state torque balance equation (the two torques in question being the electromagnetic braking torque and the viscous restoring torque) for which the island rotation frequency decreases with increasing island width are dynamically stable, whereas solutions for which the island frequency increases with increasing island width are dynamically unstable.

4.1 Interaction of Tearing Mode with Resonant Magnetic Perturbation

In the following, we only consider the toroidal equations of motion. Due to strong poloidal flow damping, poloidal effects are negligible in our analysis.

However, we present the poloidal equations in the Appendix for completeness.

We will adopt a version of the previously established error-field theory [14] as a model for the interaction of tearing mode with resonant magnetic perturbation. In this model, the dynamics of the interaction are governed by the plasma torque balance and the nonlinear magnetic island evolution [41].

The basic formulation of our problem is identical to the one that we defined in the previous chapter; we are considering a large aspect-ratio, low-β tokamak plasma whose magnetic flux surfaces map out almost concentric circles in the poloidal plane. Such a plasma can be satisfactorily approximated as a periodic cylinder. Let a be the *minor radius* of the plasma. We will adopt the standard right-handed cylindrical coordinates (r, θ, z). The system will be assumed to be periodic in the z-direction with period $2\pi R_0$, where $R_0 \gg a$ is the simulated plasma major radius. For consistency with the parameters of toroidal geometry, it is convenient to define the simulated toroidal angle $\phi = z/R_0$. We are adopting standard, large aspect-ratio tokamak orderings, according to which $B_z \gg B_\theta$, $R_0 \gg a$ and $q \sim \mathcal{O}(1)$.

The model will comprise a closed set of equations, consisting of:

1. The plasma equation of toroidal angular motion given the no-slip constraint for the nonlinear regime,

2. The net torque exerted in the vicinity of the rational surface, and

3. The magnetic island phase evolution (Rutherford) equation.

Each one of the components of this model will be studied individually.

4.2 Plasma Equation of Toroidal Angular Motion Equation

Let $\Omega_\phi(r,t) = \Omega_\phi^{(0)}(r) + \Delta\Omega_\phi(r,t)$ be the plasma toroidal angular velocity profile, where:

1. $\Omega_\phi^{(0)}(r)$ is the steady-state profile in the absence of braking electromagnetic (EM) torque, and

2. $\Delta\Omega_\phi(r,t)$ is the modification to the profile due to the error-field.

The plasma toroidal equation of motion [14] is written:

$$\rho\, r R_0^2 \frac{\partial \Delta\Omega_\phi}{\partial t} - \mu \frac{\partial}{\partial r}\left(r R_0^2 \frac{\partial \Delta\Omega_\phi}{\partial r}\right) = \frac{T_{\phi_{EM}}(t)}{4\pi^2 R_0}\,\delta(r - r_s)\,, \tag{4.1}$$

where ρ and μ are assumed to be uniform across the plasma (mass density and perpendicular viscosity, respectively).

The physical boundary conditions satisfied by the perturbed toroidal angular velocity profile are:

$$\frac{\partial \Delta\Omega_\phi(0,t)}{\partial r} = \Delta\Omega_\phi(\alpha,t) = 0 \tag{4.2}$$

4.3 No-slip constraint

The conventional *no-slip constraint* that we have introduced when studying the *nonlinear response* to tearing modes demands that the island chain

co-rotates with the plasma at the rational surface. This constraint holds for island widths much larger than the linear layer width at the rational surface. We can write:

$$\Psi_s(t) = |\Psi_s|(t) \exp\left[-i \int_0^t \omega(t')\, dt'\right], \tag{4.3}$$

where:

$$\omega = m\,\Omega_\theta(r_s) - n\,\Omega_\phi(r_s) = \omega_0 - n\,\Delta\Omega_\phi(r_s, t) \tag{4.4}$$

The first term in the right hand side of the previous equation is absorbed into ω_0 (the plasma poloidal angular velocity profile is fixed) due to strong poloidal flow damping, and $\omega_0 = m\,\Omega_\theta(r_s) - n\,\Omega_\phi^{(0)}(r_s, t)$ is the steady-state island rotation frequency in the absence of the braking torque.

4.4 Normalized Plasma Equation of Toroidal Angular Motion

Let us introduce *normalized* variables:

1. $\hat{r} = r/a$,
2. $\hat{r}_s = r_s/a$,
3. $\tau_V = a^2\rho/\mu$,
4. $\Omega(\hat{r}, t) = n\Delta\Omega_\phi(r_s, t)/\omega_0$,
5. $\tau_H = \dfrac{R_0}{B_\phi}\dfrac{\sqrt{\mu_0\,\rho(r_s)}}{n\,s}$,

where τ_V is the momentum confinement timescale, and τ_H is the hydromagnetic timescale [14]. We are assuming that $\mu(r)$, $\rho(r)$ possess *flat profiles* across the plasma, for the sake of simplicity; all dependence on viscosity and density is included in τ_V and τ_H, respectively.

We can normalize Equation (4.4) as:

$$\omega = \omega_0 - n\,\Delta\Omega_\phi\left(\hat{r}_s, t\right) = \omega_0\left[1 - \Omega\left(\hat{r}_s, t\right)\right], \tag{4.5}$$

which, in turn, yields the normalized plasma equation of toroidal angular motion:

$$\tau_V\,\frac{\partial\Omega}{\partial t} - \frac{1}{\hat{r}}\frac{\partial}{\partial\hat{r}}\left(\hat{r}\frac{\partial\Omega}{\partial\hat{r}}\right) = -\,T_{\phi_{EM}}\left(t\right)\frac{\delta\left(\hat{r} - \hat{r}_s\right)}{\hat{r}} \tag{4.6}$$

4.4.1 Solution of Normalized Plasma Equation of Toroidal Angular Motion

The partial differential equation (4.6), together with the physical boundary conditions (4.2), can be reduced into a system of ordinary differential equations, upon defining a set of velocity eigenfunctions and eigenvalues [51]:

$$\frac{d}{dr}\left(r\,\mu\,\frac{du_k}{dr}\right) + r\beta_k\,u_k = 0, \tag{4.7}$$

$$\frac{du_k(0)}{dr} = u_k(a) = 0 \tag{4.8}$$

From Equation (4.7) one gets:

$$u_k(r) = C_k\,J_0\left(\frac{r}{a}\,j_{0,k}\right); \qquad \beta_k = \frac{j_{0,k}^2}{\tau_V}, \tag{4.9}$$

where $j_{0,k}$ is the k^{th} zero of the J_0 Bessel function.

Let us expand Ω (i.e., the normalized modification of the toroidal rotation profile due to the error-field) in terms of Bessel functions:

$$u_k(\hat{r}) = \frac{\sqrt{2} J_0(j_{0,k}\,\hat{r})}{j_{0,k}}. \tag{4.10}$$

From Abramowitz & Stegun [1] it can be easily demonstrated that, upon defining

$$C_k \equiv \left(\int_0^a r\, J_0^2\left[(r/a) j_{0,k}\right]\, dr \right)^{-1/2}, \tag{4.11}$$

we satisfy the *orthonormality condition*

$$\int_0^1 \hat{r}\, u_k(\hat{r})\, u_{k'}(\hat{r})\, d\hat{r}' = \delta_{kk'},$$

as well as:

$$\delta(\hat{r} - \hat{r}_s) = \sum_{k=1}^{\infty} \hat{r}\, u_k(\hat{r})\, u_{k'}(\hat{r})$$

According to the Sturm-Liouville theory, the eigenfunctions u_k form a complete set. Therefore we can expand the toroidal angular velocity as:

$$\Omega(\hat{r}, t) = \sum_{k=1}^{\infty} h_k(t)\, \frac{u_k(\hat{r})}{u_k(\hat{r}_s)}, \tag{4.12}$$

which automatically satisfies the boundary conditions (4.2). Note that:

$$\left(\frac{d^2}{d\hat{r}^2} + \frac{1}{\hat{r}} \frac{d}{d\hat{r}} \right) u_k = -\, j_{0,k}^2\, u_k \tag{4.13}$$

Using the orthonormality relation, and substituting into the equation of motion (4.6) we obtain a simplified, numerable set of ordinary differential equations for $h_k(t)$:

$$\tau_V \frac{dh_k}{dt} + j_{0,k}^2\, h_k = -\, \frac{T_{\phi_{EM}}(t)}{4\pi^2\, R_0^3\, \mu} \left[u_k(\hat{r}_s)\right]^2 \tag{4.14}$$

Finally, Equations (4.5) and (4.12) give:

$$\omega\,(t) = \omega_0 \left(1 - \sum_{k=1}^{\infty} h_k\right) \tag{4.15}$$

4.5 Torques

4.5.1 Electromagnetic Braking Torque

The flux-surface integrated toroidal electromagnetic torque acting on the plasma is given by:

$$T_{\phi_{EM}} = \oiint d\theta\, d\phi\, r R_0^2\, (\mathbf{j}\times\mathbf{B})_\phi = \oiint d\theta\, d\phi\, r R_0^2\, (j_r\, b_\theta - j_\theta\, b_r) \tag{4.16}$$

Due to the angular integrations, only the product of the perturbations gives a contribution in (4.16). The marginally-stable ideal MHD equations incorporate $\mathbf{j}\times\mathbf{B} = \nabla p$ [47]. It follows immediately from the form of Equation (4.16), and from the assumed periodicity of the system in the toroidal direction, that $T_{\phi_{EM}}$ is *zero* in the region of the plasma governed by ideal MHD (i.e., the outer region). Thus, any net electromagnetic torques acting on the plasma must develop in the vicinity of the rational surfaces, where ideal MHD breaks down, and large perturbed helical currents flow (i.e., in the inner region) [14].

Let us consider a general (m, n) magnetic perturbation

$$\delta\mathbf{B} = \delta\mathbf{B}(r)\exp\left(i\,\xi\right), \tag{4.17}$$

where $\xi = m\,\theta - n\,\phi - \int^t \omega\,(t')\; dt'$, and $\omega(t)$ is the instantaneous mode (angular) rotation frequency. The perturbed current, $\delta\mathbf{j}$, is also assumed to be of this form.

Suppose that the large perturbed helical currents flowing in the vicinity of the rational flux surfaces are "sheet"-like; i.e., $|\delta j_r| \ll |\delta j_\theta|, |\delta j_\phi|$ in the inner region. The expression for the magnetic perturbation, the Ampère - Maxwell equation, and current conservation ($\nabla \delta\mathbf{j} = 0$) imply that:

$$\delta\mathbf{B} \cdot \mathbf{B}_0 \simeq 0 \tag{4.18}$$

in the inner region, where $\mathbf{B}_0$ is the equilibrium magnetic field.

Electromagnetic torques can also develop *outside* the plasma due, for instance, to eddy currents induced in conducting walls or helical currents flowing around external windings. If the system is cylindrically symmetric (as in our case), and if these external currents are localized in radius (i.e., any walls or external windings are thin), then the external currents are also sheet-like. The inner region is extended to include those regions where the external helical currents flow. Likewise, the outer region is extended to include those regions outside the plasma where no helical currents flow. Clearly, in a cylindrically symmetric system the external "sheet" eddy currents induced by an (m, n) tearing mode have the same helical pitch as the equilibrium magnetic field at the rational surfaces inside the plasma. Similarly, this is the optimal pitch for external helical windings interacting with (m, n) modes. It follows that the jumps with respect to the various resonant surfaces give rise to Dirac-like localized torques:

$$T_{\phi_{EM}} \simeq \sum_k T_{\phi_{EM_k}} \delta\left(r - r_k\right), \tag{4.19}$$

where $T_{\phi_{EM_k}}$ are the components of the toroidal electromagnetic torque which develops in a portion of the inner region centered on r_k, where r_k are the radii, extended to include both the radii of rational surfaces inside the plasma and the radii of any conducting walls or helical windings outside the plasma.

Finally, let us note that the ratio of poloidal to toroidal torques is $(-m/n)$ in all parts of the inner region.

The toroidal electromagnetic torque exerted in the immediate vicinity of the rational surface as a consequence of the interaction of the tearing mode with the resonant magnetic perturbation is

$$T_{\phi_{EM}} = \frac{4\pi^2\, m\, n R_0}{\mu_0} |\Psi_v||\Psi_s| \sin\left(\phi_s - \phi_v\right) \tag{4.20}$$

Without loss of generality, we can write $\phi_s - \phi_v = \phi$ (we can assume that $\phi_v = 0$). We can rewrite the expressions for the true and vacuum magnetic island width as:

$$W = 4\left(\frac{q_s}{s_s}\frac{R_0}{B_\phi}|\Psi_s|\right)^{1/2}, \tag{4.21}$$

$$W_v = 4\left(\frac{q_s}{s_s}\frac{R_0}{B_\phi}|\Psi_v|\right)^{1/2}, \tag{4.22}$$

where the subscript s denotes evaluation at $r = r_s$.

Taking the definition for the electromagnetic braking torque into account, we can revisit the expression for the plasma toroidal angular equation of motion. After some algebra, it follows that:

$$\tau_V \frac{dh_k}{dt} + \hat{\jmath}_{0,k}^2\, h_k = \frac{1}{2^8}\frac{n}{m}\left(\frac{W}{r_s}\right)^2\left(\frac{W_v}{r_s}\right)^2\left(\frac{r_s}{R_0}\right)^2 \frac{\tau_V}{\tau_H^2}\left[\hat{u}_k\right]^2 \sin\left(\phi_s - \phi_v\right), \tag{4.23}$$

where the "hatted" quantities are defined as: $\hat{\mathrm{j}}_{0,k} = \hat{r}_s\, \mathrm{j}_{0,k}$ and $\hat{u}_k = \hat{r}_s\, u_k(\hat{r}_s)$.

Tokamak plasmas possess strong parallel (to the magnetic field) viscosity which opposes the plasma compression associated with poloidal rotation. In conventional tokamak plasmas, this viscosity is sufficiently large to prevent any error-field-induced change in the poloidal rotation. Thus, in practice, the plasma does not respond to the poloidal component of the electromagnetic torque exerted in the vicinity of the rational surface by the error-field. However, for the sake of completeness of our analysis, a treatment of poloidal electromagnetic torques will be presented in the Appendix.

The reader is strongly recommended to refer to Appendix A of [51] for a generalized discussion of Newcomb's equation and electromagnetic torques generated by nonlinear interaction among tearing modes.

4.5.2 Viscous Restoring Torque

The *toroidal* viscous torque exerted at rational surface is [14]:

$$T_{\phi_{VS}} = \frac{-4\pi^2 R_0^3}{\displaystyle\int_{r_s}^{a} dr/r\mu}\,\frac{\omega_0 - \omega}{n} = \frac{4\pi^2 R_0^3}{\displaystyle\int_{r_s}^{a} dr/r\mu}\,\frac{\omega - \omega_0}{n} \tag{4.24}$$

4.5.3 Toroidal torque balance

According to [15], it is easily demonstrated that *zero* net torque can be exerted on flux surfaces located in a region of the plasma which is governed by the equations of ideal MHD. Thus, the electromagnetic torque exerted on the plasma by the error-field develops in the immediate vicinity of the rational

surface, where ideal MHD breaks down. Similarly, perpendicular viscosity gives rise to a localized viscous torque, acting in the vicinity of the rational surface, which *opposes* the error-field-induced change in the plasma rotation. This change gives rise to a modification of the "slip frequency".

In *steady state* ($d/dt \to 0$), the equation of motion (4.14) yields:

$$j_{0,k}^2 h_k = -\frac{T_{\phi_{EM}}(t)}{4\pi^2 R_0^3 \mu} \left[u_k\left(\hat{r}_s\right)\right]^2, \tag{4.25}$$

which implies

$$h_k = -\frac{T_{\phi_{EM}}(t)}{4\pi^2 R_0^3 \mu} \frac{\left[u_k\left(\hat{r}_s\right)\right]^2}{j_{0,k}^2}. \tag{4.26}$$

Using the identity [1]:

$$\sum_{k=1}^{\infty} \frac{\left[u_k\left(\hat{r}_s\right)\right]^2}{j_{0,k}^2} \equiv \ln\left(\frac{1}{\hat{r}_s}\right), \tag{4.27}$$

we can rewrite the expression for the *normalized frequency* as:

$$\hat{\omega} = \omega/\omega_0 \tag{4.28}$$

or:

$$\hat{\omega} = 1 - \sum_{k=1}^{\infty} h_k, \tag{4.29}$$

and:

$$1 - \hat{\omega} = -\frac{T_{\phi_{EM}}(t)}{4\pi^2 R_0^3 \mu} \ln\left(\frac{1}{\hat{r}_s}\right) \tag{4.30}$$

The left hand side of the *torque balance equation* (4.30) corresponds to the *viscous torque*, acting to maintain plasma rotation, and the right hand side corresponds to the *electromagnetic braking torque*.

Both toroidal electromagnetic torque ($T_{\phi_{EM}}(t)$) and the modification to the toroidal angular velocity profile ($\Delta\Omega_\phi(r,t)$) can be expressed as combinations of time-independent (constant) and time-dependent (oscillatory) terms [16]:

$$T_{\phi_{EM}}(t) = \langle T_{\phi_{EM}} \rangle + \widetilde{T}_{\phi_{EM}} \exp(i\,\omega\,t)\,, \tag{4.31}$$

$$\Delta\Omega_\phi(r,t) = \Delta\Omega_\phi(r) + \Delta\widetilde{\Omega}_\phi(r) \exp(i\,\omega\,t)\,, \tag{4.32}$$

where in both cases: $\omega = \omega_0 - n\,\Delta\Omega_\phi(\hat{r}_s)$.

We will treat the constant (time-independent) and the oscillatory (time-dependent) parts of the expressions above separately.

4.5.3.1 Time-Independent

Recall, at steady state: $d/dt \to 0$.

The plasma toroidal angular equation of motion for the locked mode can be written as:

$$-4\pi^2 R_0^3 \frac{d}{dr}\left(\mu\, r \frac{d\Delta\Omega_\phi}{dr}\right) = \langle T_{\phi_{EM}} \rangle\, \delta(r - r_s)\,, \tag{4.33}$$

satisfying the physical boundary conditions:

$$\frac{d\Delta\Omega_\phi(0)}{dr} = \Delta\Omega_\phi(\alpha) = 0, \tag{4.34}$$

where:

$$\Delta\Omega_\phi(0) = \Delta\Omega_\phi(r_s) \begin{cases} 1 & \text{if } r < r_s \\ \left[\int_r^\alpha dr/r\mu \Big/ \int_{r_s}^\alpha dr/r\mu\right] & \text{if } r > r_s \end{cases}, \tag{4.35}$$

with

$$\Delta\Omega_\phi\left(r_s\right) = \frac{\langle T_{\phi_{EM}}\rangle}{4\pi^2 R_0^3}\int_{r_s}^{\alpha}\frac{dr}{r\mu} \tag{4.36}$$

4.5.3.2 Time-Dependent

The plasma toroidal angular equation of motion can be written as

$$-4\pi^2 R_0^3\left[i\,\omega\,\rho\,r\,\Delta\widetilde{\Omega}_\phi - \frac{d}{dr}\left(\mu\,r\,\frac{d\Delta\widetilde{\Omega}_\phi}{dr}\right)\right] = \widetilde{T}_{\phi_{EM}}\,\delta\left(r-r_s\right), \tag{4.37}$$

satisfying the physical boundary conditions

$$\frac{d\Delta\widetilde{\Omega}_\phi\left(0\right)}{dr} = \Delta\widetilde{\Omega}_\phi\left(\alpha\right) = 0, \tag{4.38}$$

where

$$\Delta\widetilde{\Omega}_\phi\left(0\right) = \Delta\widetilde{\Omega}_\phi\left(r_s\right)\begin{cases}\exp\left[+\,\mathrm{e}^{\,i\,\pi/4}\sqrt{\omega\,\tau_V}\left(r-r_s\right)/r_s\right] & \text{if } r<r_s\\ \exp\left[-\,\mathrm{e}^{\,i\,\pi/4}\sqrt{\omega\,\tau_V}\left(r-r_s\right)/r_s\right] & \text{if } r>r_s\end{cases}, \tag{4.39}$$

with

$$\Delta\widetilde{\Omega}_\phi\left(r_s\right) = \frac{\mathrm{e}^{-\,i\,\pi/4}\widetilde{T}_{\phi_{EM}}}{4\pi^2 R_0^3\,2\,\mu(r_s)\sqrt{\omega\,\tau_V}} \tag{4.40}$$

In conventional, large aspect-ratio, ohmically heated tokamaks: $\omega\,\tau_V \gg 1$.

In the *nonlinear response regime*: $\langle T_{\phi_{EM}}\rangle \sim \widetilde{T}_{\phi_{EM}}$, and from [16],

$$\langle T\rangle \simeq \frac{0.4577\alpha}{1+0.8546\,\alpha^{5/3}}, \tag{4.41}$$

thus:

$$\langle T\rangle \simeq \widetilde{T}_{\phi_{EM}} \simeq 0.2468, \tag{4.42}$$

for $\alpha = 1$ that corresponds to intermediate rotation. Recall that $\alpha \ll 1$ corresponds to the slow rotation limit, and $\alpha \gg 1$ corresponds to the fast rotation limit.

4.6 Magnetic Island Phase Evolution

Magnetic island suppression by a resonant magnetic perturbation relative to its naturally saturated state has been observed for error-field amplitudes both above and below the threshold for mode locking [28]. When the error-field amplitude is above the threshold, there is always a transient oscillating phase before the mode locking eventually takes place. During this transient phase, it is found numerically that the time-averaged rotational frequency collapses to zero, and the island width is shrunk as a result of its modification by the error-field.

Recall the no-slip constraint from Equation (4.4):

$$\omega \equiv \frac{d\phi(t)}{dt} = \omega_0 - n\,\Delta\Omega_\phi\,(r_s) \tag{4.43}$$

Let us focus on the transient oscillating magnetic island phase, ϕ. From [19] we adopt the reasonable general *ansatz* for the phase:

$$\phi(t) = \phi_0 + \delta\phi = \omega_0\,t + a_s\,\sin(\omega_0\,t) + a_c\,\cos(\omega_0\,t)\,, \quad \delta\phi << \phi_0 \tag{4.44}$$

Now:

$$\omega = \frac{d\phi(t)}{dt} = \omega_0 + a_s\,\omega_0\,\cos(\omega_0\,t) - a_c\,\omega_0\,\sin(\omega_0\,t) = \omega_0 - n\,\Delta\Omega_\phi\,(r_s) \Rightarrow$$

$$\Rightarrow \omega_0 + a_s\,\omega_0\,\cos(\omega_0\,t) - a_c\,\omega_0\,\sin(\omega_0\,t) =$$

$$= \omega_0 - n\left\{\frac{\langle T_{\phi_{EM}}\rangle}{4\pi^2 R_0^3}\int_{r_s}^{\alpha}\frac{dr}{r\mu(r_s)} + \frac{\mathrm{e}^{-i\pi/4}\,\widetilde{T}_{\phi_{EM}}}{4\pi^2 R_0^3\,2\,\mu(r_s)\sqrt{\omega\,\tau_V}}\,\cos(\omega\,t) + \right.$$

$$\left. + \frac{i\,\mathrm{e}^{+i\pi/4}\,\widetilde{T}_{\phi_{EM}}}{4\pi^2 R_0^3\,2\,\mu(r_s)\sqrt{\omega\,\tau_V}}\,\sin(\omega\,t)\right\} \tag{4.45}$$

The trigonometric functions $\sin\phi\,(t)$ and $\cos\phi\,(t)$ are analytic. According to our ansatz, $\delta\phi\,(t) = a_s \sin(\omega_0\, t) + a_c \cos(\omega_0\, t) \ll \omega_0 t$, so we can *Taylor expand* to first order each one of them close to $\phi_0 = \omega_0 t$:

$$\cos(\omega\, t) = \cos(\phi(t)) = \cos(\phi_0 + \delta\phi)\,, \tag{4.46}$$

which implies

$$\cos(\omega_0 t + \delta\omega\, t) \simeq \cos(\omega_0\, t) + \delta\omega\, t\,(-\sin(\omega_0\, t))\,, \tag{4.47}$$

where $\delta\omega \equiv a_s\,\omega_0\,\cos(\omega_0\, t) - a_c\,\omega_0\,\sin(\omega_0\, t)$.

Hence:

$$\cos(\omega\, t) \;\simeq\; \cos(\omega_0\, t) \;-\; \{[\omega_0\, a_s\,\cos(\omega_0\, t)] - \omega_0\, a_c\,\sin(\omega_0\, t)\}\; t\,\sin(\omega_0\, t)\,, \tag{4.48}$$

thus:

$$\cos(\omega\, t) \simeq \cos(\omega_0\, t) - \left[\omega_0\, a_s\,\cos(\omega_0\, t)\,\sin(\omega_0\, t) + \omega_0\, a_c\,\sin^2(\omega_0\, t)\right]\; t, \tag{4.49}$$

or: $\cos(\omega\, t) \simeq \cos(\omega_0\, t)$ since higher order terms are negligible.

Similarly:

$$\sin(\omega\, t) \simeq \sin(\omega_0\, t) + \left[-\omega_0\, a_c\,\sin(\omega_0\, t)\,\cos(\omega_0\, t) + \omega_0\, a_s\,\cos^2(\omega_0\, t)\right]\; t, \tag{4.50}$$

or: $\sin(\omega\, t) \simeq \sin(\omega_0\, t)$.

Taking those approximations and Equation (4.45) into account, we can

write:

$$\omega = \omega_0 + a_s\,\omega_0\,\cos(\omega_0\,t) - a_c\,\omega_0\,\sin(\omega_0\,t) \simeq \omega_0 - n\left\{\frac{\langle T_{\phi_{EM}}\rangle}{4\pi^2 R_0^3}\int_{r_s}^{\alpha}\frac{dr}{r\mu(r_s)} + \right.$$

$$\left. + \frac{\mathrm{e}^{-i\pi/4}\,\widetilde{T}_{\phi_{EM}}}{4\pi^2 R_0^3\,2\,\mu(r_s)\sqrt{\omega\,\tau_V}}\,\cos(\omega_0\,t) + \frac{i\,\mathrm{e}^{+i\pi/4}\,\widetilde{T}_{\phi_{EM}}}{4\pi^2 R_0^3\,2\,\mu(r_s)\sqrt{\omega\,\tau_V}}\,\sin(\omega_0\,t)\right\} \quad (4.51)$$

Matching coefficients in Equation (4.51) yields:

$$a_s = -\frac{n\,\mathrm{e}^{-i\pi/4}\,\widetilde{T}_{\phi_{EM}}}{\omega_0\,4\pi^2 R_0^3\,2\,\mu(r_s)\sqrt{\omega\,\tau_V}}, \quad (4.52)$$

$$a_c = \frac{n\,\mathrm{e}^{+i\pi/4}\,\widetilde{T}_{\phi_{EM}}}{\omega_0\,4\pi^2 R_0^3\,2\,\mu(r_s)\sqrt{\omega\,\tau_V}}, \quad (4.53)$$

where $|a_s| \ll 1$, $|a_c| \ll 1$.

4.7 Magnetic Island Width Evolution

In order to complete the model system of the interaction between the tearing mode and the resonant magnetic perturbation we need to include the magnetic island nonlinear width evolution with time, governed by the *Rutherford equation* [41]:

$$0.8227\,\tau_R\,\frac{d}{dt}\left(\frac{W}{r_s}\right) = \Delta' - 2\,m\left(\frac{W_v}{W}\right)^2\cos(\phi(t))\,, \quad (4.54)$$

where

$$\cos(\phi(t)) \simeq \cos(\omega_0\,t) - \frac{1}{2}a_s^2\sin^2(\omega_0\,t)\cos(\omega_0\,t) - a_s a_c\sin(\omega_0\,t)\cos^2(\omega_0\,t) -$$

$$- \frac{1}{2}a_c^3\cos^3(\omega_0\,t) - a_s\sin^2(\omega_0\,t) - a_c\cos(\omega_0\,t)\sin(\omega_0\,t) \simeq \cos(\omega_0\,t)\,, \quad (4.55)$$

if we neglect the higher order terms.

A similar *ansatz* to the one from Equation (4.44) can be invoked for the oscillatory nature of the magnetic island width in the transient phase:

$$W(t) = W_0 + \delta W = W_0 + \delta W_s \, \sin(\omega_0 \, t) + \delta W_c \, \cos(\omega_0 \, t) \, , \quad \delta W << W_0 \quad (4.56)$$

In the equation above, we have only kept the leading terms of the angle expansions. Hence, the arguments of the trigonometric functions are $\omega_0 \, t$ instead of $\omega \, t$. We need to calculate the square of the magnetic island width since this is how it appears in the Rutherford equation:

$$\begin{aligned}
[W(t)]^2 &= [W_0 + \delta W = W_0 + \delta W_s \, \sin(\omega_0 \, t) + \delta W_c \, \cos(\omega_0 \, t)]^2 = \\
&= W_0^2 + \delta W_s^2 \sin^2(\omega_0 \, t) + \delta W_c^2 \cos^2(\omega_0 \, t) + 2 \, W_0 \, \delta W_s \sin(\omega_0 \, t) + \\
&\quad + 2 \, W_0 \, \delta W_c \cos(\omega_0 \, t) + 2 \, \delta W_s \, \delta W_c \sin(\omega_0 \, t) \cos(\omega_0 \, t) \simeq \\
&\simeq W_0^2 \, \left[1 + 2 \, \delta \hat{W}_s \sin(\omega_0 \, t) + 2 \, \delta \hat{W}_c \cos(\omega_0 \, t) \right] , \quad (4.57)
\end{aligned}$$

where:

1. We have neglected higher order terms.

2. We have introduced the normalized quantities $\delta \hat{W}_s \equiv \delta W_s / W_0$ and $\delta \hat{W}_c \equiv \delta W_c / W_0$.

We can now integrate Rutherford Equation, (4.54), over one transient oscillation period $T \equiv 2\pi / \omega_0$:

$$0.8227 \, \tau_R \left\langle \frac{d}{dt} \left(\frac{W}{r_s} \right) \right\rangle = \Delta' - 2 \, m \, W_v^2 \left\langle \cos(\phi) / W^2 \right\rangle \quad (4.58)$$

with $\langle f \rangle \equiv T^{-1} \int_0^T f\, dt$. Performing a Taylor expansion on the expression (4.57) we yielded for W^2:

$$W^2(t) \simeq W_0^2 + 2\,\delta\hat{W}_c\, W_0^2 + 2\,\omega_0\, t\,\delta\hat{W}_s\, W_0^2 = W_0^2\left[1 + 2\,\delta\hat{W}_c + \delta\hat{W}_s\,\omega_0\, t\right] \quad (4.59)$$

From Equation (4.58), the average in the right hand side yields:

$$\left\langle \cos(\phi)/W^2 \right\rangle \simeq$$
$$\frac{\pi\left[2 + 4\,\delta\hat{W}_c - 2\,a_c\,(1+a_s)\left(1 + 2\,\delta\hat{W}_c\right)\pi - 4\,\delta\hat{W}_s\,\pi + a_c^2\left(-1 - 2\,\delta\hat{W}_c + \pi\,2\,\delta\hat{W}_s\right)\right]}{\left(W_0 + 2\,\delta\hat{W}_c\, W_0\right)^2\,\omega_0} \quad (4.60)$$

Huang and Zhu in [28] argue that $\langle \cos(\phi)/W^2 \rangle$ is negative in the island evolution equation, which means that the error-field term provides a suppressing effect to the magnetic island evolution.

4.8 Time-averaged Normalized Toroidal Net Torque

Following [16], we have the following two equations for normalized electromagnetic torque and normalized viscous torque:

$$\hat{T}_{\phi_{EM}} = \left(\frac{\hat{W}}{\hat{W}_v}\right)^2 \sin\left(\phi(t)\right) \quad (4.61)$$

$$\hat{\omega} - \hat{\omega_0} \simeq -\frac{(2.104)^6}{2^5\,(0.8227)^4}\frac{1}{\hat{\delta}_{VR}}\left[\ln\left(\frac{1}{\hat{r}_s}\right)\right]\left(\frac{n}{m}\right)^2\left(\frac{r_s}{R_0}\right)^2 \hat{W}_v^2\,\hat{W}^2\,\sin\left(\phi(t)\right),$$

which implies:

$$\hat{T}_{\phi_{VS}} \simeq \frac{4\pi^2\, R_0^3}{\int_{r_s}^{a} dr/r\mu}\,\frac{1}{n}\,\frac{(2.104)^6}{2^5\,(0.8227)^4}\,\frac{1}{\hat{\delta}_{VR}}\times \\ \times\left[\ln\left(\frac{1}{\hat{r}_s}\right)\right]\left(\frac{n}{m}\right)^2\left(\frac{r_s}{R_0}\right)^2\,\hat{W}_v^2\,\hat{W}^2\,\sin\left(\phi(t)\right), \quad (4.62)$$

where the derivation of the expression for $\hat{\omega}-\hat{\omega_0}$ is presented in detail in the Appendix.

The sum of expressions (4.61) and (4.62) yields the *Normalized Toroidal Net Torque*:

$$\begin{aligned}\hat{T}_{\phi_{\rm net}} &= \hat{T}_{\phi_{EM}} + \hat{T}_{\phi_{VS}} = \\ &= \left\{\left(\frac{\hat{W}}{\hat{W}_v}\right)^2 + \frac{4\pi^2\, R_0^3}{\int_{r_s}^{a} dr/r\mu}\,\frac{1}{n}\,\frac{(2.104)^6}{2^5\,(0.8227)^4}\,\frac{1}{\hat{\delta}_{VR}}\times\right. \\ &\left.\times\left[\ln\left(\frac{1}{\hat{r}_s}\right)\right]\left(\frac{n}{m}\right)^2\left(\frac{r_s}{R_0}\right)^2\,\hat{W}_v^2\,\hat{W}^2\right\}\,\sin\left(\phi(t)\right).\end{aligned} \quad (4.63)$$

Although this expression looks fairly complicated, we can immediately see that $\hat{T}_{\phi_{\rm net}} \sim W^2 \sin\left(\phi(t)\right)$, so we can integrate it over one transient oscillation period, as we did with the Rutherford equation:

$$\left\langle W^2 \sin\left(\phi(t)\right)\right\rangle \simeq \frac{\pi\, W_0^2}{\omega_0}\times \\ \times\left[2\left(1+a_s\right)\left(1+2\,\delta\hat{W}_c\right)\pi - a_c^2\left(\pi + 2\pi\,\delta\hat{W}_c\right) + a_c\left(2+4\,\delta\hat{W}_c+4\pi\,\delta\hat{W}_s\right)\right]. \quad (4.64)$$

Again, according to the argument by Huang and Zhu, the averaged external term from the error-field is argued to be positive in the torque balance equation, which means that the error-field provides a braking effect to the mode rotation.

4.9 Bifurcation theory

Let us bring everything together for this step. We have: $\hat{t} = t/\tau_V$, $\hat{\omega} = \omega/\omega_0$, $\hat{j}_{0,k} = \hat{r}_s\, j_{0,k}$ and $\hat{u}_k = \hat{r}_s\, u_k\left(\hat{r}_s\right)$. As we show in the Appendix, the plasma toroidal angular equation of motion can be written as:

$$\frac{dh_k}{d\hat{t}} + \hat{j}_{0,k}^2\, h_k = \frac{1}{2^8}\frac{n}{m}\left(\frac{W}{r_s}\right)^2\left(\frac{W_v}{r_s}\right)^2\left(\frac{r_s}{R_0}\right)^2\frac{\tau_V}{\tau_H^2}\left(\hat{u}_k\right)^2\sin\left(\phi\left(t\right)\right) \tag{4.65}$$

As for the *normalized frequency*, recall Eq. (4.28):

$$\hat{\omega} = \omega/\omega_0 \tag{4.66}$$

or

$$\hat{\omega} = 1 - \sum_{k=1}^{\infty} h_k \tag{4.67}$$

Equations (4.65) and (4.67) are the *rotation-braking equations*. In a steady-state (i.e., $d/d\hat{t} \to 0$), Eq. (4.65) yields the velocity profile expressed in terms of Bessel functions:

$$h_k = -\frac{T_{\phi EM}(t)}{4\pi^2 R_0^3 \mu}\frac{\left[u_k\left(\hat{r}_s\right)\right]^2}{j_{0,k}^2} = \frac{1}{2^8}\frac{n}{m}\left(\frac{W}{r_s}\right)^2\left(\frac{W_v}{r_s}\right)^2\left(\frac{r_s}{R_0}\right)^2\frac{\tau_V}{\tau_H^2}\frac{\left[u_k\left(\hat{r}_s\right)\right]^2}{j_{0,k}^2}\sin\left(\phi\left(t\right)\right). \tag{4.68}$$

Using the identity from [1]:

$$\sum_{k=1}^{\infty}\frac{\left[u_k\left(\hat{r}_s\right)\right]^2}{j_{0,k}^2} \equiv \ln\left(\frac{1}{\hat{r}_s}\right),$$

we can rewrite Equation (4.67) as:

$$1 - \hat{\omega} = \frac{1}{2^8}\frac{n}{m}\left(\frac{W}{r_s}\right)^2\left(\frac{W_v}{r_s}\right)^2\left(\frac{r_s}{R_0}\right)^2\frac{\tau_V}{\tau_H^2}\ln\left(\frac{1}{\hat{r}_s}\right)\sin\left(\phi\left(t\right)\right) \tag{4.69}$$

This is the *torque balance equation*, which clearly exhibits the dependence $\hat{\omega} \sim W^2 \sin(\phi(t))$. Taking into account that $\omega = \omega_0 \hat{\omega}$ we can take the average of both sides of Eq. (4.69):

$$\langle \omega \rangle = \omega_0 - \frac{1}{2^8} \frac{n}{m} \left(\frac{1}{r_s} \right)^2 \left(\frac{W_v}{r_s} \right)^2 \left(\frac{r_s}{R_0} \right)^2 \frac{\tau_V}{\tau_H^2} \ln \left(\frac{1}{\hat{r}_s} \right) \left\langle W^2 \sin(\phi(t)) \right\rangle \quad (4.70)$$

Although we have already calculated the average in the right hand side of the expression above earlier [see Eq. (4.64)], we will further simplify it by removing higher-order, negligible terms:

$$\left\langle W^2 \sin(\phi(t)) \right\rangle \simeq \frac{\pi W_0^2}{\omega_0} (2\pi + 2\pi a_s + 2 a_c) \quad (4.71)$$

After some tidying up, Equation (4.70) for the average frequency can now be written as:

$$\langle \omega \rangle \simeq \omega_0 - \frac{1}{2^8} \frac{n}{m} \left(\frac{W_v}{r_s} \right)^2 \left(\frac{1}{R_0} \right)^2 \frac{\tau_V}{\tau_H^2} \ln \left(\frac{1}{\hat{r}_s} \right) W_0^2 \left(2\pi^2 + 2\pi^2 a_s + 2\pi a_c \right) \quad (4.72)$$

The last step is to substitute the coefficients a_s and a_c in the above equation with the expressions (4.52), (4.53) we have already found for them through matching. We will take time averages over the transient oscillation period, so instead of ω we will have $\langle \omega \rangle$ everywhere:

$$\langle \omega \rangle \simeq \omega_0 - \frac{1}{2^8} \frac{n}{m} \left(\frac{W_v}{r_s} \right)^2 \left(\frac{1}{R_0} \right)^2 \frac{\tau_V}{\tau_H^2} \ln \left(\frac{1}{\hat{r}_s} \right) \times$$

$$\times \left[2\pi^2 W_0^2 - 2\pi^2 \frac{n \, \mathrm{e}^{-i\pi/4} \widetilde{T}_{\phi_{EM}}}{\omega_0 \, 4\pi^2 R_0^3 \, 2\mu \sqrt{\langle \omega \rangle \, \tau_V}} + 2\pi \frac{n \, \mathrm{e}^{+i\pi/4} \widetilde{T}_{\phi_{EM}}}{\omega_0 \, 4\pi^2 R_0^3 \, 2\mu \sqrt{\langle \omega \rangle \, \tau_V}} \right] \quad (4.73)$$

This fairly complicated expression is an *implicit equation*. Studying the extreme behaviors (limits) for increasing island widths, we can study island locking and bifurcations.

Multiplying both sides of Equation (4.73) by $\sqrt{\langle\omega\rangle}$ yields:

$$\langle\omega\rangle^{3/2} \simeq \omega_0 \langle\omega\rangle^{1/2} + c_1 \langle\omega\rangle^{1/2} + c_2, \tag{4.74}$$

where:

$$c_1 = -\frac{1}{2^8}\frac{n}{m}\left(\frac{W_v}{r_s}\right)^2\left(\frac{1}{R_0}\right)^2\frac{\tau_V}{\tau_H^2}\ln\left(\frac{1}{\hat{r}_s}\right)2\pi^2 W_0^2, \tag{4.75}$$

and

$$c_2 = \frac{1}{2^8}\frac{n}{m}\left(\frac{W_v}{r_s}\right)^2\left(\frac{1}{R_0}\right)^2\frac{\tau_V}{\tau_H^2}\ln\left(\frac{1}{\hat{r}_s}\right)2\pi\times \\ \times\left[\frac{\pi\, n\, \mathrm{e}^{-i\pi/4}\,\widetilde{T}_{\phi_{EM}}}{\omega_0\, 4\pi^2\, R_0^3\, 2\,\mu\,\sqrt{\tau_V}} - \frac{n\,\mathrm{e}^{+i\pi/4}\,\widetilde{T}_{\phi_{EM}}}{\omega_0\, 4\pi^2\, R_0^3\, 2\,\mu\,\sqrt{\tau_V}}\right] \tag{4.76}$$

Setting $z = \langle\omega\rangle^{1/2}$, we can write the third order algebraic equation:

$$z^3 = (\omega_0 + c_1)\, z + c_2 \Rightarrow z^3 - (\omega_0 + c_1)\, z - c_2 = 0. \tag{4.77}$$

Equation (4.77) has three convoluted solutions, one of which is real.

The left hand side of Eq. (4.77) can be written as

$$f\left(\langle\omega\rangle\right) = \langle\omega\rangle^{3/2} - (\omega_0 + c_1)\langle\omega\rangle^{1/2} - c_2 \tag{4.78}$$

The frequency threshold for the onset of bifurcation will be the extremum of function (4.78):

$$\frac{df\left(\langle\omega\rangle\right)}{d\langle\omega\rangle} = \frac{-(\omega_0 + c_1) + 3\langle\omega\rangle}{2\langle\omega\rangle^{1/2}} = 0 \tag{4.79}$$

thus:

$$\langle\omega\rangle^* = \frac{\omega_0 + c_1}{3}, \tag{4.80}$$

with $\langle\omega\rangle^*$ being the *critical frequency*. The second derivative of Equation (4.78) for $\langle\omega\rangle = \langle\omega\rangle^*$ is:

$$\left.\frac{d^2 f\left(\langle\omega\rangle\right)}{d\left\langle\omega\right\rangle^2}\right|_{\langle\omega\rangle^*} = \frac{d}{d\left\langle\omega\right\rangle}\left[\frac{-\left(\omega_0 + c_1\right) + 3\left\langle\omega\right\rangle}{2\left\langle\omega\right\rangle^{1/2}}\right]_{\langle\omega\rangle^*} = \frac{\omega_0 + c_1}{2\left(\dfrac{\omega_0 + c_1}{3}\right)^{3/2}} > 0, \tag{4.81}$$

which means that the critical frequency for the onset of bifurcation is a minimum of function (4.78):

$$\langle\omega\rangle^* = \frac{\omega_0}{3} - \frac{2\pi^2 W_0^2}{3\,2^8}\frac{n}{m}\left(\frac{W_v}{r_s}\right)^2 \frac{1}{R_0^2}\frac{\tau_V}{\tau_H^2}\ln\left(\frac{1}{\hat{r}_s}\right) \tag{4.82}$$

In references [14], [15] and [16], it is argued that solutions of the torque balance equation (4.69) for which the island rotation frequency decreases as the island width increases are dynamically stable, whereas solutions for which the island rotation frequency increases as the island width increases are dynamically unstable. This argument leads to the conclusion that when the intrinsic plasma rotation is sufficiently high, the general solution of the torque balance equation exhibits a forbidden band of island rotation frequencies. This band separates a branch of dynamically stable low frequency solutions from a branch of dynamically stable high frequency solutions. Thus, when a low frequency solution crosses the lower boundary of the forbidden band, it becomes dynamically unstable, and there is presumably a bifurcation to a high frequency solution. Likewise, when a high frequency solution crosses the upper

boundary of the forbidden band, it becomes dynamically unstable, and there is presumably a bifurcation to a low frequency solution.

Chapter 5

Summary and Conclusion

In Chapter 1, we argued that our planet is ailing and that action against global warming needs to be taken fast. In search for an alternative to fossil fuels, nuclear fusion emerges indisputably as the pathway to an environmentally friendly and inexhaustible source of energy. On earth, the most promising scheme to achieve nuclear fusion is the tokamak, which confines the plasma in a magnetic field. It was our choice to make this dissertation as standalone as possible, therefore we introduced the building blocks of our study, starting with the basic principles of Magnetohydrodynamics (MHD), the theoretical framework of studying plasmas as electrically conducting fluids. The concepts of MHD Equilibrium and Stability for simple geometries are fundamental in our understanding of tokamak plasmas, however the introduction of resistivity in our equations gives rise to a potentially deleterious instability: the tearing mode. These resistive instabilities are driven by current and pressure gradients and involve a reconfiguration of the magnetic and velocity fields localized into a narrow region located at a resonant magnetic surface. While the equilibrium magnetic field lines are located on concentric nested toroidal flux surfaces, the instability creates magnetic islands in which field lines connect flux tubes together, allowing for a high radial heat transport, and thus resulting in a loss

of confinement.

Chapter 2 is dedicated to the Tearing Mode Theory; finite resistivity invalidates the ideal-MHD "frozen flux" condition and it allows magnetic field lines to break and *reconnect*, rearranging the magnetic topology. The phenomenon of magnetic reconnection is observed both in nature, (especially in space phenomena such as solar flares, coronal mass injections and reconfigurations of the Earth's magnetosphere) as well as in laboratory plasma experiments and large-scale confinement devices such as tokamaks and reverse field pinches. Through simple physical considerations, the two-dimensional slab configuration is presented as a pedagogic model of introducing the resistive instability before considering a generalized sheared magnetic field and a helical external perturbation in order to obtain the tearing mode dispersion relation. The tearing mode reconnects the magnetic field at the so called *resonant surface*. The ingenious method of asymptotic matching greatly facilitates our analysis: the plasma is effectively divided into a narrow "inner region", centered at the resonant surface, where resistive and inertial effects are important and an "outer region", comprising the bulk of the plasma, where resistivity is negligible and the ideal MHD equations are applicable. The equation describing the dynamics of the tearing mode are solved separately in each region and then they are *matched* in an intermediate matching region. Linear theory predicts that the tearing mode grows exponentially on a hybrid timescale, but when the magnetic island chain width exceeds the width of the linear layer, forces due to nonlinear eddy currents replace inertia as the dominant mecha-

nism opposing mode growth, and a significant extension of the linear theory comes into play: the nonlinear tearing mode theory. The magnetic island growth in the nonlinear regime is governed by the Rutherford equation. Note that the island does not grow indefinitely, but it eventually saturates.

In Chapter 3, we studied the linear and nonlinear response of a rotating tokamak plasma to an error-field, i.e., an externally imposed resonant magnetic perturbation, which could be attributed to a misaligned coil. First, a general analysis of the constant-ψ, resistive magnetohydrodynamical theory of the response of a rotating, quasi-cylindrical tokamak plasma to a resonant magnetic perturbation (error-field) was presented. This analysis covered both *linear plasma response*, where the width of the magnetic island chain induced at the rational surface is much less than the linear layer width, as well as *nonlinear plasma response*, where the width of the driven magnetic island chain is permitted to greatly exceed the linear layer width. We find that the response of the plasma in the immediate vicinity of the rational surface to the applied error-field can be usefully visualized as a trajectory in a kind of phase-space. If the response is linear (i.e., if the driven island width is much less than the linear layer width) then the phase-space trajectory decays to a fixed point. On the other hand, if the response is nonlinear (i.e., if the driven island width is much larger than the linear layer width) then the trajectory asymptotes to a limit cycle. The fixed point corresponds to a time-asymptotic linear response characterized by a non-rotating island chain of fixed width, through which the plasma at the rational surface flows. The limit cycle corresponds to a time-

asymptotic nonlinear response characterized by a rotating island chain that is convected by the plasma at the rational surface, and whose width periodically falls to zero. Each time this occurs, the helical phase of the chain (measured with respect to the error-field) decreases discontinuously by π radians. Consequently, although the phase is constantly increasing in time, it is nevertheless restricted to lie in a limited range of values.

The analysis predicted that, in the presence of a resonant error-field, there is a forbidden band of plasma rotation frequencies which effectively separates relatively high-rotation from relatively low-rotation states. Second, we investigated *bifurcations* between the dynamically stable low-rotation and high-rotation solution branches of the torque balance equation, triggered as the amplitude of the error-field is varied.

In Chapter 4, we extended the analysis of Chapter 3; the focus was shifted to an exhaustive investigation of the interaction of a tearing mode in a rotating tokamak plasma with a resonant magnetic perturbation (error-field). A complete set of rotation-braking equations was derived for the nonlinear regime, comprising the plasma equation of toroidal angular motion (from which we derived the angular velocity profile expressed in Bessel functions), the no-slip condition which yielded the angular velocity profile modification due to the error-field, and the magnetic island width evolution equation, i.e., Rutherford equation. Due to the oscillatory nature of the nonlinear regime, we averaged both the electromagnetic torque and the island width evolution equation over a period in order to obtain expressions for the braking and locking of

tearing mode rotation by the interaction of the mode with resonant magnetic perturbations. As we have seen before, for sufficiently large intrinsic plasma rotation, there is a "forbidden band" of tearing mode rotation frequencies that separates a branch of high-frequency solutions from a branch of low-frequency solutions.

Even though our analysis has been quite straightforward and it has greatly increased our understanding of the phenomena under consideration, it is unfortunately subject to a number of limitations: First, it only applies to large-aspect ratio, low-β, circular cross-section, tokamak plasmas. Second, it assumes that the tearing mode amplitude varies on a timescale that is much longer than the plasma momentum confinement timescale. Third, it assumes that the plasma density and perpendicular viscosity are uniform across the plasma. The simple phenomenological parameter choice of plasma viscosity in the adopted model may be further replaced by a more first-principle physics-based model for viscosity, which can include effects from both collisions and turbulence. Fourth, our model assumes that the plasma poloidal rotation profile is fixed due to the action of strong poloidal flow damping, even though we have presented a more complete set of equations in the Appendix. Fifth, it neglects the transient response of the eddy currents to the magnetic field generated by the rotating tearing mode. Finally, it ignores the presence of conducting structures, or "walls", that can be of varying thickness, resistivity, and magnetic permeability, greatly complicating the analysis needed. Other elements of the interaction between a tearing mode and an error-field are

missing in the adopted model that may potentially have significant impacts; among them are equilibrium flow, two-fluid and finite-Larmor-radius effects, additional terms in the Rutherford equation (e.g., bootstrap current and *Neoclassical Tearing Modes* [25]) as well as the study of the interaction of *multiple* error-field harmonics with multiple tearing modes, that may be seen to have a stabilizing effect on mode locking. Finally, a straightforward extension of this analysis is the inclusion of *drift effects* (e.g., semi-collisional effects in the linear regime, and the ion polarization current in the nonlinear regime).

Although derived in a fairly simple setting, the methods presented in this dissertation can be applied and extended in order to incorporate more advanced, rich phenomena, and, therefore, to be of benefit to the fusion research community. Further theoretical investigations, propelled from and enriched with feedback from experiments, will keep paving the road leading to practically endless possibilities of research, the cornerstone of which is the dream of mankind to be able to produce clean, safe, everlasting and sustainable energy for everybody from virtually limitless natural resources; putting Science at the service of Humanity.

Appendices

Appendix A

Derivation of the Grad-Shafranov Equation

We shall present a detailed, step-by-step derivation of the Grad-Shafranov Equation, as an Appendix to Chapter 1.

A.1 Derivation

Step 1

We define a *cylindrical coordinate system*, (R, ϕ, Z), about the major axis of a torus. Let the unit vectors along the axes be $(\hat{\mathbf{e}}_R, \hat{\mathbf{e}}_\phi, \hat{\mathbf{e}}_Z)$. Assume two-dimensional axisymmetric toroidal configuration: $\partial/\partial\phi = 0$.

Step 2

We will now decompose $\mathbf{B}$ and $\mathbf{j}$ into poloidal and toroidal components:

$$\mathbf{B} = \mathbf{B}_p + B_\phi \, \hat{\mathbf{e}}_\phi, \tag{A.1}$$

$$\mathbf{j} = \mathbf{j}_p + j_\phi \, \hat{\mathbf{e}}_\phi, \tag{A.2}$$

where

$$\mathbf{B}_p = B_R \, \hat{\mathbf{e}}_R + B_Z \, \hat{\mathbf{e}}_Z, \tag{A.3}$$

$$\mathbf{j}_p = j_R \, \hat{\mathbf{e}}_R + j_Z \, \hat{\mathbf{e}}_Z. \tag{A.4}$$

Step 3

Now we will express the poloidal and toroidal components of $\mathbf{B}$ and $\mathbf{j}$ in terms of the flux function ψ.

Let us start with the magnetic field. Since $\nabla\cdot\mathbf{B} = 0$, we can introduce a magnetic vector potential function, $\mathbf{A}$, such that $\mathbf{B} = \nabla\times\mathbf{A}$, and in cylindrical coordinates:

$$B_R = -\frac{\partial A_\phi}{\partial Z}, \qquad B_Z = \frac{1}{R}\frac{\partial}{\partial R}\left(R\,A_\phi\right) \tag{A.5}$$

We define the flux function $\psi \equiv R\,A_\phi$. We can now write:

$$B_R = -\frac{1}{R}\frac{\partial\psi}{\partial Z}, \qquad B_Z = \frac{1}{R}\frac{\partial\psi}{\partial R} \tag{A.6}$$

Thus, the poloidal component of $\mathbf{B}$ is:

$$\mathbf{B}_p = -\frac{1}{R}\frac{\partial\psi}{\partial Z}\,\hat{\mathbf{e}}_R + \frac{1}{R}\frac{\partial\psi}{\partial R}\,\hat{\mathbf{e}}_Z. \tag{A.7}$$

Let us also define the quantity $F \equiv R\,B_\phi/\mu_0$. The toroidal component of $\mathbf{B}$ is:

$$B_\phi = \frac{\mu_0\,F}{R} \tag{A.8}$$

We will now shift our focus to the electric current. Recall that $\mu_0\,\mathbf{j} = \nabla\times\mathbf{B}$. The individual components of $\mathbf{j}$ in cylindrical coordinates are:

$$j_R = \frac{1}{\mu_0}\frac{\partial B_\phi}{\partial Z}, \tag{A.9}$$

$$j_\phi = \frac{1}{\mu_0}\left(\frac{\partial B_R}{\partial Z} - \frac{\partial B_Z}{\partial R}\right), \tag{A.10}$$

$$j_Z = \frac{1}{\mu_0\,R}\frac{\partial}{\partial R}\left(R\,B_\phi\right). \tag{A.11}$$

$$\tag{A.12}$$

Substituting from (A.8) yields:

$$\mathbf{j}_p = -\frac{1}{R}\frac{\partial F}{\partial Z}\,\hat{\mathbf{e}}_R + \frac{1}{R}\frac{\partial F}{\partial R}\,\hat{\mathbf{e}}_Z \tag{A.13}$$

As for the toroidal component, substitutions for B_R and B_Z in terms of the flux function ψ yield:

$$j_\phi = -\frac{1}{\mu_0\, R}\left[R\,\frac{\partial}{\partial R}\left(\frac{1}{R}\frac{\partial \psi}{\partial R}\right) + \frac{\partial^2 \psi}{\partial Z^2}\right], \tag{A.14}$$

or:

$$j_\phi = -\frac{\Delta^* \psi}{\mu_0\, R}, \tag{A.15}$$

where the *elliptic operator* Δ^* is defined as:

$$\Delta^* \psi = R\,\frac{\partial}{\partial R}\left(\frac{1}{R}\frac{\partial \psi}{\partial R}\right) + \frac{\partial^2 \psi}{\partial Z^2} \tag{A.16}$$

Step 4

The next step is to show that ψ and F are surface quantities, i.e., constant over a given surface, like p and q. In cylindrical coordinates:

$$\nabla\psi = \frac{\partial \psi}{\partial R}\,\hat{\mathbf{e}}_R + \frac{\partial \psi}{\partial Z}\,\hat{\mathbf{e}}_Z = R\,B_Z\,\hat{\mathbf{e}}_R - R\,B_R\,\hat{\mathbf{e}}_Z, \tag{A.17}$$

which implies

$$\mathbf{B}\cdot\nabla\psi = B_R\,R\,B_Z - B_Z\,R\,B_R = 0 \tag{A.18}$$

Thus, ψ is constant along field lines of $\mathbf{B}$. Also:

$$\nabla F = \frac{\partial F}{\partial R}\,\hat{\mathbf{e}}_R + \frac{\partial F}{\partial Z}\,\hat{\mathbf{e}}_Z, \tag{A.19}$$

which implies

$$\mathbf{j}\cdot\nabla F = j_R\,\frac{\partial F}{\partial R} + \frac{\partial F}{\partial Z} = -\,\frac{1}{R}\frac{\partial F}{\partial Z}\frac{\partial F}{\partial R} + \frac{1}{R}\frac{\partial F}{\partial R}\frac{\partial F}{\partial Z} = 0 \tag{A.20}$$

Thus, F is constant along lines of $\mathbf{j}$. We have seen that lines of $\mathbf{B}$ and $\mathbf{j}$ lie on flux surfaces, therefore we have shown that ψ and F are surface quantities.

Step 5

The next step is a physical interpretation of ψ and F. Assume a cross section of flux surfaces in the $R-Z$ plane. Nested tori can be represented as annular regions with inner and outer radii. We will focus on the case where the inner radius corresponds to R_0 (the magnetic axis) and the outer radius will be denoted as R_{out}. Let us calculate the *poloidal flux* inside the flux surface:

$$\int \mathbf{B}\,d\mathbf{S} = \int_{R_0}^{R_{out}} B_Z\,2\pi\,R\,dR = 2\pi\int_{R_0}^{R_{out}} \frac{1}{R}\frac{\partial\psi}{\partial R}R\,dR = 2\pi\,\left[\psi\right]_{R_0}^{R_{out}}, \tag{A.21}$$

where $\psi\left(R_{out}\right) = \psi$ on the flux surface and we define $\psi\left(R_0\right) = 0$. Thus, $2\pi\psi$ is the poloidal flux inside the flux surface.

Similarly, let us now consider the poloidal current, I_p, "surrounded" by a flux surface, and an annular region determined by R_{in} and R_{out}. I_p is enclosed by either the circle of radius R_{in}, or the one of radius R_{out}. The integral form of Ampére's Law, applied to either circle, yields:

$$\oint \mathbf{B}\cdot dl = 2\pi\,R_{in/out}\,B_\phi\left(R = R_{in/out},\,Z = 0\right) = \mu_0\,I_p. \tag{A.22}$$

On the flux surface ($R = R_{in/out}$), we have $B_\phi = \dfrac{\mu_0\,F}{R}$. Thus, $2\pi\,F$ is the poloidal current surrounded by the flux surface.

Step 6

We can now use ψ to label flux surfaces:

$$p = p(\psi) \rightarrow \nabla p = \frac{dp}{d\psi}\nabla\psi, \tag{A.23}$$

$$F = F(\psi) \rightarrow \nabla F = \frac{dF}{d\psi}\nabla\psi. \tag{A.24}$$

Step 7

We will bring everything together for the last two steps of this derivation, in order to obtain the elegant Grad-Shafranov equation. Let us analyze $\mathbf{j} \times \mathbf{B}$ into its constituent terms, and focus on each one separately:

$$\begin{aligned}\mathbf{j} \times \mathbf{B} &= (\mathbf{j}_p + j_\phi\,\hat{\mathbf{e}}_\phi) \times (\mathbf{B}_p + B_\phi\,\hat{\mathbf{e}}_\phi) = \\ &= \mathbf{j}_p \times \mathbf{B}_p + \mathbf{j}_p \times B_\phi\,\hat{\mathbf{e}}_\phi + j_\phi\,\hat{\mathbf{e}}_\phi \times \mathbf{B}_p + j_\phi\,B_\phi\,\hat{\mathbf{e}}_\phi \times \hat{\mathbf{e}}_\phi\end{aligned} \tag{A.25}$$

1. The first term, $\mathbf{j}_p \times \mathbf{B}_p$, only has a ϕ component.

2. We are going to use Eqs. (A.13), (A.24), and (A.8) to manipulate the second term:

$$\begin{aligned}\mathbf{j}_p \times B_\phi\,\hat{\mathbf{e}}_\phi &= -\frac{B_\phi}{R}\frac{\partial F}{\partial R}\,\hat{\mathbf{e}}_R - \frac{B_\phi}{R}\frac{\partial F}{\partial Z}\,\hat{\mathbf{e}}_Z \\ &= -\frac{B_\phi}{R}\nabla F \\ &= -\frac{B_\phi}{R}\frac{dF}{d\psi}\nabla\psi \\ &= -\frac{\mu_0\,F}{R^2}\frac{dF}{d\psi}\nabla\psi.\end{aligned}$$

3. We are going to use Eqs. (A.7) and (A.15) to manipulate the third term:

$$\begin{aligned} j_\phi \, \hat{\mathbf{e}}_\phi \times \mathbf{B}_p &= \frac{j_\phi}{R} \frac{\partial \psi}{\partial R} \, \hat{\mathbf{e}}_R + \frac{j_\phi}{R} \frac{\partial \psi}{\partial Z} \, \hat{\mathbf{e}}_Z \\ &= \frac{j_\phi}{R} \nabla \psi \\ &= -\frac{\Delta^* \psi}{\mu_0 \, R^2} \nabla \psi. \end{aligned}$$

4. The fourth term, $j_\phi \, B_\phi \, \hat{\mathbf{e}}_\phi \times \hat{\mathbf{e}}_\phi$, is equal to zero due to the cross product of the unit vectors.

Adding the components up, we obtain:

$$\mathbf{j} \times \mathbf{B} = \mathbf{j}_p \times \mathbf{B}_p - \left(\frac{\mu_0 \, F}{R^2} \frac{dF}{d\psi} + \frac{\Delta^* \psi}{\mu_0 \, R^2} \right) \nabla \psi \tag{A.26}$$

Step 8

Finally, we will take the component of the force balance equation, $\nabla p = \mathbf{j} \times \mathbf{B}$, that is normal to the flux surface. Let us combine Eqs. (A.23) and (A.26):

$$\frac{dp}{d\psi} \nabla \psi = \mathbf{j}_p \times \mathbf{B}_p - \left(\frac{\mu_0 \, F}{R^2} \frac{dF}{d\psi} + \frac{\Delta^* \psi}{\mu_0 \, R^2} \right) \nabla \psi. \tag{A.27}$$

ψ is constant on the flux surface, which means that $\nabla \psi$ is normal to the surface. $\mathbf{j}_p \times \mathbf{B}_p$ has no component in this direction, since it is purely in the ϕ direction, as we have seen. Thus, we yield the *Grad-Shafranov equation*:

$$\frac{1}{\mu_0} \Delta^* \psi = -R^2 \, \frac{dp}{d\psi} - \mu_0 \, F \, \frac{dF}{d\psi} \tag{A.28}$$

A.2 Discussion

We have seen that, in two dimensions (assuming axisymmetry), the force balance equation reduces to the Grad-Shafranov equation, which must be solved numerically in order to yield MHD equilibria in the form of contours of constant ψ in a tokamak, i.e., flux surfaces. It is one of the most famous equations arising from MHD: given the functions $p(\psi)$ and $F(\psi)$, the Grad-Shafranov equation describes equilibrium in an axisymmetric torus. It is important to note that functions $p(\psi)$ and $F(\psi)$ are completely arbitrary, and must be determined from considerations other than the theoretical force balance. (For example, they could be determined experimentally, or from a transport calculation, or simply fabricated).

At least in principle, given the functions $p(\psi)$ and $F(\psi)$, along with the appropriate boundary conditions (generally that ψ is specified on some boundary), Eq. (A.28) can be solved for $\psi(R, Z)$. This gives the equilibrium flux distribution. However, it is important to note that the functions p and F can be (and generally are) nonlinear, so these solutions are not guaranteed to either exist, or to be unique; there may be no solution, or many solutions, satisfying both Eq. (A.28), and the boundary conditions. It comes as no surprise that a rather large and specialized "cottage industry" has grown around finding solutions of the Grad-Shafranov equation: a large number of codes is available to evaluate those equilibria.

Appendix B

Poloidal Equations

In tokamaks, poloidal components can be neglected due to strong flow. We are presenting the poloidal equations here as an Appendix to Chapter 4.

B.1 Plasma Equation of Poloidal Angular Motion

Let $\Omega_\theta(r,t) = \Omega_\theta^{(0)}(r) + \Delta\Omega_\theta(r,t)$ be the plasma poloidal angular velocity profile, where:

1. $\Omega_\theta^{(0)}(r)$ is the steady-state profile in the absence of net poloidal braking electromagnetic (EM) torque, and

2. $\Delta\Omega_\theta(r,t)$ is the modification to the profile due to the error-field.

The plasma poloidal equation of motion is written [14]:

$$\rho\, r^3 \frac{\partial \Delta\Omega_\theta}{\partial t} - \mu \frac{\partial}{\partial r}\left(r^3 \frac{\partial \Delta\Omega_\theta}{\partial r}\right) + \frac{\rho\, r^3}{\tau_D}\Delta\Omega_\theta = \frac{T_{\theta_{EM}}}{4\pi^2 R_0}\delta(r - r_s), \qquad \text{(B.1)}$$

where ρ and μ are assumed to be uniform across the plasma (plasma mass density, and perpendicular viscosity, respectively).

The physical boundary conditions satisfied by the perturbed poloidal

angular velocity profile are:

$$\frac{\partial \Delta\Omega_\theta\left(0,t\right)}{\partial r} = \Delta\Omega_\theta\left(a,t\right) = 0, \tag{B.2}$$

where a is the plasma minor radius.

B.2 Normalized Plasma Equation of Poloidal Angular Motion

Let us introduce *normalized* variables:

1. $\hat{r} = r/a$,
2. $\hat{r}_s = r_s/a$,
3. $\tau_V = a^2\rho/\mu$,

where τ_V is the momentum confinement timescale [14]. We can write the normalized plasma equation of poloidal angular motion:

$$\tau_V \frac{\partial \Delta\Omega_\theta}{\partial t} - \frac{1}{\hat{r}^3}\frac{\partial}{\partial \hat{r}}\left(\hat{r}^3 \frac{\partial \Delta\Omega_\theta}{\partial \hat{r}}\right) + \frac{\tau_V}{\tau_D}\Delta\Omega_\theta = \frac{T_{\theta_{EM}}}{4\pi^2 R_0 \hat{r}_s^3 \mu a^2}\delta\left(\hat{r}-\hat{r}_s\right), \tag{B.3}$$

and the spatial boundary conditions:

$$\frac{\partial \Delta\Omega_\theta\left(0,t\right)}{\partial \hat{r}} = \Delta\Omega_\theta\left(1,t\right) = 0. \tag{B.4}$$

We can now introduce the function $Y(\hat{r},t) = \hat{r}\,\Delta\Omega_\theta\left(\hat{r},t\right)$ so that Eq. (B.3) is written as:

$$\tau_V \frac{\partial Y}{\partial t} - \left(\frac{\partial^2}{\partial \hat{r}^2} + \frac{1}{\hat{r}}\frac{\partial}{\partial \hat{r}} - \frac{1}{\hat{r}^2} + \frac{\tau_V}{\tau_D}\right) Y = \frac{T_{\theta_{EM}}}{4\pi^2 R_0 \hat{r}_s^2 \mu a^2}\delta\left(\hat{r}-\hat{r}_s\right) \tag{B.5}$$

B.2.1 Solution of Normalized Plasma Equation of Poloidal Angular Motion

The partial differential equation (B.3), together with the physical boundary conditions (B.4), can be reduced into a system of ordinary differential equations, upon defining a set of velocity eigenfunctions and eigenvalues [51]:

$$\frac{d}{dr}\left(r^3\,\mu\,\frac{dv_k}{dr}\right)+r^3\,\rho\,\gamma_k\,v_k=0, \tag{B.6}$$

$$\frac{dv_k(0)}{dr}=v_k(a)=0. \tag{B.7}$$

From Eq. (B.6) one gets:

$$v_k(r)=E_k\,\frac{J_1\,\left(\frac{r}{a}\,j_{1,k}\right)}{r};\qquad \gamma_k=\frac{j_{1,k}^2}{\tau_V}, \tag{B.8}$$

where $j_{1,k}$ is the k^{th} zero of the J_1 Bessel function.

From Abramowitz & Stegun [1] it can be easily demonstrated that, upon defining

$$E_k\equiv\left(\int_0^a r\,J_1^2\left[(r/a)j_{1,k}\right]\,dr\right)^{-1/2}, \tag{B.9}$$

we satisfy the *orthonormality condition*

$$\int_0^1 \hat{r}^3\,v_k\left(\hat{r}\right)v_{k'}\left(\hat{r}\right)d\hat{r}'=\delta_{kk'},$$

as well as:

$$\delta\left(\hat{r}-\hat{r}_s\right)=\sum_{k=1}^{\infty}\hat{r}\,v_k\left(\hat{r}\right)v_{k'}\left(\hat{r}\right).$$

According to the Sturm-Liouville theory, the eigenfunctions v_k form a complete set. Therefore we can expand the poloidal angular velocity as:

$$Y\left(\hat{r},t\right)=\sum_{k=1}^{\infty}\hat{r}_s\,g_k\left(t\right)\frac{v_k\left(\hat{r}\right)}{u_k\left(\hat{r}_s\right)}, \tag{B.10}$$

which automatically satisfies the boundary conditions (B.4).

Using the orthonormality relation, and substituting into the equation of motion (B.5), we obtain a simplified, numerable set of ordinary differential equations for $g_k(t)$:

$$\tau_V \frac{dg_k}{dt} + \left(\mathrm{j}_{1,k}^2 + \frac{\tau_V}{\tau_D} \right) g_k = \frac{T_{\theta_{EM}}}{4\pi^2 R_0 r_s^2 \mu} \left[v_k \left(\hat{r}_s \right) \right]^2 \tag{B.11}$$

Also, the modification to the angular velocity profile:

$$\Delta\Omega_\theta \left(\hat{r}, t \right) = \sum_{k=1}^{\infty} g_k \left(t \right) \frac{\hat{r}_s}{\hat{r}} \frac{v_k(\hat{r})}{v_k(\hat{r}_s)} \tag{B.12}$$

B.3 Slip Frequency

The slip frequency is defined as [14]:

$$\omega = m\, \Omega_\theta \left(\hat{r}_s, t \right) - n\, \Omega_\phi \left(\hat{r}_s, t \right), \tag{B.13}$$

where m, n are the poloidal and toroidal mode numbers respectively. Let:

$$\Omega_\theta \left(\hat{r}, t \right) = \Omega_\theta^{(0)} + \Delta\Omega_\theta \left(\hat{r}, t \right) \tag{B.14}$$

$$\Omega_\phi \left(\hat{r}, t \right) = \Omega_\phi^{(0)} + \Delta\Omega_\phi \left(\hat{r}, t \right) \tag{B.15}$$

Using the results from Eqs. (B.12) and (4.12), we can write (B.13) as:

$$\omega \left(t \right) = \omega_0 + \sum_{k=1}^{\infty} \left[m\, g_k(t) - n\, h_k(t) \right], \tag{B.16}$$

where the *natural frequency*, ω_0 is given by

$$\omega_0 = m\, \Omega_\theta^{(0)} - n\, \Omega_\phi^{(0)}. \tag{B.17}$$

B.4 Torques

B.4.1 Poloidal Electromagnetic Torque

The poloidal electromagnetic torque exerted at rational surface is [14]:

$$T_{\theta_{EM}} = -\frac{4\pi^2\, m^2\, R_0}{\mu_0}|\Psi_v||\Psi_s|\sin\left(\phi_s - \phi_v\right). \tag{B.18}$$

Recall the expressions for the true and vacuum magnetic island width:

$$W = 4\left(\frac{q_s}{s_s}\frac{R_0}{B_\phi}|\Psi_s|\right)^{1/2}, \tag{B.19}$$

$$W_v = 4\left(\frac{q_s}{s_s}\frac{R_0}{B_\phi}|\Psi_v|\right)^{1/2}, \tag{B.20}$$

where the subscript s denotes evaluation at $r = r_s$.

Taking this definition for the poloidal electromagnetic torque into account, we can revisit the expression for the poloidal equation of motion. After some algebra it follows that:

$$\tau_V\,\frac{dg_k}{dt} + \left(\hat{\mathrm{j}}^2_{1,k} + \frac{\tau_V}{\tau_D}\right) g_k = -\frac{1}{2^8}\left(\frac{W}{r_s}\right)^2\left(\frac{W_v}{r_s}\right)^2\frac{\tau_V}{\tau_H^2}\left[\hat{v}_k\right]^2\sin\left(\phi_s - \phi_v\right), \tag{B.21}$$

where the "hatted" quantities are defined as: $\hat{\mathrm{j}}_{1,k} = \hat{r}_s\,\mathrm{j}_{1,k}$, and $\hat{v}_k = \hat{r}_s\, v_k(\hat{r}_s)$.

Tokamak plasmas possess strong parallel (to the magnetic field) viscosity, which opposes plasma compression associated with poloidal rotation. In conventional tokamak plasmas this viscosity is sufficiently large to prevent any error-field-induced change in the poloidal rotation. Thus, in practice, the plasma does not respond to the poloidal component of the electromagnetic torque exerted in the vicinity of the rational surface by the error-field.

B.4.2 Poloidal Viscous Torque

From Equations (30) and (46) of Ref. [14], the poloidal viscous torque exerted at rational surface is:

$$T_{\theta_{VS}} = 4\pi^2 R_0 \left[\mu r^3 \frac{\partial \Delta\Omega_\theta}{\partial r}\right]_{r_s-}^{r_s+} = -4\pi^2 R_0 (\omega - \omega_0) \left(\frac{\mu ((r_{s-})\ r_{s-}^3}{\delta_{D-}} + \frac{\mu (r_{s+})\ r_{s+}^3}{\delta_{D+}}\right), \tag{B.22}$$

where:

$$\frac{\delta_{D\pm}}{a} = \left(\frac{\mu}{a^2 \rho} \tau_D\right)_{r_{s\pm}}^{1/2} = \left(\frac{\tau_D}{\tau_V}\right)_{r_{s\pm}}^{1/2}. \tag{B.23}$$

The above expression for $\Delta\Omega_\theta(r)$ is only valid in the limit where the localization length scales $\delta_{D\pm}$ are much less than the minor radius a.

Recall from Chapter 4 that the spatial boundary condition at the edge of the plasma is $\Delta\Omega_\phi(a,t) = 0$. In other words, the plasma is clamped at the edge, and is not substantially modified by the error field [14].

The poloidal velocity shift profile is localized around the rational surface, owing to the action of *strong poloidal flow damping*. We ignore poloidal torque components, since τ_D is normally relatively small.

B.5 Magnetic Island Evolution Equations

For the sake of completeness, we will now present our analysis for both the poloidal and toroidal equations of angular motion, completing the missing steps of the presentation in Chapter 4.

Let:

$$\hat{\omega}_0 = \left[\frac{r_s}{\delta_{VR}}\frac{\tau_R}{(-\Delta')}\right]\omega_0,$$

$$\bar{g}_k = \left[\frac{r_s}{\delta_{VR}}\frac{\tau_R}{(-\Delta')}\right]g_k,$$

$$\bar{h}_k = \left[\frac{r_s}{\delta_{VR}}\frac{\tau_R}{(-\Delta')}\right]h_k.$$

Then:

$$\hat{\omega} = \hat{\omega}_0 + \sum_{k=1}^{\infty}\left[m\,\bar{g}_k - n\,\bar{h}_k\right], \tag{B.24}$$

and the plasma equations of angular motion can be written as:

$$\left(\frac{\tau_V}{\tau_R}\frac{r_s}{\delta_{VR}} - \Delta'\right)\frac{d\bar{g}_k}{d\hat{t}} + \left(\hat{\mathrm{j}}_{1,k}^2 + \frac{\tau_V}{\tau_D}\right)\bar{g}_k =$$
$$= -\frac{1}{2^8}\left(\frac{2}{0.8227}\frac{\delta_{VR}}{r_s}\right)^4\left(-\frac{\Delta'}{2m}\right)\left(\frac{\delta_{VR}}{r_s}\frac{1}{-\Delta'}\right)\frac{\tau_R\,\tau_V}{\tau_H^2}\times\hat{W}^2\,\hat{W}_v^2\,\hat{v}_k^2\,\sin\phi, \tag{B.25}$$

and

$$\left(\frac{\tau_V}{\tau_R}\frac{r_s}{\delta_{VR}} - \Delta'\right)\frac{d\bar{h}_k}{d\hat{t}} + \hat{\mathrm{j}}_{0,k}^2\,\bar{h}_k =$$
$$= \frac{n}{m}\left(\frac{r_s}{R_0}\right)^2\frac{1}{2^8}\left(\frac{2}{0.8227}\frac{\delta_{VR}}{r_s}\right)^4\left(-\frac{\Delta'}{2m}\right)\left(\frac{\delta_{VR}}{r_s}\frac{1}{-\Delta'}\right)\frac{\tau_R\,\tau_V}{\tau_H^2}\times\hat{W}^2\,\hat{W}_v^2\,\hat{u}_k^2\,\sin\phi \tag{B.26}$$

We will simplify these expressions by further normalizing our variables. Let:

$$-m\,\bar{g}_k = \hat{g}_k, \tag{B.27}$$

$$n\,\bar{h}_k = \hat{h}_k\,\frac{n^2}{m^2}\left(\frac{r_s}{R_0}\right). \tag{B.28}$$

The normalized slip frequency is now written as:

$$\hat{\omega} = \hat{\omega}_0 - \sum_{k=1}^{\infty} \left[\hat{g}_k + \left(\frac{n}{m}\right)^2 \left(\frac{r_s}{R_0}\right)^2 \hat{h}_k \right], \tag{B.29}$$

and our set of plasma poloidal/toroidal equations of motion:

$$-\Delta' \frac{\tau_V}{\tau_R} \frac{d\hat{g}_k}{d\hat{t}} + \hat{\delta}_{VR} \left(\hat{\mathrm{j}}_{1,k}^2 + \frac{\tau_V}{\tau_D} \right) \hat{g}_k = \frac{(2.104)^6}{2^5 \, (0.8227)^4} \hat{W}^2 \, \hat{W}_v^2 \, \hat{v}_k^2 \, \sin\phi, \tag{B.30}$$

$$-\Delta' \frac{\tau_V}{\tau_R} \frac{d\hat{h}_k}{d\hat{t}} + \hat{\delta}_{VR} \hat{\mathrm{j}}_{0,k}^2 \, \hat{h}_k = \frac{(2.104)^6}{2^5 \, (0.8227)^4} \hat{W}^2 \, \hat{W}_v^2 \, \hat{u}_k^2 \, \sin\phi, \tag{B.31}$$

where $\hat{\delta}_{VR} = \delta_{VR}/r_s$.

B.6 Complete Equations

Finally, we are bringing everything together, so as to:

1. Derive compact equations of angular motion for the plasma, both in the poloidal and the toroidal direction.

2. Consider the analytic limit $d/dt \to 0$ for the locked mode, in order to obtain analytic expressions for the velocity profiles and the slip frequency.

From Chapter 3, recall the normalized island evolution equations for both the visco-resistive and the Rutherford regime:

$$\left.\begin{aligned} \frac{d\hat{W}}{d\hat{t}} &= \frac{\hat{W}}{2}\left(-1+\frac{\hat{W}_v^2}{\hat{W}^2}\cos\phi\right), \\ \frac{d\phi}{d\hat{t}} - \hat{\omega} &= -\frac{\hat{W}_v^2}{\hat{W}^2}\sin\phi, \end{aligned}\right\} \quad \text{Linear - visco-resistive regime}$$

for $0 \leq \hat{W} \leq 1$, and

$$\left.\begin{aligned} \frac{d\hat{W}}{d\hat{t}} &= \frac{1}{2}\left(-1+\frac{\hat{W}_v^2}{\hat{W}^2}\cos\phi\right), \\ \frac{d\phi}{d\hat{t}} - \hat{\omega} &= 0, \end{aligned}\right\} \quad \text{Nonlinear - Rutherford regime}$$

for $\hat{W} > 1$.

The expression for the slip frequency, $\hat{\omega}$, can be written as

$$\hat{\omega} = \hat{\omega}_0 - \frac{(2.104)^6}{2^5\,(0.8227)^4}\frac{1}{\hat{\delta}_{VR}} \times \sum_{k=1}^{\infty}\left[\hat{v}_k^2\,G_k + \left(\frac{n}{m}\right)^2\left(\frac{r_s}{R_0}\right)^2\hat{u}_k^2\,H_k\right], \qquad \text{(B.32)}$$

with

$$\left[\frac{(-\Delta')}{\hat{\delta}_{VR}}\frac{\tau_V}{\tau_R}\right]\frac{dG_k}{d\hat{t}} + \left(\hat{\jmath}_{1,k}^2 + \frac{\tau_V}{\tau_D}\right)G_k = \hat{W}^2\hat{W}_v^2\sin\phi, \qquad \text{(B.33)}$$

and

$$\left[\frac{(-\Delta')}{\hat{\delta}_{VR}}\frac{\tau_V}{\tau_R}\right]\frac{dH_k}{d\hat{t}}+\hat{\mathrm{j}}_{0,k}^2 H_k=\hat{W}^2\hat{W}_v^2\sin\phi. \tag{B.34}$$

Let us consider steady-state ($d/dt\rightarrow 0$) conditions. The differential equations in the previous sections can be transformed into algebraic equations and solved for the g,h velocity profile parameters. Let us start with the *poloidal* equation of plasma angular motion, (B.11), and $d/dt\rightarrow 0$:

$$\left(\mathrm{j}_{1,k}^2+\frac{\tau_V}{\tau_D}\right)g_k=\frac{T_{\theta_{EM}}}{4\pi^2\,R_0\,r_s^2\,\mu}\left[v_k\left(\hat{r}_s\right)\right]^2, \tag{B.35}$$

so the *poloidal angular velocity profile* is:

$$g_k=\frac{\tau_D\,T_{\theta_{EM}}}{4\pi^2\,R_0\,r_s^2\,\mu\left(\mathrm{j}_{1,k}^2\,\tau_D+\tau_V\right)}\left[v_k\left(\hat{r}_s\right)\right]^2, \tag{B.36}$$

and the modification to the profile due to the error-field:

$$\Delta\Omega_\theta\left(\hat{r},t\right)=\sum_{k=1}^{\infty}g_k(t)\frac{\hat{r}_s}{\hat{r}}\frac{v_k(\hat{r})}{v_k(\hat{r}_s)}, \tag{B.37}$$

thus:

$$\Delta\Omega_\theta\left(\hat{r},t\right)=\sum_{k=1}^{\infty}\frac{\tau_D\,T_{\theta_{EM}}}{4\pi^2\,R_0\,r_s^2\,\mu\left(\mathrm{j}_{1,k}^2\,\tau_D+\tau_V\right)}\,v_k\left(\hat{r}\right)v_k\left(\hat{r}_s\right). \tag{B.38}$$

Similarly, for the *toroidal* equation of plasma angular motion, (4.14), and $d/dt\rightarrow 0$:

$$\mathrm{j}_{0,k}^2\,h_k=\frac{T_{\phi_{EM}}}{4\pi^2\,R_0^3\,\mu}\left[u_k\left(\hat{r}_s\right)\right]^2, \tag{B.39}$$

so the *toroidal angular velocity profile* is:

$$h_k=\frac{T_{\phi_{EM}}}{\mathrm{j}_{0,k}^2\,4\pi^2\,R_0^3\,\mu}\left[u_k\left(\hat{r}_s\right)\right]^2, \tag{B.40}$$

and the modification to the profile due to the error-field:

$$\Delta\Omega_{\phi}\left(\hat{r},t\right)=\sum_{k=1}^{\infty}\hat{r}_{s}\,h_{k}(t)\frac{u_{k}\left(\hat{r}\right)}{u_{k}\left(\hat{r}_{s}\right)}, \tag{B.41}$$

thus:

$$\Delta\Omega_{\phi}\left(\hat{r},t\right)=\sum_{k=1}^{\infty}\frac{T_{\phi_{EM}}}{\hat{\mathrm{j}}_{0,k}^{2}\,4\pi^{2}\,R_{0}^{3}\,\mu}\,u_{k}\left(\hat{r}\right)u_{k}\left(\hat{r}_{s}\right). \tag{B.42}$$

Using these definitions of g_k and h_k, and Eq. (B.16), we obtain the following expression for the *slip frequency*:

$$\omega\left(t\right)=\omega_{0}+\sum_{k=1}^{\infty}\left[m\,\frac{\tau_{D}\,T_{\theta_{EM}}}{4\pi^{2}\,R_{0}\,r_{s}^{2}\,\mu\left(\hat{\mathrm{j}}_{1,k}^{2}\,\tau_{D}+\tau_{V}\right)}\left[v_{k}\left(\hat{r}_{s}\right)\right]^{2}-n\,\frac{T_{\phi_{EM}}}{\hat{\mathrm{j}}_{0,k}^{2}\,4\pi^{2}\,R_{0}^{3}\,\mu}\left[u_{k}\left(\hat{r}_{s}\right)\right]^{2}\right] \tag{B.43}$$

After we introduced the expressions for the poloidal and toroidal electromagnetic torque, we wrote the respective differential equations of motion (B.21), and (4.23). Their algebraic counterparts can be easily obtained if we consider equilibrium conditions, where nothing varies in time, as before.

Let us start from the poloidal equation of electromagnetic torque, (B.21), and $d/dt\rightarrow 0$:

$$\left(\hat{\mathrm{j}}_{1,k}^{2}+\frac{\tau_{V}}{\tau_{D}}\right)g_{k}=-\frac{1}{2^{8}}\left(\frac{W}{r_{s}}\right)^{2}\left(\frac{W_{v}}{r_{s}}\right)^{2}\frac{\tau_{V}}{\tau_{H}^{2}}\left[\hat{v}_{k}\right]^{2}\sin\left(\phi_{s}-\phi_{v}\right), \tag{B.44}$$

which implies

$$g_{k}=-\frac{1}{2^{8}}\frac{\tau_{V}\,\tau_{D}}{\tau_{H}^{2}}\left(\frac{W}{r_{s}}\right)^{2}\left(\frac{W_{v}}{r_{s}}\right)^{2}\frac{1}{\left(\hat{\mathrm{j}}_{1,k}^{2}\,\tau_{D}+\tau_{V}\right)}\left[\hat{v}_{k}\right]^{2}\sin\left(\phi_{s}-\phi_{v}\right). \tag{B.45}$$

We are now considering the toroidal equation of electromagnetic torque, (4.23), and $d/dt \to 0$:

$$\hat{\mathrm{j}}^2_{0,k}\, h_k = \frac{1}{2^8}\,\frac{n}{m}\left(\frac{W}{r_s}\right)^2\left(\frac{W_v}{r_s}\right)^2\left(\frac{r_s}{R_0}\right)^2\frac{\tau_V}{\tau_H^2}\,[\hat{u}_k]^2\sin(\phi_s-\phi_v), \tag{B.46}$$

which implies

$$h_k = \frac{1}{2^8}\frac{n}{m}\,\frac{1}{\hat{\mathrm{j}}^2_{0,k}}\left(\frac{W}{r_s}\right)^2\left(\frac{W_v}{r_s}\right)^2\left(\frac{r_s}{R_0}\right)^2\frac{\tau_V}{\tau_H^2}\,[\hat{u}_k]^2\sin(\phi_s-\phi_v). \tag{B.47}$$

Recall that, after introducing the island evolution equations, and the tearing stability index Δ', we wrote the plasma equations of angular motion, (B.25), and (B.26). After the simple substitutions (B.27) and (B.28) these equations were written as (B.30) and (B.31). In the interest of completeness of our presentation, let us transform these differential equation to algebraic ones with $d/dt \to 0$ and solve for the respective $\bar{g}_k, \bar{h}_k, \hat{g}_k$ and $\hat{g}_k$. Let us start with the poloidal equation of motion:

$$\left(\hat{\mathrm{j}}^2_{1,k}+\frac{\tau_V}{\tau_D}\right)\bar{g}_k = \\ = -\frac{1}{2^8}\left(\frac{2}{0.8227}\frac{\delta_{VR}}{r_s}\right)^4\left(-\frac{\Delta'}{2m}\right)\left(\frac{\delta_{VR}}{r_s}\frac{1}{-\Delta'}\right)\frac{\tau_R\,\tau_V}{\tau_H^2}\times\hat{W}^2\,\hat{W}_v^2\,\hat{v}_k^2\,\sin(\phi_s-\phi_v), \tag{B.48}$$

which implies

$$\bar{g}_k = -\frac{1}{2^8}\left(\frac{2}{0.8227}\frac{\delta_{VR}}{r_s}\right)^4\left(-\frac{\Delta'}{2m}\right)\left(\frac{\delta_{VR}}{r_s}\frac{1}{-\Delta'}\right)\frac{\tau_D}{\left(\hat{\mathrm{j}}^2_{1,k}\,\tau_D+\tau_V\right)}\times \\ \times\,\frac{\tau_R\,\tau_V}{\tau_H^2}\hat{W}^2\,\hat{W}_v^2\,\hat{v}_k^2\,\sin(\phi_s-\phi_v). \tag{B.49}$$

Similarly for the toroidal equation of motion:

$$\hat{\mathrm{j}}^2_{0,k}\,\bar{h}_k = \\ = \frac{n}{m}\left(\frac{r_s}{R_0}\right)^2 \frac{1}{2^8}\left(\frac{2}{0.8227}\frac{\delta_{VR}}{r_s}\right)^4 \left(-\frac{\Delta'}{2m}\right)\left(\frac{\delta_{VR}}{r_s}\frac{1}{-\Delta'}\right)\frac{\tau_R\,\tau_V}{\tau_H^2}\times \\ \times\,\hat{W}^2\,\hat{W}_v^2\,\hat{u}_k^2\,\sin\left(\phi_s-\phi_v\right), \quad \text{(B.50)}$$

which implies

$$\bar{h}_k = \frac{n}{m}\left(\frac{r_s}{R_0}\right)^2 \frac{1}{2^8}\left(\frac{2}{0.8227}\frac{\delta_{VR}}{r_s}\right)^4 \left(-\frac{\Delta'}{2m}\right)\left(\frac{\delta_{VR}}{r_s}\frac{1}{-\Delta'}\right)\frac{1}{\hat{\mathrm{j}}^2_{0,k}}\times \\ \times\,\frac{\tau_R\,\tau_V}{\tau_H^2}\hat{W}^2\,\hat{W}_v^2\,\hat{u}_k^2\,\sin\left(\phi_s-\phi_v\right) \quad \text{(B.51)}$$

Similarly for the "hatted" velocity profiles:

$$\hat{g}_k = \frac{(2.104)^6}{2^5\,(0.8227)^4}\frac{1}{\hat{\delta}_{VR}}\frac{\tau_D}{\left(\hat{\mathrm{j}}^2_{1,k}\,\tau_D+\tau_V\right)}\times\hat{W}^2\,\hat{W}_v^2\,\hat{v}_k^2\,\sin\left(\phi_s-\phi_v\right), \quad \text{(B.52)}$$

and

$$\hat{h}_k = \frac{(2.104)^6}{2^5\,(0.8227)^4}\frac{1}{\hat{\delta}_{VR}}\frac{1}{\hat{\mathrm{j}}^2_{0,k}}\times\hat{W}^2\,\hat{W}_v^2\,\hat{u}_k^2\,\sin\left(\phi_s-\phi_v\right). \quad \text{(B.53)}$$

Finally, the *Complete Equations*, (B.33) and (B.34), can be solved for G_k and H_k if we set $d/dt \to 0$. The poloidal case:

$$\left(\hat{\mathrm{j}}^2_{1,k}+\frac{\tau_V}{\tau_D}\right)G_k = \hat{W}^2\,\hat{W}_v^2\,\sin\left(\phi_s-\phi_v\right), \quad \text{(B.54)}$$

thus:

$$G_k = \frac{\tau_D}{\left(\hat{\mathrm{j}}^2_{1,k}\,\tau_D+\tau_V\right)}\times\hat{W}^2\,\hat{W}_v^2\,\sin\left(\phi_s-\phi_v\right), \quad \text{(B.55)}$$

and the toroidal case:

$$\hat{\mathrm{j}}^2_{0,k} H_k = \hat{W}^2 \, \hat{W}_v^2 \, \sin\left(\phi_s - \phi_v\right), \tag{B.56}$$

thus:

$$H_k = \frac{1}{\hat{\mathrm{j}}^2_{0,k}} \times \hat{W}^2 \, \hat{W}_v^2 \, \sin\left(\phi_s - \phi_v\right). \tag{B.57}$$

The "complete" velocity profiles, (B.55) and (B.57), can be substituted into the expression for $\hat{\omega}$, (B.32), to yield a complete expression for the slip frequency:

$$\hat{\omega} = \hat{\omega}_0 - \frac{(2.104)^6}{2^5 \, (0.8227)^4} \frac{1}{\hat{\delta}_{VR}} \times$$
$$\times \sum_{k=1}^{\infty} \left[\frac{\tau_D}{\left(\hat{\mathrm{j}}^2_{1,k} \, \tau_D + \tau_V \right)} \hat{v}_k^2 + \left(\frac{n}{m} \right)^2 \left(\frac{r_s}{R_0} \right)^2 \frac{1}{\hat{\mathrm{j}}^2_{0,k}} \hat{u}_k^2 \right] \hat{W}^2 \, \hat{W}_v^2 \, \sin\left(\phi_s - \phi_v\right). \tag{B.58}$$

This equation can of course be rewritten in terms of $\hat{\omega} - \hat{\omega}_0$, since this expression appears in the definition of the toroidal viscous torque, Eq. (4.24).

Bibliography

[1] Milton Abramowitz and Irene A Stegun. *Handbook of Mathematical Functions*. Dover Publications, New York, 1964.

[2] Glenn Bateman. *MHD instabilities*. MIT Press, Cambridge, Mass., 1978.

[3] Carl M Bender and Steven A Orszag. *Advanced Mathematical Methods for Scientists and Engineers I*. Springer Science & Business Media, 1999.

[4] Willard H Bennett. Magnetically self-focussing streams. *Physical Review*, 45(12):890, 1934.

[5] Dieter Biskamp. *Nonlinear Magnetohydrodynamics*, volume 1 of *Cambridge Monographs on Plasma Physics*. Cambridge University Press, 1997.

[6] Dieter Biskamp. *Magnetic Reconnection in Plasmas*, volume 3 of *Cambridge Monographs on Plasma Physics*. Cambridge University Press, 2005.

[7] Allen H. Boozer. Physics of magnetically confined plasmas. *Rev. Mod. Phys.*, 76:1071–1141, Jan 2005.

[8] SI Braginskii. Transport processes in a plasma. *Reviews of plasma physics*, 1:205, 1965.

[9] BE Chapman, R Fitzpatrick, D Craig, P Martin, and G Spizzo. Observation of tearing mode deceleration and locking due to eddy currents induced in a conducting shell. *Physics of Plasmas (1994-present)*, 11(5):2156–2171, 2004.

[10] Bruno Coppi, John M Greene, and John L Johnson. Resistive instabilities in a diffuse linear pinch. *Nuclear Fusion*, 6(2):101, 1966.

[11] Michael Coppins. Lecture notes: Magnetohydrodynamics I & II. Culham Plasma Physics Summer School, 2011.

[12] R.K. Pachauri Core Writing Team and L.A. Meyer (eds.). Climate change 2014: Synthesis report. Technical report, 2014. 151 pp.

[13] PC De Vries, MF Johnson, B Alper, P Buratti, TC Hender, HR Koslowski, V Riccardo, JET-EFDA Contributors, et al. Survey of disruption causes at JET. *Nuclear Fusion*, 51(5):053018, 2011.

[14] R Fitzpatrick. Interaction of tearing modes with external structures in cylindrical geometry (plasma). *Nuclear Fusion*, 33(7):1049, 1993.

[15] Richard Fitzpatrick. Bifurcated states of a rotating tokamak plasma in the presence of a static error-field. *Physics of Plasmas (1994-present)*, 5(9):3325–3341, 1998.

[16] Richard Fitzpatrick. Linear and nonlinear response of a rotating tokamak plasma to a resonant error-field. *Physics of Plasmas (1994-present)*, 21(9):092513, 2014.

[17] Richard Fitzpatrick. *Plasma Physics: An Introduction*. CRC Press, 2014.

[18] Richard Fitzpatrick. Braking of tearing mode rotation by ferromagnetic conducting walls in tokamaks. *Physics of Plasmas (1994-present)*, 22(9):092506, 2015.

[19] Richard Fitzpatrick and François L Waelbroeck. Two-fluid magnetic island dynamics in slab geometry. ii. islands interacting with resistive walls or resonant magnetic perturbations. *Physics of Plasmas (1994-present)*, 12(2):022308, 2005.

[20] Jeffrey P Freidberg. *Ideal Magnetohydrodynamics*. Plenum Press, New York, NY, 1987.

[21] Harold P Furth, John Killeen, and Marshall N Rosenbluth. Finite-resistivity instabilities of a sheet pinch. *Physics of Fluids (1958-1988)*, 6(4):459–484, 1963.

[22] DA Gates and TC Hender. Resistive wall induced forbidden bands of mode rotation frequency on the COMPASS-D tokamak. *Nuclear Fusion*, 36(3):273, 1996.

[23] Harold Grad. Toroidal containment of a plasma. *Physics of Fluids (1958-1988)*, 10(1):137–154, 1967.

[24] Richard D Hazeltine and James D Meiss. *Plasma Confinement*. Courier Corporation, 2003.

[25] F. L. Hinton and R. D. Hazeltine. Theory of plasma transport in toroidal confinement systems. *Rev. Mod. Phys.*, 48:239–308, Apr 1976.

[26] Qiming Hu, Bo Rao, Q Yu, Yonghua Ding, Ge Zhuang, Wei Jin, and Xiwei Hu. Understanding the effect of resonant magnetic perturbations on tearing mode dynamics. *Physics of Plasmas (1994-present)*, 20(9):092502, 2013.

[27] Qiming Hu, Q Yu, Bo Rao, Yonghua Ding, Xiwei Hu, Ge Zhuang, et al. Effect of externally applied resonant magnetic perturbations on resistive tearing modes. *Nuclear Fusion*, 52(8):083011, 2012.

[28] Wenlong Huang and Ping Zhu. Mode locking and island suppression by resonant magnetic perturbations in Rutherford regime. *Physics of Plasmas (1994-present)*, 22(3):032502, 2015.

[29] I. B. Bernstein, E. A. Frieman, M. D. Kruskal, R. M. Kulsrud. An energy principle for hydromagnetic stability problems. *Proceedings of the Royal Society of London. Series A, Mathematical and Physical Sciences*, 244(1236):17–40, 1958.

[30] K Ida, M Yoshinuma, H Tsuchiya, T Kobayashi, C Suzuki, M Yokoyama, A Shimizu, K Nagaoka, S Inagaki, K Itoh, et al. Flow damping due to stochastization of the magnetic field. *Nature Communications*, 6, 2015.

[31] Kruskal, M. D. and Johnson, J. L. and Gottlieb, M. B. and Goldman, L. M. Hydromagnetic instability in a stellarator. *Physics of Fluids*, 1(5):421–429, 1958.

[32] Kenro Miyamoto. *Plasma Physics and Controlled Nuclear Fusion*, volume 38. Springer Science & Business Media, 2006.

[33] Nave, MFF and Wesson, JA. Mode locking in tokamaks. *Nuclear Fusion*, 30(12):2575, 1990.

[34] William A Newcomb. Hydromagnetic stability of a diffuse linear pinch. *Annals of Physics*, 10(2):232–267, 1960.

[35] Edwin F. Northrup. Some newly observed manifestations of forces in the interior of an electric conductor. *Phys. Rev. (Series I)*, 24:474–497, Jun 1907.

[36] Francesco Porcelli. Viscous resistive magnetic reconnection. *Physics of Fluids (1958-1988)*, 30(6):1734–1742, 1987.

[37] Eric Ronald Priest. *Solar Magnetohydrodynamics*. Springer Science & Business Media, 2012.

[38] B Rao, YH Ding, QM Hu, WF Shi, XQ Zhang, M Zhang, XS Jin, JY Nan, KX Yu, G Zhuang, et al. Tearing mode suppression by using resonant magnetic perturbation coils on J-TEXT tokamak. *Physics Letters A*, 377(3):315–318, 2013.

[39] John Ashworth Ratcliffe. *Introduction to the Ionosphere and Magnetosphere*. Cambridge University Press, New York, 1972.

[40] CT Russell. Planetary magnetospheres. *Science Progress (1933-)*, pages 93–105, 1991.

[41] Paul Harding Rutherford. Nonlinear growth of the tearing mode. *Physics of Fluids*, 16(11):1903, 1973.

[42] VD Shafranov. On magnetohydrodynamical equilibrium configurations. *Soviet Phys. JETP*, 6, 1958.

[43] JA Snipes, DJ Campbell, PS Haynes, TC Hender, M Hugon, PJ Lomas, NJ Lopes Cardozo, MFF Nave, and FC Schüller. Large amplitude quasi-stationary MHD modes in JET. *Nuclear Fusion*, 28(6):1085, 1988.

[44] Thomas H Stix. Decay of poloidal rotation in a tokamak plasma. *Physics of Fluids (1958-1988)*, 16(8):1260–1267, 1973.

[45] Suydam, B. R. *Proceedings of the Second International Conference on the Peaceful Uses of Atomic Energy, Geneva*, 31:157, 1958.

[46] A Thyagaraja. Perturbation analysis of a simple model of magnetic island structures. *Physics of Fluids (1958-1988)*, 24(9):1716–1724, 1981.

[47] Wesson, John and Campbell, David J. *Tokamaks*, volume 149 of *International Series of Monographs on Physics*. Oxford University Press, 2011.

[48] R. B. White. Resistive reconnection. *Rev. Mod. Phys.*, 58:183–207, Jan 1986.

[49] Roscoe B White, DA Monticello, Marshall N Rosenbluth, and BV Waddell. Saturation of the tearing mode. *Physics of Fluids (1958-1988)*, 20(5):800–805, 1977.

[50] Edmund Po-ning Yu. *Evolution Equations for Magnetic Islands in a Reversed Field Pinch*. PhD thesis, The University of Texas at Austin, 2001.

[51] P Zanca. Avoidance of tearing modes wall-locking in a reversed field pinch with active feedback coils. *Plasma Physics and Controlled Fusion*, 51(1):015006, 2009.

[52] Hartmut Zohm. *Magnetohydrodynamic Stability of Tokamaks*. John Wiley & Sons, 2014.

Vita

Nikolaos Vergos was born November 2, 1982 to parents Apostolos and Irene. He grew up in Volos, Greece, and he attended the National Technical University of Athens, where he earned his Diploma in Applied Mathematics & Physics in 2009. In August of 2009 he began his doctoral studies under Professor Richard Fitzpatrick at the University of Texas at Austin. During the summer of 2012 he attended the Culham Plasma Physics Summer School, UKAEA Culham Laboratories in Abingdon, Oxfordshire, UK.

"Wir müssen wissen – wir werden wissen!" – David Hilbert

Permanent address: 55, Deligiorgi St.
Volos, Greece 38221

This dissertation was typeset with LaTeX[†] by the author.

[†]LaTeX is a document preparation system developed by Leslie Lamport as a special version of Donald Knuth's TeX Program.